

**THE EFFECTS OF DOSAGE AND DURATION OF
METHYLPHENIDATE ON CEREBELLAR STRUCTURE**

Robert Lin

02/09/2024

Westmount Charter School

LOG BOOK

SECTION I

Summary Report

Abstract

Problem

Research Questions

OLD VERSION: THE EFFECTS OF DOSAGE AND DURATION OF METHYLPHENIDATE ON CEREBELLAR STRUCTURE

By: Robert Lin

Submitted February 9, 2024

Westmount Charter School Science Fair

Abstract

Impacting up to 8.4% of children worldwide, attention deficit hyperactivity disorder (ADHD) is among the most common neurodevelopmental disorders in the world. Methylphenidate is currently the most prescribed treatment for ADHD, acting as a reuptake inhibitor for dopamine and norepinephrine. In response to inconsistent reports on the effects of methylphenidate (MPH) on the cerebellar structure of individuals with ADHD, this present study aims to combine detailed medical histories of patients with the SUIT toolbox to definitively correlate MPH dosages and usage duration with changes in localized cerebellar volume. From the various statistics and analytical tools used, the following results were obtained: (1) a statistically significant decrease ($p=0.02$) in cerebellar volume localized the left lobule IV and left IX regions can be found between neurotypical individuals and MPH-using ADHD individuals; (2) a statistically significant decrease ($p=0.02$) in cerebellar volume localized the right fastigial region can be found between MPH-using individuals with ADHD and drug-naive individuals with ADHD; (3) the median total cerebellar volume is lower in individuals who use MPH and highest in neurotypical individuals; (4) a strong positive correlation exists between medication dosage and the volume of the right fastigial nucleus ($r=0.77$), (5) a moderate positive correlation exists between medication intensity and regional volume in the Left I_IV region ($r=0.58$); and (6) a moderate correlation exists between medication duration and total cerebellar volume ($r=0.67$). Further analysis should focus on: (1) expanding the sample size of the study; (2) examining apoptotic and inflammatory factors in the most affected regions; (3) comparing the effect of MPH and amphetamines to see if the latter provides a suitable alternative.

I. Introduction

Attention deficit hyperactivity disorder (ADHD) is a neurodevelopmental disorder classified by differences in executive functioning and motivation, with estimates suggesting the condition affects up to 8.4% of children and 2.5% of adults (Harpin, 2005). From a neuroimaging standpoint, ADHD is classified by changes in overall brain volume. Methylphenidate (MPH), a

psychostimulant, is the most commonly used medication prescribed for ADHD treatment, oftentimes under brand names such as Ritalin. As a reuptake inhibitor, MPH increases the concentration of dopamine in the synapse, which has dramatic effects on the dopaminergic pathway in the mesolimbic system. Despite the many benefits of MPH as a medication, existing literature demonstrates that particular

doses and usage durations of MPH can have a variety of effects on brain structure and composition, many of which are still not fully understood. In particular, some existing works highlight the effects of MPH on the cerebellar structures, especially in the context of apoptosis pathways, cortical thickness, and increased disease risk (Raofi et. al, 2020; Bahcelioglu et al. 2009; 2017; Reus et al., 2014; Quansah et al., 2018; Curtin et al., 2018; Mackey et al., 2013). The effects of MPH also appear to extend to the prefrontal cortex, hippocampus, and striatum (Motaghinejad et al., 2016; Schmitz et al., 2012; Lizanne et al., 2012). Much of this existing literature, however, is still contradictory and little consistency exists in the results from one study to another. Given the prevalence of MPH use in children with ADHD, as well as the continued gaps in scientific knowledge, these findings are cause for concern. As such, this project aims to find the correlation between MPH dosage and usage duration by performing volumetric analyses on T1 weighted MR images. To differentiate itself from the inconsistency in existing literature, results from the volumetric analysis will be coupled with detailed medication history to eliminate confounding variables. Ultimately, this project aims to (1) elucidate the structural changes that occur in the cerebellum; (2) identify how dosage and duration impact these structural changes, and (3) illuminate the possible mechanisms for harmful effects as a result of cerebellar degeneration.

II. Method

II.I Overview

T1 weighted images from individuals between the ages of 5 and 18 will be gathered or repurposed from a neuromelanin study and the TAG-IT demographics project. Remaining gaps will be filled out by collecting data from volunteers. Using the SUIT toolbox, the volumes of the various regions of the

cerebellum will be extracted. SUIT's ability to create a surface-based representation of the cerebellum will be used to identify three to five main structures as having the greatest change between MPH-using individuals and psychostimulant-negative individuals with ADHD. Each of these regions is visually represented using three graphs. The first scatterplot will plot medication dosage (mg) against regional volume (mm³). The second scatter plot will plot MPH medication duration (years) against regional volume (mm³). The third graph will use a coding system, in which letters correspond to medication dosage and numbers correspond to medication duration. For the letter system, code A refers to no medication, code B refers to <30mg, code C refers to >30mg and <60mg, and code D refers to >60mg. For the number system, number 1 refers to <2 years, number 2 refers to >2 years and <4 years, and number 3 refers to >4 years. Each letter and number will be uniquely paired, forming ten medication and dosage categories in total. The average volume for subjects meeting the criteria for each distinct category is then plotted as a bar graph, which can elucidate which combination of dosage and medication period have the greatest effect.

II.II Phase I

The first phase is a pilot study using eight T1 MR images. These eight images were originally collected for a separate study at BrainKids Lab, but was reused given it: (1) contains structural image data of children with ADHD, (2) includes children who both use and do not use methylphenidate, (3) comes with detailed patient information including duration and dose of the drug, and (4) was reliably collected and reused with the consent of the subjects. All eight of the images did not contain defects that prevented the data from being usable. It should be noted that subject number four had a metal retainer in their mouth, but the distortion in the image mostly and does not

disturb the cerebellum or brainstem. As such, this scan was not excluded.

II.III Phase II

A larger sample size is required for inferential statistics. A study conducted with BrainKids Lab contained T1 weighted images from children with a mean age of around 11 to 12 (n=40). However, certain exclusion criteria must be applied to the scans when gathering data on MPH-using individuals: (1) no artifacts or distortions may be present in the cerebellum in any dimensions, (2) subject must currently be taking a MPH stimulant medication for ADHD, (3) subject must include dose and duration of their current medication. A similar exclusion criteria must be applied when selecting data for the non-MPH-using subjects: (1) no artifacts or distortions may be present in any dimensions, (2) subject must not be currently taking MPH for ADHD, or have taken the medication for in the past, (3) subject must not be on any psychostimulant, and (4) must explicitly state no prior medication history. Lastly, the TAG-IT demographics also includes data from non-ADHD patients which can be used as a negative control when interpreting results. Exclusion criteria for this group include: (1) no artifacts or distortions may be present in the cerebellum in any of the three dimensions, (2) subject must not be currently taking a methylphenidate stimulant medication for ADHD, or have taken the medication for an extended period of time in the past, (3) subject must not be on any additional psychostimulant medication, including amphetamines, (4) must not have a diagnosis for ADHD or any other neurocognitive disability (must be neurotypical).

II.IV Phase III

Depending on the number of participants that meet the exclusion criteria from the TAG-IT study, additional and specific data may be required. The exclusion criteria for

study participants will be similar to those mentioned in Phase II, although groups underrepresented in the Phase II data may be emphasized during recruitment. In order to obtain this data, this study will first have to be approved by the University of Calgary's Internal Review Board, and the Alberta Children's Hospital's research MRI must finish renovating (mid-2024). A CAIR Level 0 certification has been obtained. In order to schedule MRI use, however, a CAIR Level 1 certification must be obtained. As such, Phase III will likely be implemented after the completion of science fair in mid 2024.

II.V SUIT Introduction

SUIT is a specialized program developed by Diedrichsen Lab using voxel-based morphometry to analyze the cerebellum from one individual to another. Specialized cerebellar atlases are provided as part of the SUIT MATLAB toolbox. SUIT was chosen because it can: (1) Automatically isolate cerebellar structures from an anatomical image; (2) Achieve accurate normalization of the cerebellum into atlas space using the Dartel algorithm; (3) Display data on a surface-based flatmap representation; and (4) Use VBM to determine patterns of growth or shrinkage. The most commonly used atlas template for brain imaging is the ICBM152 template, which does not show any clear differentiation for the cerebellum, making analysis of specific regions of the cerebellum difficult. To remedy this, Diedrichsen lab developed a cerebellar atlas based on the average anatomy of twenty healthy individuals aged 22-45. Certain characteristics about this template enable it to be specialized to the cerebellum, such as how it: (1) is specifically based on brainstem and cerebellum, (2) preserves the anatomical accuracy of the cerebellum to a far greater extent than the ICBM152 template, and (3) reduces spatial variance and improves overlap of deep cerebellar

nuclei.

II.VI SUIT Procedure

To use the SUIT program, the first function used is "suit_isolate_seg". This function takes the original T1 weighted image and produces gray and white matter probability maps, representing the distribution of white and gray matter in the subject, as well as a cerebellar mask. In most cases, this cerebellar mask must be edited in MRICron. The isolation function is performed in the native space of the original image, meaning that the image needs to be normalized to the cerebellar atlas in order to compare between various images. As such, the normalization function "suit_normalize_dartel" deforms the image from the native space to SUIT space, changing location but not size. The Dartel algorithm uses the tissue segmentation maps -- in this case white matter and gray matter maps -- to find the nonlinear deformation in the form of a three-dimensional mathematical model known as a flowfield. The normalization function may encounter the common error message stating the image is stated too far apart, in which the origin of the original T1 weighted image must be reset to a bundle of white matter in the brain known as the anterior commissure. This normalization function produces an affine matrix and non-linear flowfield. It is important to note that the normalization feature does not reslice the image into the atlas space, but only calculates the changes that would be necessary to make such a change. The next step in the process is to reslice the image into SUIT space using the "suit_reslice_dartel_inv". This function uses the products from the normalization function, as well as the SUIT cerebellar atlases and the original T1 weighted image, to reslice the image. This, in turn, produces a file that has split the cerebellum up into its specific volumes. Using the product of the reslice function as the input for the "suit_vol" function, the program generates

the following information: number of voxels per region, volume in mm³ per region, and volume of one voxel. The key information here is the volume in mm³ per region, which should be recorded in a separate data table. Once both groups have been analyzed, a surface-based representation of the cerebellum can be created, which will allow for the display and comparison of volume-averaged cerebellar data between groups.

II.VII Data Analysis

In order to establish the relationship, or the lack of one, between methylphenidate and changes in cerebellar structures, multiple forms of data analysis must be performed. Before commencing data analysis, outliers within each group should be identified and removed using the 1.5 IQR rule. A least-squares regression line will be created for each scatterplot, allowing for the Pearson's correlation coefficient (r value) and the R² squared value. In turn, this will allow for the nature of the correlation, as well as the strength of the correlation, to be revealed. After calculating the sample means and standard deviations for each region in both methylphenidate-using and medication-free individuals with ADHD, a standard t test can be conducted. Setting the confidence interval to 95%, any differences must have a p-value of less than 0.05 in order to show statistical significance. Comparisons can be made using all regions, as well as between each ADHD medication level and the negative control (individual without ADHD). The use of a t test will allow for the comparison between the use of methylphenidate and medication free individuals. Further analysis can be conducted using an ANOVA test. Analysis of variance tests can show how the dependent variable changes with varying levels of the independent variable. In this case, the dependent variable is the cerebellar regional volume, while the independent variable levels are the dosage and duration of medication. A one way

ANOVA test can be used to gain a better understanding how each independent variable affects cerebellar structure, but a two-way ANOVA test will also be used to understand how both dosage and duration of methylphenidate use will impact the cerebellum.

III. Research

III.I ADHD

Attention deficit hyperactivity disorder (ADHD) is a chronic and debilitating disorder that affects individuals in areas such as academic and professional achievements, interpersonal relationships, and daily functioning (Harpin, 2005). Estimates suggest that 8.4% of children have ADHD, while a lower proportion, 2.5% of adults have the condition. In particular, the disorder leads to decreases in executive function and changes motivation patterns. While some theories postulate the genetic basis for the condition, the true cause remains unknown. With the exclusion of Parent-Child Interaction Therapy (PCIT) for preschool-aged children, the most commonly prescribed medications for ADHD are psychostimulants, usually amphetamines and methylphenidates. Twin studies show heritability estimates of 0.6 to 0.9, with the most studied genetic variations being those occurring in the dopamine D4 receptor and dopamine transporter (DAT1). New findings suggest the role of COMT, an enzyme that is involved in metabolizing catecholamine neurotransmitter, val 158/108 met variant in influencing conduct problems. The most consistent finding between individuals with the condition is an overall reduction in total brain size that continues into adolescence, as well as reduced dimensions of specific brain regions, including: the caudate nucleus, prefrontal cortex white matter, corpus callosum and the cerebellar vermis. The structures with decreased size are most commonly those with a high density of dopamine receptors.

III.II Methylphenidate (MPH)

Methylphenidate treats ADHD in children and adults (Verghese & Abdijadid), working as a norepinephrine (NE) and dopamine(DA) reuptake inhibitor. In preclinical studies, it was found MPH results in the inhibition of NET and DAT, agonist activity at 5-HT1A receptor, inhibition of MAO, and redistribution of VMAT-2. This results in higher DA and NE levels. In neuroimaging studies, MPH increases activation of the parietal and prefrontal cortices during working memory tasks. In an uncertain environment, MPH resulted in increased activation in left and right parahippocampal regions and cerebellar regions. MPH-caused improvements in working memory tasks corresponded with decreased oxyhemoglobin levels in the right lateral prefrontal cortex.

III.III The Cerebellum

Anatomy: As the largest structure in posterior fossa, the cerebellum is attached to dorsal pons and rostral medulla by three peduncles: the superior, middle, and inferior peduncles. The former of the two carries output from the cerebellum, and decussates in the midbrain, while the latter carries inputs. The cerebellum consists of the midline vermis situated in between two larger cerebellar hemispheres, which are in turn divided into anterior and posterior lobes by the primary fissure, as well as the flocculonodular lobe by the posterolateral fissure. The vermis and flocculonodular lobes control proximal and trunk muscles. The intermediate part of the cerebellar hemisphere is involved in control of distal appendicular muscles, while the lateral part of the cerebellar hemisphere controls motor planning. All outputs of the cerebellum pass through the four deep cerebellar nuclei, from most lateral to most medial: dentate, emboliform, globose, and fastigial. The position of the deep cerebellar nuclei directly corresponds to their input.

Circuitry: The cerebellar cortex has three

layers: the granule layer contains granule cells; the purkinje layer contains purkinje cells; and the molecular layer contains the unmyelinated axons of granule cells, dendrites of purkinje cells, as well as several types of interneurons. There are two types of synaptic inputs to the cerebellum, mossy fibers and climbing fibers. Mossy fibers ascend from various regions and form excitatory synapses with dendrites of granule cells. In turn, granule cells send axons into the molecular layer, which bifurcate, forming parallel fibers that run perpendicular and form excitatory synapses with the dendrites of the purkinje cells. All outputs from cerebellar cortex carried by axons of purkinje fibers into the cerebellar white matter. Purkinje cells form inhibitory synapses with deep cerebellar and vestibular nuclei, which convey information from the cerebellum to other regions through excitatory synapses, regulating information exiting so as to avoid overstimulation. The other kind of input to cerebellum is climbing fibers, which arise exclusively from neurons in the contralateral inferior olivary nucleus. Climbing fibers wrap around the cell body and proximal dendritic tree of purkinje fibers, forming excitatory synapses. These cells have a strong modulatory effect on purkinje cells, and can cause significant decline in response to parallel fiber stimulation. Basket cells and stellate cells are located in the molecular layer, and are excited by synaptic input from parallel fibers, which respond by inhibiting adjacent purkinje cells. Golgi cells can be found at the granule cell layer. These cells are also stimulated by the parallel fibers, and provide feedback inhibition on granule cell dendrites. The result of golgi cell's inhibitory property is regulation of the temporal domain of signals, leading to enhanced signal resolution. Similarly, the result of stellate and basket cell inhibitory property is regulation of the spatial domain of signals, also leading to enhanced signal resolution.

III.IV Magnetic Resonance Imaging (MRI)

MRI provides images of body tissues and their chemical compositions with exceptional clarity and little risk. When a magnetized species exists, it can absorb the energy from a magnetic field of equal strength. The nucleus has a net positive charge, with each proton and neutron in the nucleus having its own spin. A nucleus must possess overall spin to respond to MRI. In the absence of external forces, these varying spin states are of equal energy. When hydrogen protons are exposed to a magnetic field, they will tend to orient themselves with the field to maximize stability. At the beginning of a spin echo sequence, a 90 degree RF pulse is applied. The net magnetization vector becomes perpendicular to its original orientation, eliminating longitudinal magnetization and generating a transverse magnetization vector. During recovery, the longitudinal magnetization increases, and the transverse magnetization decreases, causing energy to be released and recorded by the MRI. The point at which 63% of the longitudinal magnetization has been recovered is called T1. The time at which 63% of the transverse magnetization has been lost is called T2. Both values are unique to specific tissue types. Time to echo (TE) is the latency between the RF pulse and the echo, while repetition time (TR) is the time to run a pulse sequence at one time. Images created with a short TE and TR are known as T1-weighted images. When T1 effects are minimized by having a long TE and TR, T2 weighted images are produced.

III.V The Mesolimbic System

The mesolimbic system, or reward system, is composed of brain structures responsible for mediating the physiological and cognitive processing of rewards. Dopamine plays a key role in the reward value of food, drink, sex, social interaction, and substance abuse. As such, the mesolimbic system

primarily refers to the dopaminergic pathway, which is formed by projections of midbrain dopamine neurons of the ventral tegmental area (VTA) to the striatum, prefrontal cortex, amygdala, hippocampus, and many structures of the limbic system. Some abnormalities exist in the mesolimbic system for individuals with ADHD. Usually, the repetition of a positive stimulus means the time of the reward transfers to earlier and earlier predictors of the reward. The dopamine transfer deficit theory suggests that the transfer of the cell's response to dopamine fails to predict the reinforcement that will occur in children with ADHD. Dopamine transporters (DATs) are responsible for terminating the dopamine signal. In many diagnosed with ADHD, the dopamine transporter 1 (DAT1) gene varies in length due to a variable number tandem repeat (VNTR) of a 40 base pair repeat. The alleles with 10 copies (10R) have been associated with ADHD. In vitro, it was found that DAT binding site density for the 10R polymorphism was elevated 50% over that of the 9R allele. In addition, individuals homozygous for the 10R allele showed significantly hypoactivation in the left dorsal anterior cingulate cortex (dACC), a structure found in the cerebral cortex associated with executive function. Hypoactivation was also shown in the left cerebellar vermis and right lateral prefrontal cortex. Polymorphisms of D4 and D5 receptors are associated with ADHD. D4 is expressed presynaptically, giving it regulatory powers over both the presynaptic and postsynaptic neuron. This receptor is associated with the rapid translocation of the CaMKII II protein from the cytosol to the prefrontal cortex neurons, which activates synaptic proteins responsible for developing plasticity. Coupled to adenylyl cyclase, D5 receptors

will result in increased cyclic AMP levels upon activation. This process is key for the development of plasticity for the dopamine pathway, as well as the development of long term potentiation between the cerebral cortex and striatum.

IV. Conclusion

Without full experimental results, it is difficult to form a conclusion on the effects of methylphenidate dosage and usage duration on cerebellar structure. Purely from conducting literature review, prior studies suggest the MPH has the most profound effects on cerebellar cortical thickness and composition, increases in cerebellar-related diseases, and increases in tissue degeneration and inflammation factors. Due to the method of this study, obtained results will only indirectly correspond to the findings in the literature review. The main reason for this is the fact that only anatomical scans are being used. Additionally, inflammation factors cannot be tested for in subjects who are still alive. The literature review serves to elucidate the unique nature of this project. While previous studies have focused primarily on the degeneration of the outer layers of the cerebellar hemispheres, the use of SUIT allows this study to examine medial structure as well. As such, this study has the potential to yield novel insights into the dangers of methylphenidate.

V. Acknowledgements

I would like to thank Dr. Kara Murias at the University of Calgary for her guidance and advice throughout this entire project. I would also like to thank all the members of BrainKids Lab, especially Ryan Verbitsky, who helped me on issues from downloading MATLAB to drawing masks in MRIcron.

Abstract

Impacting up to 8.4% of children worldwide, attention deficit hyperactivity disorder (ADHD) is among the most common neurodevelopmental disorders in the world. Methylphenidate is currently the most prescribed treatment for ADHD, acting as a reuptake inhibitor for dopamine and norepinephrine. In response to inconsistent reports on the effects of methylphenidate (MPH) on the cerebellar structure of individuals with ADHD, this present study aims to combine detailed medical histories of patients with the SUIT toolbox to definitively correlate MPH dosages and usage duration with changes in localized cerebellar volume. From the various statistics and analytical tools used, the following results were obtained: (1) a statistically significant decrease ($p=0.02$) in cerebellar volume localized the left lobule IV and left IX regions can be found between neurotypical individuals and MPH-using ADHD individuals; (2) a statistically significant decrease ($p=0.02$) in cerebellar volume localized the right fastigial region can be found between MPH-using individuals with ADHD and drug-naive individuals with ADHD; (3) the median total cerebellar volume is lower in individuals who use MPH and highest in neurotypical individuals; (4) a strong positive correlation exists between medication dosage and the volume of the right fastigial nucleus ($r=0.77$), (5) a moderate positive correlation exists between medication intensity and regional volume in the Left I_IV region ($r=0.58$); and (6) a moderate correlation exists between medication duration and total cerebellar volume ($r=0.67$). Further analysis should focus on: (1) expanding the sample size of the study; (2) examining apoptotic and inflammatory factors in the most affected regions; (3) comparing the effect of MPH and amphetamines to see if the latter provides a suitable alternative.

Introduction

Attention deficit hyperactivity disorder (ADHD) is a neurodevelopmental disorder classified by differences in executive functioning and motivation, with estimates suggesting the condition affects up to 8.4% of children and 2.5% of adults (Harpin, 2005). From a neuroimaging standpoint, ADHD is classified by changes in overall brain volume, although these changes can be partially localized to some regions. Methylphenidate (MPH), a psychostimulant, is the most commonly used medication prescribed for ADHD treatment, oftentimes under brand names such as Ritalin. As a reuptake inhibitor, MPH increases the concentration of dopamine in the synapse, which has dramatic effects on the dopaminergic pathway in the mesolimbic system. Despite the many benefits of MPH as a medication, existing literature demonstrates that particular doses and usage durations of MPH can have a variety of effects on brain structure and composition, many of which are still not fully understood. In particular, some existing works highlight the effects of MPH on the cerebellar structures, especially in the context of apoptosis pathways, cortical thickness, and increased disease risk (Raoufi et al., 2020; Bahcelioglu et al., 2009; 2017; Reus et al., 2014; Quansah et al., 2018; Curtin et al., 2018; Mackey et al., 2013). The effects of MPH also appear to extend to the prefrontal cortex, hippocampus, and striatum (Motaghinejad et al., 2016; Schmitz et al., 2012; Lizanne et al., 2012). Much of this existing literature, however, is still contradictory and little consistency exists in the results from one study to another. Given the prevalence of MPH use in children with ADHD, as well as the continued gaps in scientific knowledge, these findings are cause for concern. As such, this project aims to examine the correlation between methylphenidate dosage and usage duration by performing volumetric analyses on T1 weighted MR images. To differentiate itself from the inconsistency existing in existing literature, results from the volumetric analysis will be coupled with detailed medication history to eliminate confounding variables. Ultimately, this project aims to (1) elucidate the structural changes that occur in the cerebellum; (2) identify how dosage and duration impact these structural changes, and (3) illuminate the possible mechanisms for harmful effects as a result of cerebellar degeneration.

Research Question

How does the dosage and usage duration of methylphenidate as a prescription medication for ADHD affect cerebellar structure and volume?

Background Research

- ADHD
 - Types of ADHD medication
 - Causes of ADHD
 - Structural changes in the brain that occur because of ADHD
 - Mechanisms of impairment for ADHD
- Dopamine reward pathway in the brain
- Methylphenidate
 - What is methylphenidate
 - How does it act on the brain in relation to ADHD
- Cerebellum
 - What is the anatomy and physiology of the cerebellum
 - What are some notable functions and pathways
- MRIs
 - MRI physics - how does it work
 - What are different types of MRI layers
 - Artifacts, etc.
- Data analysis techniques
 - Voxel based morphometry
 - SUI toolbox
 - Editing layers in MRICron

Literature Review

- SUI: <file:///C:/Users/rober/Documents/cerebellar%20volumesHIE%20SUI.pdf>

SECTION II

Basic Research

ADHD

Dopamine

Methylphenidate

Cerebellum

MRI Physics

Literature Review

Synthesis

Basic Research on the Brain

Structure and function

- Most organelles are located in the **cell body**, which is studded with highly branched extensions called **dendrites**
 - Dendrites receive signals
- Axon is the extension that transmits signals to other cells
 - Longer than dendrites
 - Uses pulses of electrical current to transmit information
 - Cone shaped base of axon, called an axon hillock, is where the signal is generated
- Axons transmit information to another cell at a junction called a synapse
 - Part of axon that forms synapse is called the synaptic terminal
- Neurotransmitters pass information from the neuron to the receiving cell

Information processing

- 3 steps: sensory input, integration, and motor output
- Types of neurons
 - Sensory neurons transmit information about external stimuli and internal conditions
 - Interneurons form local signals in the brain, responsible for integration
 - Motor neurons transmit signals to muscle cells, causing them to contract
- All types transmit information in the same information despite structural variations between the three
- More highly branched dendrites = more input and output
- When grouped together, axons of neurons form bundles we call nerves
- Generally...
 - Processing and integration are in the CNS, including the brain or a simpler cluster called ganglia
 - Neurons that carry info in and out of the CNS constitute the PNS
 - Glial cells, or glia, support neurons

White and gray matter

- Peripheral NS is all white matter
- Unmyelinated neurons are referred to as gray matter, myelinated neurons are referred to as white matter

Overview

- Ions are unequally distributed between the interior and exterior of neurons, leading to the inside having a negative charge relative to the exterior

- Difference in charge, or voltage, is called membrane potential
 - Typically between -60 and -80 millivolts (mV)

Formation of resting potential

- In most neurons, the concentration of K⁺ is higher inside the cell, while the concentration of Na⁺ is higher outside
- These concentration gradients are maintained by the sodium-potassium pump
 - Uses energy of ATP to actively transport Na⁺ out of the cell, and K⁺ into the cell

Ion	Intracellular concentration (mM)	Extracellular concentration (mM)
K ⁺	140	5
Na ⁺	15	150
Cl ⁻	10	120
Large anions, such as proteins, inside the cell	100	n/a

- Sodium-potassium pump transports 3 Na⁺ out of the cell for every 2 K⁺ that enter
 - Generates a net negative charge
 - Acts slowly
- Negative charge is created thanks to ion movement through ion channels, pores formed by protein clusters
 - As ions move through, they carry with them units of electrical charge
 - Move rapidly
- K⁺ ions can freely move along their concentration gradient and out of the cell again due to K⁺ channels (sometimes called leak channels), which establishes a negative resting potential
- Excess negative charge inside the cell exerts an attractive force that opposes the flow of potassium ions out the cell
 - Creates an electrical gradient that counterbalances the concentration gradient

Modeling Resting Potential

- The magnitude of the membrane voltage at equilibrium for a particular ion is called that ion's equilibrium potential (E_{ion})
 - The Nernst Equation can calculate E_{ion}

$$E_{\text{ion}} = 62 \text{ mV} \left(\log \frac{[\text{ion}]_{\text{outside}}}{[\text{ion}]_{\text{inside}}} \right)$$

- this specific equation only works at human body temperature (37 C), and for an ion with a net charge of 1+
 - Concentration of ions are measured in mM
 - When the outside concentration of K⁺ is 140mM and the inside concentration is 5mM, the E_{ion} is -90mv
- The real resting potential is slightly lower than the Nernst equation thanks to the small but steady movement of Na⁺ into the cell via the few open sodium channels
 - If there is a tenfold higher concentration of Na⁺ in the extracellular environment, and all of the Na⁺ ions are open, the flow of ions into the cell results in an equilibrium potential of +62 mv
- Neither K⁺ or Na⁺ is at equilibrium in a resting neuron, as there is a net flow of each ion across the membrane

Overview

- Neuron changes membrane potential by opening gated ion channel in response to stimuli
 - When channels open and close, the membrane's permeability changes

Hyperpolarization and depolarization

- If gated potassium channels in a resting neuron is opened, the membrane's permeability to K⁺ increases
 - Diffusion of K⁺ out of the neuron, bringing the membrane potential towards E_{K}
 - This increase in magnitude of the membrane potential is known as **hyperpolarization**
 - Results from any stimulus that increases outflow of positive ions or inflow of negative ions
- A reduction in the magnitude of the membrane is called depolarization
 - In neurons, depolarization occurs when gated sodium channels open, causing the membrane potential to shift towards E_{Na}

Graded potentials and action potentials

- Sometimes the response to depolarization or hyperpolarization is just a shift in membrane potential, which is referred to as **graded potential**
 - Magnitude varies with stimuli
 - Induces a small current that dissipates as it flows along the membrane
 - Decay with time and distance from their source
- If depolarization shifts membrane potential significantly, a large change in voltage, called action potential, occurs
 - Have constant magnitude and can regenerate in adjacent regions of the membrane

- If depolarization increases membrane potential to a level called threshold, the voltage-gated ion channels open
 - Inflow of Na⁺ further raises membrane potential, leading to more ion channels opening (positive feedback)
 - Result: very rapid opening of many voltage-gated sodium channels
 - Threshold is about -55mv
- The magnitude of action potential is independent of the magnitude of the stimulus
 - Either occur or do not, all-or-none scenario

Action Potential Deep Dive

- Resting potential
 - Most voltage gated sodium channels are closed, but some potassium channels are open
 - Most K⁺ voltage gated channels are closed
- Depolarization
 - Stimulus depolarizes the membrane, some gated sodium channels open, allowing Na⁺ to diffuse in
 - If stimulus is strong enough, the positive feedback loop occurs and more channels open
- Rising phase of action potential
 - Positive feedback cycle really kicks in, bringing the membrane potential close to E_{Na}
- Falling phase of action potential
 - Voltage-gated sodium channels inactivate soon after opening, preventing the inflow of Na⁺
 - Most voltage-gated K⁺ channels open, causing a rapid outflow of K⁺ ions
 - These two events bring the membrane potential back to E_K
- Undershoot (hyperpolarization)
 - Membrane permeability to K⁺ is at its highest, so the membrane is closest to E_K that it will ever be
 - Gated potassium channels close, and the membrane potential returns to the resting potential

Action potential extra info

- The sodium voltage gated channels become inactivated because they can only close when the membrane returns to resting potential
 - However, the falling phase require a reduction in the inflow of sodium ions, and the inactivation of these proteins provides the perfect mechanism
- Sodium channels remain inactivated during the falling phase and the early part of undershoot

- If a second depolarizing stimulus during this period, action potential cannot be initiated
 - This is known as the refractory period

Conduction of action potentials

- At the site where action potential is initiated (usually the axon hillock), Na⁺ inflow creates an electrical current that successfully depolarizes the neighboring region of the axon membrane
 - If this reaches threshold, another action potential will occur
 - All-or-none means magnitude and duration of action potential will be the same down the entire neuron
- Current can spread down the neuron via many successive action potentials, from the cell body to the synaptic terminals, like dominos falling
- Thanks to the refractory period, the inward current can only depolarize the membrane ahead of the action and not behind it
 - Action potential travels in one direction
- After the refractory period is complete, depolarization of the axon hillock will trigger and new action potential
 - Since action potentials last ~2 milliseconds, firing rate can reach hundreds of action potentials per second
- Rate at which action potentials are produced is proportional to the strength of input signal strength
 - Louder sounds will result in more frequent action potentials
- Mutations of ion channel genes for neurons can cause epilepsy, where nerve cells fire simultaneously and excessively, producing seizures

Evolution of axon structure

- Rate of action potentials is advantageous and closely connected to natural selection
- Wider axon provides less resistance to the current associated with action potential
 - Think skinny hose v wide hose
- Vertebrates have skinny axons but can still conduct action potentials quickly thanks to electrical insulation, analogous to wire casing
 - Causes depolarizing current to travel farther along the axon interior, bringing more distant regions to the threshold sooner
 - Prevents current from leaking out of the axon, increases the distance along the axon that a current can flow passively
- Myelin sheaths serve as the electrical insulation
 - Produced by glia
 - Oligodendrocytes in the CNS and Schwann cells in the PNS
 - In myelinated axons, voltage-gated sodium channels are restricted to gaps in the myelin sheath called the Nodes of Ranvier

- Extracellular fluid is in contact with the axon only at the nodes
- As a result, action potentials are not generated at in the regions between the nodes
- Action potential at a node travels within the axon all the way to the next node
 - As a result, action potentials appear to jump from node to node as it travels along the axon
- Action potentials propagate more rapidly in myelinated axons because the time-consuming process of opening and closing ion channels only occurs in select places along the axons
 - Known as saltatory conduction (saltare=to leap) because the action potential appears to jump from one node to another
- Myelinated axon with diameter of 20 micrometers has a faster conduction rate than a unmyelinated axon that is 40 times greater in diameter
 - More than 2000 myelinated axons can be packed into the space of one giant axon

Overview

- Transmission of information from neurons to other cells occurs at synapses, which can either be electrical or chemical
- Electrical synapses contain gap junctions that allow electrical current to flow directly from one neuron to another
 - Play a role in synchronizing the activity of neurons that direct rapid unvarying behaviors
- Chemical synapses (majority) rely on the release of a neurotransmitter by the presynaptic neuron to transfer information to the target cell
 - Neurotransmitters are synthesized at the synaptic terminal and packaged in membrane-enclosed compartments called synaptic vesicles
- When the action potential arrives at the synaptic terminal, Ca^{2+} voltage gated channels open
 - The elevated levels of calcium causes the vesicles to fuse with the membrane, releasing the neurotransmitter
- Released neurotransmitters diffuse across the synaptic cleft, the gap between the presynaptic neuron and the target
 - Short diffusion time, distance = 50nm
- NT binds and activates specific receptor
- The receptor for a neurotransmitter could be a ligand-gated ion channel
 - As receptor binds, the ion channel opens allowing for the diffusion of Na^{+} and K^{+}
- Information transfer at chemical synapses can be modified by altering the amount of neurotransmitter that is released
 - Can also be modified by altering the responsiveness of the postsynaptic cell

- These are the mechanisms allowing for adaptation to stimuli and the basis of learning

Postsynaptic potentials

- NTs often bind to ligand-gated ion channels
- Binding of NTs result in inflow of ions, which results in a postsynaptic potential, a graded potential
- At some synapses, the channel becomes permeable to both K^+ and Na^+
 - Membrane potential will depolarize towards a value midway between the two equilibriums
 - This brings the membrane toward threshold, and is called an excitatory postsynaptic potential (EPSP)
- At other synapses, the channel is only permeable to K^+ and Cl^-
 - When these channels open, the postsynaptic membrane hyperpolarizes
 - Known as inhibitory postsynaptic potential (IPSP) because it moves the membrane further from threshold

Summation of postsynaptic potentials

- Input of an individual synapse is insufficient to trigger a response, as the EPSP degrades before it reaches the axon hillock
- Sometimes individual postsynaptic potentials can combine to produce a larger signal (summation)
- If two EPSPs occur at the same time, with the second one occurring before the membrane as returned to its resting potential, the two signals can combine in a process called temporal summation
- Summation can involve multiple synapses; if two synapses are active at the same time, the resulting EPSP's can add together through spatial summation
- IPSPs can also combine in the same ways, producing a larger hyperpolarizing effect
 - Can also counter the effects of an EPSP
- Axon hillock is the main integrating center, membrane potential represents the summed effects of all EPSPs and IPSPs

Termination

- Chemical synapse returns to its resting state after a response is triggered
 - happen by clearing the NT from the synaptic cleft
 - Some NTs are inactivated by enzymatic hydrolysis
 - Others are recaptured into the presynaptic neuron
 - After reuptake, the NTs are repackaged in vesicles or transferred to glia for metabolism or recycling

Modulated signaling at synapses

- At some synapses, the NT binds to a G protein-coupled receptor, activating a signal transduction pathway involving a secondary messenger
 - Also called metabotropic receptors
- Advantages: signal amplification
 - One molecule of norepinephrine can open many channels
- Many NTs have both ionotropic and metabotropic receptors
 - G-proteins have slower but longer lasting effects

Neurotransmitters

- Acetylcholine (ACH)
 - Muscle stimulation, memory formation, and learning
 - Has a ligand-gated ion channel
 - Know most about its function at the neuromuscular junction, where a synapse forms between a motor neuron and skeletal muscle cell (excitatory)
 - GCPR is found in locations that include the CNS and heart
 - Will inhibit adenylyl cyclase and open potassium channels, reducing heart rate
 - Nicotine acts as a stimulant by binding to an ionotropic ACH receptor in the CNS
- Glutamate
 - Amino acid NT
 - Serves as the ACH for invertebrates at the neuromuscular junction
 - Most common NT in vertebrates, key for long term memory
- Glycerine
 - Amino acid
 - Inhibitory synapses in parts of the CNS outside the brain
- GABA
 - Amino acid is the NT at most inhibitory synapses
 - Increases membrane permeability of Cl⁻, resulting in IPSP
- Biogenic amines
 - Group of NTs are synthesized from amino acids and include norepinephrine
 - Dopamine (made from tyrosine) and serotonin (made from tryptophan) impact sleep, mood, attention, and learning
- Neuropeptides
 - Short chains of amino acids that serve as NTs, operate on GPCRs
 - Produced by the cleavage of larger protein precursors
 - substance P is an excitatory NT that mediates pain perception
 - Endorphins decrease pain perception, reduce urine output, decrease respiration, and produce euphoria
- Gasses

- Some neurons release NO into the erectile tissue of the penis during sexual arousal
 - Relaxes smooth muscles in blood vessels, allowing the erectile tissue to fill with blood
- NO is not stored in cytoplasmic vesicles, but synthesized on demand

Vertebrate Nervous System

- The CNS develops from a hollow dorsal nerve cord, characteristic of chordates
- Cavity of the nerve cord gives rise to the narrow central canal of the spine and the ventricles of the brain
 - Both the central canal and ventricles are filled with cerebrospinal fluid, which is formed in the brain by filtering arterial blood
 - Supplies the CNS with nutrients and hormones and carries away wastes
 - Circulates through the ventricles and central canals, drains into veins
- Brain and spinal cord have gray and white matter
 - Grey matter composed of neuron cell bodies
 - White matter consists of bundled (myelinated) axons
- White matter forms the outer layer in the spinal cord and the inner layer of the brain
- Spinal cord acts independently of the brain to produce reflexes, which provide rapid, involuntary responses to stimuli

The PNS

- transmits information to and from the CNS, regulating internal environment and locomotion
- Sensory information reaches the CNS via the PNS afferent neurons
 - Information is processed, and exits via the efferent neurons
- Two components
 - Motor system carries signals to skeletal muscles
 - Can be voluntary (raising hand) or involuntary (knee-jerk reaction)
 - Autonomic nervous system is generally involuntary
 - Parasympathetic and sympathetic divisions regulate organs of the cardiovascular, excretory, and endocrine systems
 - Enteric nervous system, another subunit, regulates the digestive tract, pancreas, and gallbladder
- Homeostasis often relies on cooperation between autonomic and motor system
 - When body temp drops, motor signal causes shivering while autonomic system constricts surface blood vessels
- Activation of sympathetic NS corresponds to energy generation (flight or fight)
 - Heart beats faster, digestion is inhibited, release of epinephrine, liver converts glycogen to glucose, pupils dilate, inhibits bladder emptying

- Activation of parasympathetic division causes the opposite effects of sympathetic, with the exclusion of genitals
 - Sympathetic promotes ejaculation and vaginal contractions, parasympathetic promotes erection
- Parasympathetic nerves exit the CNS at the base of the brain or spinal cord and form synapses in ganglia located just outside of the spinal cord
- In both divisions, the pathway for information flow involves a preganglionic neuron and a postganglionic neuron, with the ganglia in between
 - In both, the preganglionic releases ACH
 - In the sympathetic, the postganglionic neuron releases norepinephrine, while the postganglionic neuron in the parasympathetic division releases ACH again

Glia

- Schwann cells myelinate neurons in the PNS, oligodendrocytes myelinate neurons in the CNS
- Embryonic glial cells
 - Radial glia form tracks along which newly formed neurons migrate from the neural tube, which is the structure that gives rise to the CNS
 - Astrocytes are adjacent to brain capillaries and form the blood-brain barrier
 - Filters blood to prevent many substances from entering the CNS
- Radial glial cells and astrocytes can both serve as stem cells
- Ependymal cells line the ventricles of the brain and have cilia that circulate the cerebrospinal fluid
- Astrocytes also facilitate information transfer, regulator extracellular ion concentration, and promote blood flow to neurons
- Microglia are immune cells in the CNS
- Forebrain contains olfactory bulb and cerebrum, activities include processing of smells, sleep regulation, learning, and complex processing
- Midbrain coordinates routing of sensory input
- Hindbrain controls involuntary activities and motor activities

Brain development

- As the embryo develops, the neural tube forms three anterior bulges (forebrain, midbrain, hindbrain) that produce the adult brain
- Midbrain and hindbrain give rise to the brainstem, which connects to the SC
- Most of the hindbrain is the cerebellum
- Forebrain develops into the diencephalon, which includes the neuroendocrine tissues of the brain, and the telencephalon, which becomes the cerebrum
- Rapid growth of telencephalon causes the outer portion, or cortex, of the cerebrum to extend around most of the brain

The cerebrum

- Controls skeletal muscle contraction
- Center for learning, emotion, memory, and perception
- Outer layer called cerebral cortex
 - Vital for perception, voluntary movement, learning
- Left side of cerebral cortex receives info and controls the right side of the body, vice versa
- Thick band of axons, corpus callosum, connect L and R
- Deep in white matter, clusters of neurons called basal nuclei serve as centers for planning and learning movement sequences
- Damage results in cerebral palsy, disruption in motor commands to muscles

Cerebellum

- Coordinates movement and balance
- Also learning and remembering motor skills
- Allows us to keep track of where our body is
- Monitors motor commands from the cerebrum
- Hand eye coordination

Diencephalon

- Composed of thalamus, hypothalamus, and epithalamus
- Thalamus is the main input center for sensory info going to the cerebrum
 - Formed of two masses, each the size of a walnut
- Hypothalamus constitutes the body's thermostat and central biological clock
 - Regulates pituitary gland, meaning it also regulates hunger, thirst, sexual desire, and initiates the fight or flight response
 - Source of posterior pituitary hormones and release hormones that act on the anterior pituitary
 - Thalamus includes pineal gland, the source of melatonin

Brainstem

- Consists of midbrain, pons, and medulla oblongata
- Midbrain receives and integrates sensory information and sends it to specific regions of the forebrain
 - Sensory axons in hearing either terminate or pass through the midbrain
 - Also coordinates visual reflexes
- Pons and medulla transfer info between the PNS and the midbrain and forebrain
 - Also coordinate large scale body movement, such as running
 - Axons carry info cross from one side of the CNS to the other, which is why right brain controls left body

- Medulla also controls autonomic homeostatic functions
 - Respiration, heart rate, swallowing, digestion
- Pons also controls some of these, eg. regulates breathing centers in medulla

Arousal and sleep

- We think sleep and dreams are involved in learning and consolidating memory, with sleep-deprived subjects having a reduced ability to recall when particular events occurred
- Arousal and sleep are controlled partly by the reticular formation, a diffuse network formed primarily of neurons in the midbrain and pons
 - Control the timing of sleep periods characterized by REM and nREM stages
 - Also regulated by the biological clock
- Sleep is a state where external stimuli is received but not consciously perceived

Biological clock regulation

- Cycles of sleep and wakefulness are an example of a circadian rhythm, a daily cycle of biological activity
 - Relies on a biological clock, a molecular mechanism that directs periodic gene expression and cellular activity
 - Typically synchronized to light and dark, but can maintain a roughly 24-hour cycle in the absence of environmental cues
- In mammals, circadian rhythms are regulated by clustered neurons in the hypothalamus
 - Forms a structure called the suprachiasmatic nucleus (SCN)
 - Acts as a pacemaker in response to stimuli, synchronizing the biological clock in cells throughout the body

Emotions

- Generation and experience of emotions relies on many different structures, including the amygdala, hippocampus, and thalamus
 - Borders the brainstem and are called the limbic system (limbus=border)
- Limbic system stores emotional experiences as memories that can be recalled by similar circumstances
 - Eg. recalling a frightening memory can trigger a sympathetic NS response
 - Storage and recall of emotional memory are dependent on the amygdala, found close the base of the cerebrum
- Often generating and experiencing emotion require interactions between different regions of the brain
 - Laughing and crying need both limbic system and parts of the forebrain
- Forebrain attach feelings to survival-related functions, such as aggression, feeding, and sex
- Amygdala also allows people to experience autonomic arousal

- Eg. participants were shown an image and given a shock
 - Participants shown the image without the shock still reacted with increased perspiration and heart rate
 - Exception: people with damage to amygdala did not show autonomic arousal

Neuroimaging

- First widely used imaging technique was positron emission tomography (PET), which involved the injection of radioactive glucose as a display for metabolic activity
- fMRI scans for the flow of oxygen rich blood into a particular region
- Subjects who hear sad music experience increased activities in the amygdala
- Happy music = activity increase in the nucleus accumbens, a brain structure for the perception of pleasure
- fMRI is used today to monitor recovery from a stroke, map abnormalities in the brain, and assist in brain surgery

Agonists

- A mimic or copycat for a neurotransmitter
- Produces more of or an enhanced effect for whatever that neurotransmitter does by fitting into the receptor site the same way

Antagonists

- Blocks the neurotransmitter from being released by the axon terminal or blocks the neurotransmitter from being picked up at the receptor site by entering the receptor site itself
- Produces less of or no effect for whatever the neurotransmitter does

Affecting Re-uptake

- Neurotransmitters are released into the synapse, picked up at receptor sites
 - Some neurotransmitters travel back from the synapse and into the pre-synaptic terminal and are picked back up by vesicles

Reuptake inhibitor

- Blocks nt from being absorbed back into the presynaptic axon terminal
- Produces more of the neurotransmitter at the synapse the next time the neuron fires
- The neuron will fire and release the regular amount of neurotransmitter
 - The newly fired amount and the pre-existing amount in the synapse will cause the neurotransmitter to have a greater impact
 - Net amount of neurotransmitter increases

Background Research

ADHD

Overview of ADHD

- Attention-deficit/hyperactivity disorder is one of the most common mental disorders affecting children
- Includes inattention, hyperactivity, and impulsivity
- Chronic and debilitating disorder affects individuals in areas such as academic and professional achievements, interpersonal relationships, and daily functioning (Harpin, 2005)
 - Also poor self-esteem and social function (Harpin et al. 2016)
- 8.4% of children have ADHD, 2.5% of adults
- Inattentive type
 - Challenges with staying on task, focus, and organization
- Hyperactive/impulsive type
 - Excess motion eg. fidgeting, excess energy, not sitting still, super talkative
 - Performs actions without thinking them through
- Combined type can also occur
 - No specific blood type or routine imaging involved in diagnosis
- Cause could possibly be genetic, but no specific gene combinations have been identified yet
 - Anatomical differences between children with and without ADHD exist
 - Children with ADHD have reduced gray and white brain matter volume and demonstrate different brain region activation during certain tasks (Pliszka, 2007)
 - the frontal lobes, caudate nucleus, and cerebellar vermis of the brain are affected in ADHD (Tripp & Wickens, 2009)
 - Relatives of children with adhd are frequently also affected
 - Non-genetic factors include: low birth weight, premature birth, teratogens, extreme stress during pregnancy
- Treatment
 - In preschool and younger
 - Behavioral strategies in the form of parent-management training and school intervention
 - Parent-Child Interaction Therapy (PCIT)
 - Broken down into two phases: first stage involves establishing a solid relationship between parent and child, while the second stage involves informing the parents on how to deal with challenging behaviors
 - Everyone else

- Psychostimulants (amphetamines and methylphenidates) are first line pharmaceutical treatments for ADHD
 - Only amphetamines are FDA approved for use in preschool aged children
 - Methylphenidates may be more effective than amphetamines
 - Other approved medications: Alpha agonists (clonidine and guanfacine) and the selective norepinephrine reuptake inhibitor (atomoxetine)
 - Newer approved medications: Jornay (methylphenidate extended-release) which is taken at night and starts the medication effect the next morning, Xelstrym (dextroamphetamine) which is an amphetamine patch, Qelbree (viloxazine) which is a non-stimulant, Adhansia (methylphenidate hydrochloride), Dyanavel (amphetamine extended-release oral suspension), Mydayis (mixed salts amphetamine product), and Cotempla (methylphenidate extended-release orally disintegrating tablets)
- Diagnostic test for ADHD in DSM IV includes 9 descriptions of symptoms in each of the two domains, and at least 6 symptoms must be met

Causes and Mechanisms of ADHD

- Heredity
 - Consistent strong familial genetic contribution
 - Twin studies show heritability estimates of 0.6 to 0.9
 - 0.6 indicates 60% of all the phenotypic variation for that trait is due to variation in genotypes for that trait
 - Most studied genetic variations are in the dopamine D4 receptor and dopamine transporter (DAT1)
 - Mutations exert weak effects and neither gene is necessary or sufficient for ADHD
 - Literature review from 1991 to 2004 show the four most associated genes are : the dopamine D4 and D5 receptors, and the dopamine and serotonin transporters
 - More recent literature indicates that COMT val 158/108 met variant influences conduct problems
 - COMT is an enzyme that is involved in metabolizing catecholamine neurotransmitters, including dopamine and epinephrine
 - Individual DNA variants have very small effects on ADHD (Faraone & Larsson)
 - Genome wide analysis suggest a third of ADHD heritability is due to a polygenic component, where many common variants have small effects that accumulate
 - Rare insertion and deletion mutations also account for part of

- Many genes did not show statistical significance during GWAS (previously thought to play a role)
 - p level was set to less than 0.00000005
 - FOX P2 gene regulates dopamine in ADHD-associated areas
 - DUSP6 regulates dopamine levels in the synapses

Structural differences with ADHD

- Most consistent finding: overall reduction in total brain size that continues into adolescence and reduced dimensions of specific brain regions
 - Includes caudate nucleus, prefrontal cortex white matter, corpus callosum and the cerebellar vermis
 - the caudate nucleus and globus pallidus, which both contain a high density of dopamine receptors are smaller in ADHD
- Decreased blood flow to regions in the striatum and changes in dopamine transporter binding can be found in the striatum
- Regional decrease in cortical thickness has been associated with the DRD4-7 repeat allele, which is commonly associated with the diagnosis of ADHD
 - Usually resolves during adolescence
- DT-MRI has shown difference in frontal and cerebellar white matter in children and adolescents
- fMRI results
 - Reduced activation in prefrontal and striatal regions has been shown a number of times
 - Local fMRI signals provide an indirect measure of dopamine release
 - Dopamine may postsynaptic neurons by creating action potentials in the corticostriatal synapses, which increase local fMRI signals
 - As it should occur:
 - Activation of dorsal striatum seems to occur in relation to reinforcement of an action
 - Activation of nucleus accumbens occurs in anticipation of reinforcement
 - Ventral striatal area was affected by prediction error in both classical and operant conditioning
 - Dorsal striatal was affected only by instrumental conditioning
 - Preference for immediate reinforcement is associated with magnitude of ventral striatal activity
 - In ADHD
 - Reduced activation of the ventral striatum in reward anticipation

Key differences between people with and without ADHD (Tripp & Wickens)

- Executive functions

- Defined as neurocognitive processes that maintain an appropriate problem-solving set to attain a later goal
 - Eg. to plan ahead and meet goals
- ADHD is likely not specifically associated with executive function impairments
 - Associated with weaknesses in several key domains of EF, such as inhibition, vigilance, and working memory
 - Effect size was moderate and these deficits were not specific to children with ADHD
 - Occur in children with other disorders and are not uncommon for children with no disorders
- Motivation
 - Altered response to reinforcement demonstrated in children with ADHD, and has been proposed as an underlying mechanism for particular symptoms
 - Most consistent finding is a preference for immediate over delayed reinforcement

Underlying Neural Features

- Dopamine system
 - Repetition of a positive stimulus means the time of the reward (dopamine release) transfers earlier and earlier predictors of the reward
 - If reward is silenced in some trials, dopamine cells stop firing to the point where an expected reward is not developed
 - Reward-prediction error theory of dopamine function
 - Dopamine release directly encodes the difference between expected and received reward
 - Unexpected reward is a positive prediction error because reward exceeds expectations
 - Signaled by increase of dopamine release
 - Omission of predicted reward is a negative prediction error because reward is less than expected
 - Inputs
 - NT systems that control the firing of dopamine cells not completely understood
 - VTA and pars compacta receive glutamatergic, GABAergic, cholinergic, serotonergic and noradrenergic afferent inputs
 - At least 70% are GABAergic and come from the neostriatum, external segment of the globus pallidus, and the substantia nigra pars reticulata
 - Glutamatergic come from the prefrontal cortex, subthalamic, laterodorsal tegmental and pedunculo-pontine tegmental nuclei
- Dopamine transporters
 - Free diffusion of dopamine from synaptic cleft into surrounding extracellular tissue

- This form of synaptic signaling has been called volume transmission in other systems
 - Dopamine transporter (DAT) is responsible for terminating the dopamine signal
 - DAT1 variation
 - At molecular level, DAT1 gene varies in length due to a variable number tandem repeat (polymorphism) of a 40 base pair repeat
 - VNTR is a location in DNA where a short nucleotide sequence is organized as a tandem repeat with variations in length between individuals
 - A tandem repeat is a sequence (2 or greater) of DNA bases that are repeated numerous times in a head-to-tail manner on a chromosome
 - Polymorphism is the presence of two or more variant forms of a specific DNA sequence that can occur among different individuals or populations
 - The alleles with 10 copies (10R) have been associated with ADHD
 - VNTR often occurs at noncoding sites, and affects the expression, not the properties of the transporter
 - In vitro, it was found that DAT binding site density for the 10R polymorphism was elevated 50% over that of the 9R allele
 - Depending on other conditions, increases and decreases in DAT expression levels can be found when comparing other alleles (not specific to 10R?)
 - Explains the variations in the direction (whether it increases or decreases) of changed DAT binding in humans with ADHD
 - More on the 10R allele (Brown et al.)
 - Individuals homozygous for the 10R allele showed significantly hypoactivation in the left dorsal anterior cingulate cortex (dACC) compared to 9R carriers
 - dorsal anterior cingulate cortex is a structure found in the cerebral cortex associated with executive function
 - Also hypoactivation in the left cerebellar vermis and right lateral prefrontal cortex
 - Means the dopamine transporter gene (SLC6A3) influences the attention networks found previously to be associated with ADHD
 - Genotype may contribute to the heterogeneity of brain alterations found within ADHD samples

Cellular actions of dopamine

- Physiological effects of dopamine mediated by g-coupled protein receptors
- Based on ligand binding and cAMP assays, D1 and D2

- Each have different biochemical properties and have selective agonists and antagonists
- Five dopamine receptors have been identified and classified into D1-like and D2-like groups
 - D1-like: D1, D5
 - D2-like: D2, D3, D4
- D1 and D2 receptors are more or less uniformly expressed throughout the striatum at high levels, found in lower levels in the prefrontal cortex
- Polymorphisms of D4 and D5 are associated with ADHD
- D4 is expressed at very low levels in the striatum but at moderate levels in the prefrontal cortex (found in both interneurons and pyramidal neurons)
 - Pyramidal neurons are the most populous excitatory neuron
 - D4 is expressed presynaptically in the terminals of the corticostriatal afferents (neurons going from cortices to striatum)
 - Function is unclear at present
 - Associated with the rapid translocation of the Ca²⁺/calmodulin-dependent protein kinase II (CaMKII) from the cytosol to postsynaptic sites in prefrontal cortex neurons
 - This event is important to synaptic plasticity
 - Activated by increase of intracellular calcium levels
 - Regulates many synaptic proteins by phosphorylation
 - May also control the excitability of prefrontal cortex neurons by controlling the
- D5 receptors are expressed in cortex, hippocampus, and striatum
 - Coupled to adenylyl cyclase, meaning its activation will result in increase cyclic AMP levels
 - Important for synaptic plasticity, as well as signal transduction
 - Most highly expressed in the striatum, associated with reward-related learning
 - Also involved in long term potentiation between cerebral cortex and striatum
 - LTP - process involving strengthening of synapses that leads to a long-lasting increase in signal transmission between two neurons
- Dopamine release is critical for positive reinforcement learning
 - Mechanism that underlies the learning involves synaptic plasticity that leads to strengthening of specific synapses
 - Three factor rule for synaptic modification
 - Learning mechanism requires
 - Presynaptic activity in cortical inputs to the striatum
 - Postsynaptic striatal cell activity
 - Phasic release of dopamine
- Dopamine transfer deficit theory

- In normal children, the cell response to dopamine acts as positive reinforcement and transfers to earlier cues that predict reinforcement
 - Provides immediate cellular level reinforcement when behavioral reinforcement is delayed
- In children with ADHD with ADHD, the transfer of the cell's response to dopamine fails to predict the reinforcement that will occur
 - Leads to delayed reinforcement at cellular and behavioral level
- Unclear why this occurs from a biological perspective, as defects in DAT1 or DRD4 and DRD5 would not cause such a large difference

Dopamine Reward Pathway

- (Lewis et. al)
- Mesolimbic system, or reward system, is composed of brain structures responsible for mediating the physiological and cognitive processing of rewards
 - Reward: when brain associates a stimulus with a positive outcome
 - Results in adjustment of an individual's behavior so that they search for that particular stimulus
 - Requires the coordinated release of many heterogeneous neurotransmitters
 - Dopamine plays a key role in the reward value of food, drink, sex, social interaction, and substance abuse
- Mesolimbic system primarily refers to dopaminergic pathway
 - Formed by projections of midbrain dopamine neurons of the ventral tegmental area (VTA) to the striatum, prefrontal cortex, amygdala, hippocampus, and many structures of the limbic system
 - When a reward is obtained, the dopamine neurons will release dopamine to the desired target nuclei
- Ventral striatum, which includes the nucleus accumbens (NAcc), is heavily involved in reward
- Dorsal striatum is critically involved in action selection and habitual behavior
 - Both ventral and dorsal striatum have collaborative roles in mediating reward
- NAcc is most known for its role in evaluation and incentive based learning

Medium spiny neurons (MSNs)

- Most prominent striatal neurons because they produce γ -aminobutyric acid (GABA)
- Make up 90-95% of the neuronal population and are the sole output from the striatum
- Generate two pathways
 - Direct pathway
 - Formed by dopamine D1 receptor (D1R) expressed in medium spiny neurons (dMSNs)
 - Indirect pathway

- Formed by dopamine D2 receptor (D2R) expressed in medium spiny neurons (iMSNs)
 - Coordinated dopamine signaling to dMSNs and iMSNs within the striatum helps with integrating and responding to rewards
- Other 5-10% of striatal neurons are interneurons, which regulate MSN activity
 - Majority are inhibitory GABAergic interneurons, which control reward by signaling to MSNs and expressing a variety of modulatory peptides
 - 1-2% are formed by tonically active (fire irregularly) cholinergic interneurons, which are critical in regulating MSNs despite their low abundance
 - Linked to the prominence of events

Methylphenidate

Overview

- FDA approved for treating ADHD in children and adults (Verghese & Abdijadid)
- Children should be older than 6 years before starting
- Basic mechanism
 - Blocks the reuptake of norepinephrine and dopamine in presynaptic neurons
 - By inhibiting the transporters of these NTs, it increases the concentration of dopamine and NE in the synaptic cleft, thereby increasing the effect of the NT on the next firing
 - Main effect is in the prefrontal cortex
 - Chemically derives from phenethylamine and benzylpiperazine
 - Undergoes metabolism by the liver to ritalinic acid through de-esterification via carboxylesterase CES1A1
 - Increases the firing rate of neurons
 - Weak agonist at the 5HT1A receptor, which helps contribute to higher dopamine levels
- Amphetamine (AMP) and Methylphenidates (MPH) seem to have comparable efficacy, though some studies state AMP has slightly greater effect
 - Safety profiles also comparable
 - Both drugs increase NE and dopamine (DA) in the synapse

Mechanism

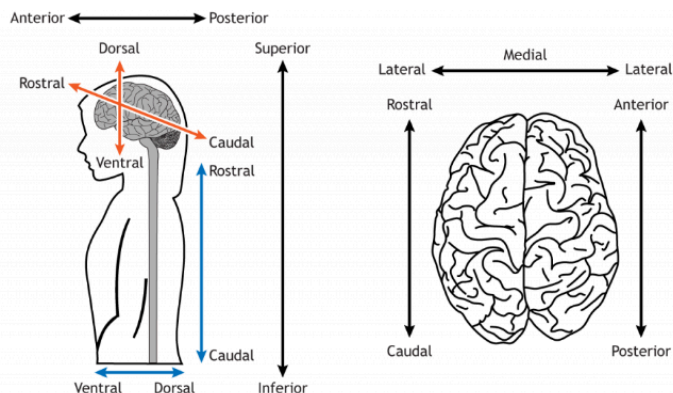
(Faraone)

- Amphetamine in Preclinical studies
 - Main mechanism is to increase synaptic extracellular DA and NE levels by acting as a reuptake inhibitor
 - AMP initially increases surface concentration of DAT and thereby DA uptake

- Continuous exposure results in decreased surface expression of DAT and lower uptake
 - Reduces binding potential of ligands for DA and NE receptors
 - Indicates increased competition for binding sites resulting from increased DA and NE
 - Increases the amount of DA released from vesicles in an action potential by inhibiting the vesicular monoamine transporter 2 (VMAT-2)
 - VMAT-2 is usually responsible for the correct packaging of DA into vesicles
 - Disrupting it results in more DA in each vesicle
 - Also promotes the the reverse transport of DA by DAT
 - DAT releases DA from inside the cell into the synapse, rather than the other way around
 - Also inhibits monoamine oxidase activity (MAO) activity, which normally breaks down monoamines such as dopamine
 - Principal area of action is in the striatum, where DAT is the highest, but also impacts the cortex and the VTA
 - Increased whole brain cerebral blood flow (CBF)
 - Caused widespread increases in blood-oxygen-level-dependent signal
- Methylphenidate in Preclinical trials
 - Direct effects include inhibition of NET and DAT, affinity for and agonist activity at 5-HT1A receptor, and redistribution of VMAT-2
 - Elevated extracellular DA and NE levels
 - 5-HT1A receptor agonists reduce the activity of serotonergic projections that inhibit dopaminergic nigrostriatal neurons, therefore increasing dopamine levels in the striatum (Bantick et. al)
 - Activates α_2 adrenergic receptors and stimulates cortical excitability'
 - Notable given two α_2 adrenergic receptor agonist drugs are indicated for ADHD treatment
- AMP in neuroimaging studies
 - DA release increased in dorsal and ventral striatum, substantia nigra, and regions of the cortex
 - Alter regional CBF to areas of the brain connected to DA activities, including the striatum, anterior cingulate cortex, prefrontal and parietal cortex, inferior orbital cortex, thalamus, cerebellum, and amygdala
 - Appear to be dose-dependent
 - Lower doses decreasing rates of blood flow in the frontal and temporal cortices and in the striatum
 - Higher does increasing blood flow to anterior cingulate cortex, caudate nucleus, putamen, and thalamus
- MPH in neuroimaging studies
 - Also increases striatal DA availability

- MPH dose-dependently blocks the NET in the thalamus and other NET-rich regions
- Increases activation of the parietal and prefrontal cortices and increases deactivation of the insula and posterior cingulate cortex during visual attention and working memory tasks
- Activation in the putamen when a response-inhibition error occurred but not when a response was successfully inhibited
 - Effects of MPH are context dependent
- Altered connectivity strength across various cortical networks, increasing activation in left and right parahippocampal regions and cerebellar regions under conditions of uncertainty
- Reduces regional CBF in the prefrontal cortex and increase CBF in the thalamus and precentral gyrus
 - MPH-associated improvements in working memory task corresponded with decreased oxy-hemoglobin levels in the right lateral prefrontal cortex, again indicating lower neural activation

Cerebellum Physiology

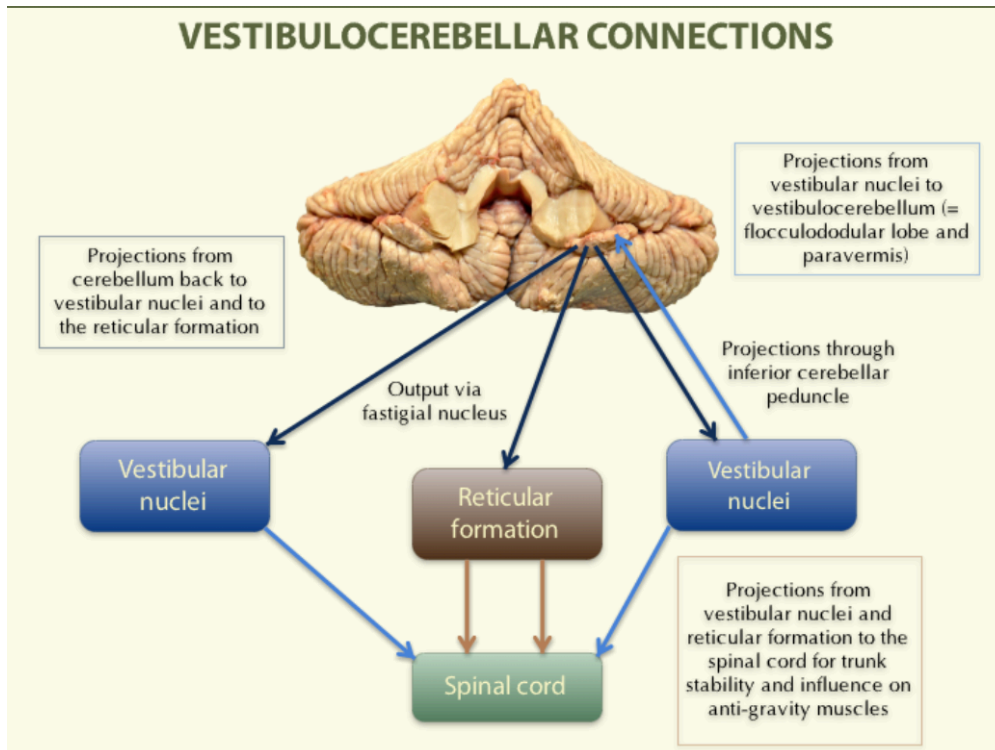


- Introduction
 - Motor movement regulation and balance control
 - Coordinates gait and maintains posture, controls muscle tone and voluntary muscle activity
 - Cannot initiate muscle contraction
 - Damage to this area = no fine movements, maintain posture, and motor learning
- Location
 - In the posterior cranial fossa
 - Behind pons and medulla oblongata
 - An extension of the dura mater, called tentorium cerebelli, separates the cerebellum from the cerebrum
 - Embryologically related to the pons
 - Connected to the brainstem by three cerebellar peduncles

- Fourth ventricle between pons and cerebellum
- Structure
 - Two hemispheres separated by the cerebellar vermis
 - Two large lobes, anterior and posterior, with a smaller lobe, the flocculonodular lobe

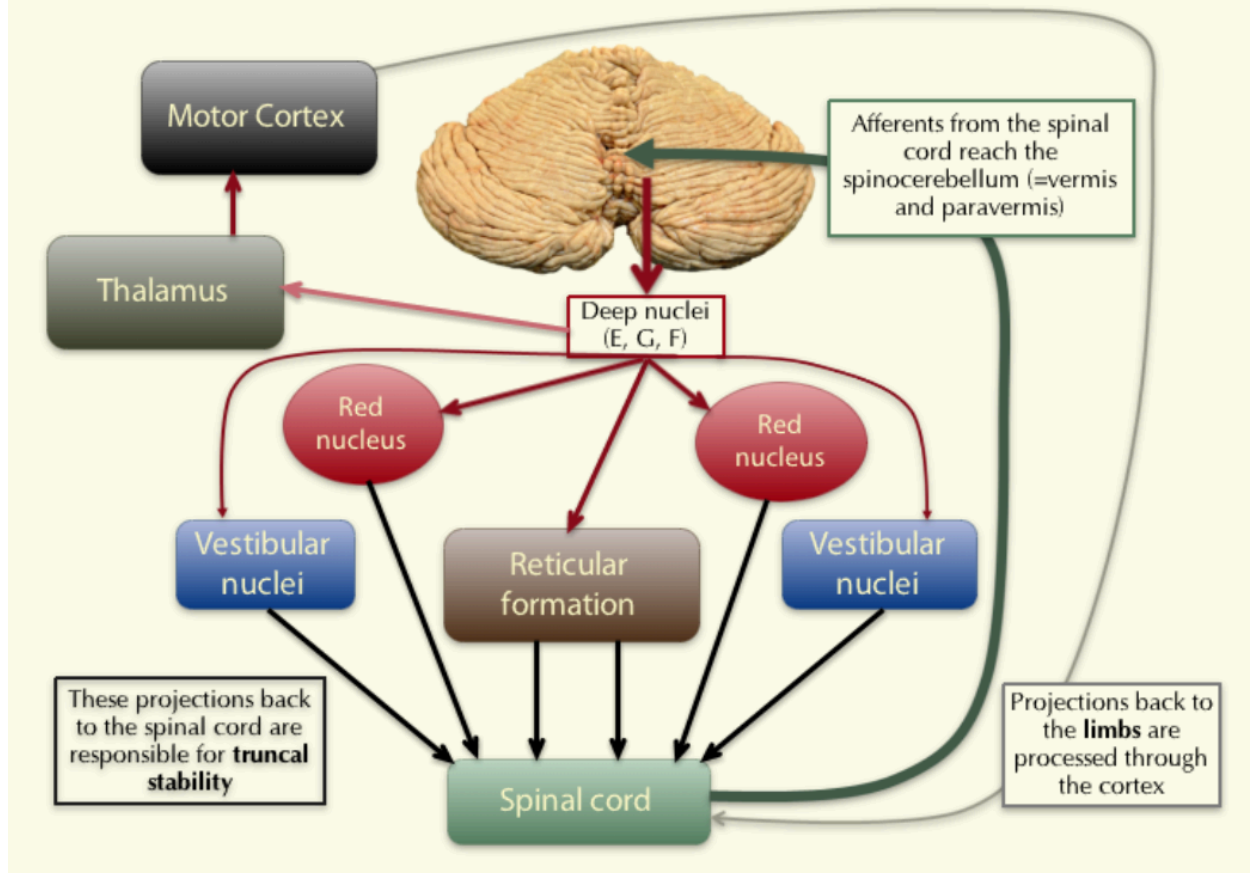
UBC Cerebellum Intro Video

- Connected with CNS
- Influences all cortical functions and output
- Receives proprioceptive information and vestibular input
- Vast connections to the cerebral cortex
- Coordinator and predictors of cortical output
- Anatomical overview
 - Tentorium cerebelli isolates the cerebellum in the posterior cranial fossa
 - Connected to the brainstem through 3 cerebellar peduncles
 - Peduncles can be found on the anterior surface
 - Superior, middle and inferior cerebellar peduncle
 - The flocculus is connected to the nodule, forming the floccular-nodular lobe, which is responsible for balance
 - From the posterior surface, you can see the vermis on the midline
 - Sits on foramen magnum, the hole in the base of the skull where the spinal cord sits
 - Increased intracranial pressure causes the cerebellar tonsils to herniate into the foramen magnum and press onto the brainstem where the breathing center is located
 - Very high surface area= millions of neurons= more than the entire CNS combined
- Balance/posture



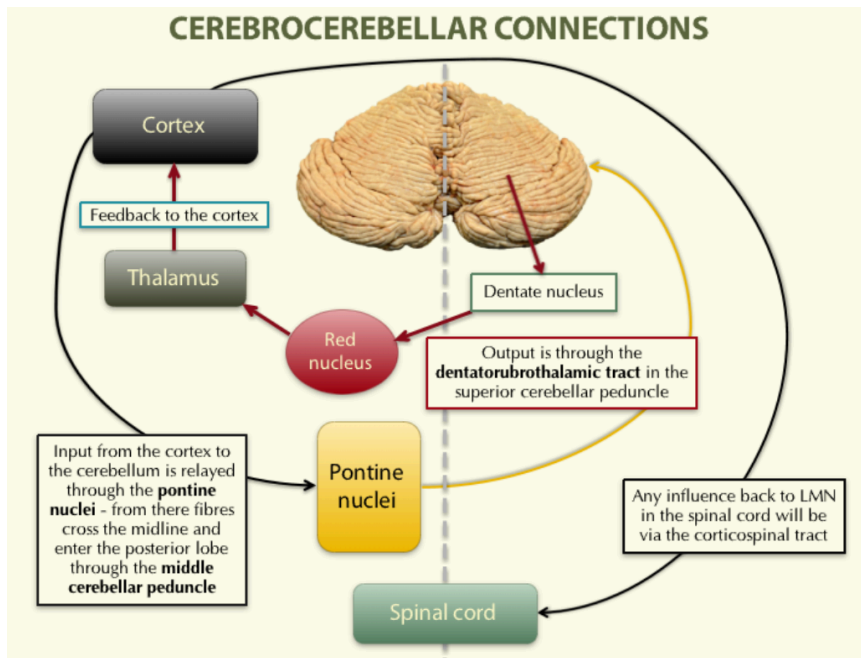
- Vestibular nuclei → Inferior cerebellar peduncle → vestibulocerebellum (flocculonodular lobe and vermis) → fastigial nucleus → vestibular nuclei → reticular formation → Spinal cord
- Oldest function taken on by the cerebellum
- Receives input from labyrinth in inner ear, balance organ
 - Influence core and limb muscles
- Anterior side of cerebellum shows the lobe for balance
 - Flocculonodular lobe
 - Flocculus and nodule
 - Closely connected to the vermis
 - Trunk musculature is coordinated through the vermis
 - Vestibular nuclei send projections to the FN lobe through the inferior cerebellar peduncle
 - In the FN lobe, the information is analyzed and sent back to the vestibular nuclei and reticular formation
 - Projections go to the lower motor neuron system in the SC to ensure truncal stability
- Limb movement and gait

SPINOCEREBELLAR CONNECTIONS



- Stimuli from spinal cord → superior cerebellar peduncle → spinocerebellum (vermis & paravermis)
- Ongoing movement is detected and coordinated
- Error detection systems allow of immediate correction of movement
- On the superior and posterior surface of the cerebellum, we can see the anterior lobe
 - Separated from the posterior lobe through the primary fissure
 - Cerebellum receives info from proprioceptors in the musculoskeletal system
 - Projects to the anterior lobe through the posterior spinocerebellar tract, which enters through the inferior cerebellar peduncle
 - Info from muscle spindles, joint receptors, golgi tendon organs
 - Gives info about the position of our limbs in space
 - Anterior spinocerebellar tract swings of the superior cerebellar peduncle and enters the anterior lobe as well
 - Originates from the spinal border cells, which send a copy of the actual motor command reaching the motor neurons
 - Cerebellum can compare motor command to the actual movement of limbs

- Rapidly corrects mistakes
- Can project directly to the lower motor neuron system
 - For limb movement, the information feeds back to the cerebral cortex through the thalamus
 - CC sends info to the lower motor neuron system in the SC
 - Connections allows for the coordination of limb movement, error detection and correction
- Fine motor skills



- Hand eye coordination
- Largest part of the cerebellum (posterior lobe) is connected to the CC
- Also allows us to have motor interaction, receives environmental cues
- Cerebellum can analyze movement patterns and predict the consequence of these movements, adjusts our movement accordingly
- Large cerebellar peduncles contain millions of connections that come from the CC
 - Cortical fibers descend to the pons, where they have synapses in the pontine nuclei
 - These fibers cross the midline and enter the contralateral side of the cerebellum in the posterior lobe
 - Info is processed and streamlined
 - Coordinated output is fed back to the CC
 - Output is sent through the dentate nucleus
 - From here, the fibers exit through the superior cerebellar peduncle and cross over to the contralateral side of the midbrain to the thalamus and cortex
- Nucleus is a cluster of neurons located deep within the cerebral hemispheres

- Peduncles are a large cluster of fiber bundles in the ventral midbrain, originating in the cerebral cortex
 - Usually connects with nuclei in the pons and terminates in the cerebellum or spinal cord
 - Dentate nucleus is the main output nucleus

Peduncle	Afferents	Efferents
Superior peduncle	Anterior spinocerebellar tract, acoustic and optic info	Dentatothalamic tract
Middle peduncle	Pontocerebellar tract	
Inferior peduncle	Vestibulocerebellar tract Posterior spinocerebellar tract	Cerebello-vestibular tract

- Vestibulocerebellar loop
 - Balance, vestibulo-ocular reflex, output to lower motor neurons for trunk stability
- Spinocerebellar loop
 - Limb movement coordination
- Cerebrocerebellar loop
 - Streamlining of cortical input
- Two major parts
 - Cerebellar deep nuclei are the sole output structures
 - Encased by a highly convoluted sheet of tissue called cerebellar cortex
 - Contains almost all the neurons in the cerebellum
- Divisions of the cerebellum
 - Two fissures run mediolaterally divide the cerebellar cortex into three primary subdivisions

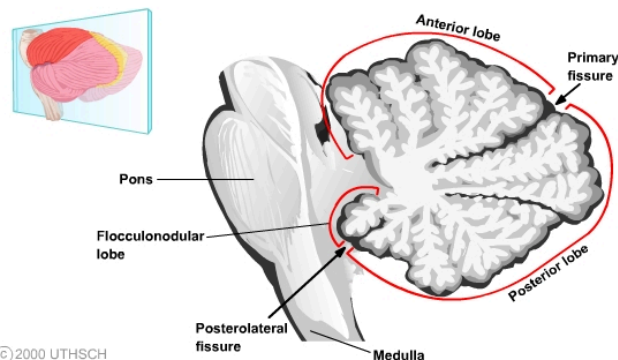


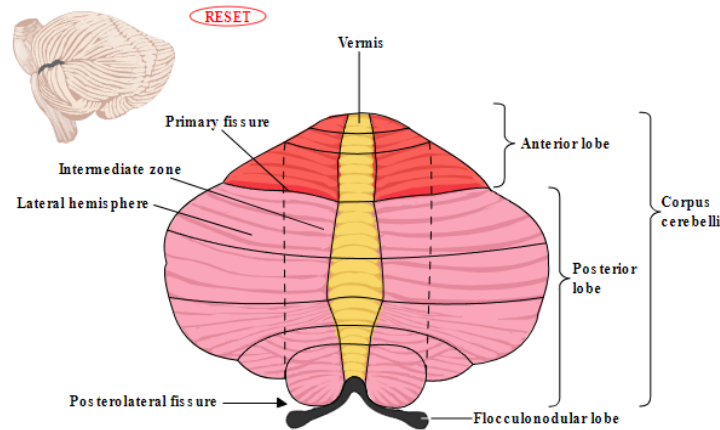
Figure 5.3
Midsagittal cross-section of cerebellum showing the three primary lobes of the cerebellum.

- © 2000 UTHSCH
 - Posterolateral fissure separates the flocculonodular lobe from the corpus cerebelli (main body)

- Primary fissure separates the anterior and posterior lobe
- Also divided sagittally into three zones

Cerebellar cortex

© 2000 UTHSCH



- Vermis is located along the midsagittal plane of the cerebellum
 - On either side of the vermis is the intermediate zone
 - Lateral hemispheres located lateral to the intermediate zone
- Cerebellar nuclei
 - All outputs from the cerebellar deep nuclei
 - Lesion to the cerebellar nuclei has the same effect as complete cerebellar lesion
 - Fastigial nucleus
 - Most medially located of cerebellar nuclei
 - Receives input from the vermis
 - Cerebellar afferents carry vestibular, proximal somatosensory, auditory, and visual information
 - Projects information to vestibular nuclei and reticular formation
 - Assists in spinocerebellum pathway
 - Interposed nuclei
 - Comprised of the emboliform nucleus and globose nucleus
 - Situated lateral to the fastigial nucleus
 - Receive input from the intermediate zone
 - Cerebellar afferents contain spinal, proximal somatosensory, auditory, and visual information
 - Project to the contralateral red nucleus (origin of the rubrospinal tract)
 - Assists in spinocerebellum pathways
 - Dentate nucleus
 - Located lateral to the interposed nuclei
 - Receives input from the lateral hemisphere
 - Cerebellar afferents carry information from the cerebral cortex (via pontine nucleus)
 - Projects to the contralateral red nucleus and ventrolateral thalamic nucleus

- Cerebrocerebellum pathways
 - Vestibular nuclei
 - Located outside the cerebellum in the medulla
 - Considered to be functionally equivalent to the cerebellar nuclei due to similar connectivity patterns
 - Input from the flocculonodular lobe and vestibular labyrinth
 - Project to motor nuclei and originate the the vestibulospinal tracts
 - Vestibulocerebellum pathways
 - All cerebellar nuclei and regions of the cerebellum get special inputs from the inferior olive of the medulla
- Cerebellar peduncles
 - Inferior cerebellar peduncle
 - Also called restiform body
 - Afferent fibers from medulla
 - Efferents to the vestibular nuclei
 - Middle cerebellar peduncle
 - Also called brachium pontis
 - Afferents from the pontine nucleus
 - Superior cerebellar peduncle
 - Also called brachium conjunctivum
 - Efferent fibers to cerebellar nuclei
 - Afferents from spinocerebellar tract
 - Inputs to the cerebellum are conveyed primarily through inferior and and middle peduncles
 - Outputs conveyed primarily through the superior peduncle
 - Inputs arise from the ipsilateral side of the body and outputs also go to the ipsilateral side of the body
 - Ipsilateral control
 - Even when outputs go to the contralateral red nucleus, they are double crossed back to the ipsilateral side due to the rubrospinal tract
- Functional subdivisions of the cerebellum
 - Vestibulocerebellum
 - Comprises the flocculonodular lobe and its connections with the lateral vestibular nuclei
 - Involved in vestibular reflexes and maintaining posture
 - Spinocerebellum
 - Comprises the vermis and the intermediate zones of the cerebellum, as well as the fastigial and interposed nuclei
 - Receives major inputs from the spinocerebellar tract
 - Output to the rubrospinal, vestibulospinal, and reticulospinal tracts
 - Involved in the integration of sensory input with motor commands to produce adaptive motor responses

- Cerebrocerebellum
 - Largest functional subdivision
 - Comprised of the lateral hemispheres and the dentate nucleus
 - Extensively connected to the cerebrum
 - Afferents pontine nucleus, efferents ventrolateral thalamic nucleus
 - Cognitive functions of the cerebellum

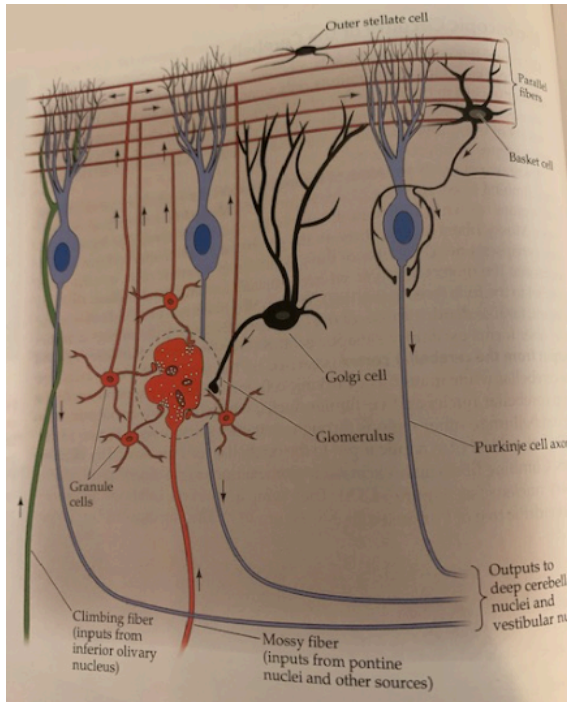
Neuroanatomy Through Clinical cases

Anatomy

- No direct connections to lower motor neurons, but instead exerts influence through connections with motor cortex and brainstem
- Largest structure in posterior fossa
- Attached to dorsal pons and rostral medulla by peduncles (feet)
- Consists of
 - Midline vermis, named for wormlike appearance
 - Two large cerebellar hemispheres
- Primary fissure separates the cerebellum into anterior and posterior lobules
- Visible from the ventral side, the posterolateral fissure separates the posterior lobe from the FN lobe
 - Two flocculi connected to the nodulus by thin pedicles
 - Nodulus is most inferior structure
- Another inferior structure is the cerebellar tonsils
 - Elevated intracranial pressure can cause tonsils to swell
- Grey and white matter is in branching patterns, sometimes referred to as arbor vitae
 - Folia, meaning leaves, refer to the ridges that run from medial to lateral
- Removing the cerebellum from the brainstem (dorsal view of cerebellum) reveals the three cerebellar peduncles (superior, middle, inferior), forms the walls of the fourth ventricle
 - Superior carries output, decussates (crosses over) in the midbrain
 - Also known as brachium conjunctivum, because striking conjunction of fibers in decussation
 - Middle and inferior mainly carries inputs
 - Middle peduncle very connected to the pons, aka brachium pontis
 - Inferior peduncle, aka restiform body, aka ropelike body
- Three functional regions
 - Vermis and flocculonodular lobes
 - Respectively important in proximal and trunk muscle control and in vestibulo-ocular control
 - Proximal muscles are those closest to the core, including including the upper legs, hips, upper arms, shoulders
 - Distal muscles are those further away from the core, including the muscles of the lower arms and legs and the hands and feet

- Trunk muscles include those that move the vertebral column, the muscles that form the thoracic and abdominal walls, and those that cover the pelvic outlet
 - Regulates balance and eye movements through interactions with the vestibular circuitry
 - Intermediate part of the cerebellar hemisphere involved in control of distal appendicular muscles in arms and legs
 - Lateral part of the cerebellar hemisphere
 - Largest
 - Involved in planning the motor program for extremities
 - Large portion can be removed unilaterally without significant impacts
 - Cerebellar nuclei
 - All outputs from cerebellum are relayed by these nuclei
 - Also receive collateral fibers (axon side branches) of cerebellar inputs on path to cerebellar cortex
 - Deep cerebellar nuclei from lateral to medial: dentate, emboliform, globose, fastigial
 - Don't eat greasy foods
 - Dentate nuclei
 - Largest
 - Receive projections from lateral cerebellar hemispheres
 - Active just before movement
 - Interposed
 - Emboliform and globose nuclei
 - Input from intermediate parts
 - Active during movement
 - Fastigial receive input from the vermis, smaller input for FN lobe
 - Most fibers leaving the inferior vermis and FN lobe project to the vestibular nuclei (located in brainstem but act similarly to deep cerebellar nuclei)

Circuitry



- Cerebellar cortex has three layers
- Granule cell layer tightly packed with small granule cells (so numerous) they rival total number of cells in rest of NS
- Purkinje layer cell bodies of large flask shaped purkinje cells
- Molecular layer contains
 - Unmyelinated axons of granule cells
 - Dendrites of purkinje cells
 - Several types of interneurons
- Two types of synaptic inputs to the cerebellum, mossy fibers and climbing fibers
 - Mossy fibers ascend through cerebellar white matter to form excitatory synapses with dendrites of granule cells
 - Arise from various regions
 - Granule cells send axons into the molecular layer, which split into two (bifurcate), forming parallel fibers that run perpendicular to the dendrites of the purkinje cells
 - These fibers form many ex synapses with the purkinje cells they pass
- All outputs from cerebellar cortex carried by axons of purkinje fibers into the cerebellar white matter
 - Purkinje cells form inhibitory synapses with deep cerebellar and vestibular nuclei, which convey information from the cerebellum to other regions through excitatory synapses
 - In other words regulates information exiting so as to avoid overstimulation
- Other kind of input to cerebellum is climbing fibers

- Arise exclusively from neurons in the contralateral inferior olivary nucleus
 - contralateral inferior olivary nucleus in the brainstem, regulates spinal cord signals to the cerebellum
- Wrap around cell body and proximal dendritic tree of purkinje fibers, forming excitatory synapses
- Single fiber can branch to support 10 purkinje cells
 - However each cell is excited by just one fiber
- Strong modulatory effect on purkinje, can cause significant decline in response to parallel fiber stimulation
- Inhibitory interneurons
 - Basket cells and stellate cells located in molecular layer
 - Excited by synaptic input from granule cell parallel fibers
 - Signals then travel in the rostral-caudal direction, perpendicular to the parallel fibers, where they cause inhibition of adjacent purkinje cells
 - Stellate cells terminate on purkinje cell dendrites
 - Basket cells form on purkinje cell bodies
 - Named for strong inhibitory basket-like connections
- Golgi cells found at granule cell layer
 - Receive excitatory signals from the parallel fibers, provide feedback inhibition on granule cell dendrites
 - Tends to shorten the duration of granule excitatory inputs to granule cells
 - Result of golgi cell's inhibitory property is regulation of the temporal domain of signals, leading to enhanced signal resolution
 - Result of stellate and basket cell inhibitory property is regulation of the spatial domain of signals, also leading to enhanced signal resolution
- Complex synaptic interaction occur in the granule cell layer in a specialized region called the cerebellar glomerulus
 - Glomeruli are visible as small clearings among the granule cells
 - Contains axons and dendrites contained in a glial sheath
 - Two types of inputs (large mossy fiber axon terminals and golgi cell axon terminals), which form synapses onto one type of postsynaptic cell (granule cell dendrites), which in turn excite inhibitory purkinje cells
 - Mossy fibers → granule cell dendrites → excites purkinje cells

Name	Acts on	Effect	Originates
Mossy Fibers	Granule cells	Excitatory	White matter
Granule cells	Purkinje as parallel fibers in molecular layer	Excitatory (on purkinje cells)	Granule layer

Purkinje cells	Deep Cerebellar and Vestibular Nuclei	Inhibitory	Dendrites in molecular layer
Climbing fibers	Molecular layer (purkinje dendrites)	Inhibitory	contralateral inferior olivary nucleus
Basket & Stellate Cells	Purkinje fibers (cell body and dendrites respectively)	Inhibitory	Molecular layer Result = enhanced signal transmission on spatial plane
Golgi cells	Granule cell dendrites	Inhibitory	Granule layer Result = increased signal transmission on temporal plane
Cerebellar glomerulus	n/a	Site of where mossy fiber, granule cell, purkinje cell interactions take place	n/a

Cerebellar output pathways

- Medial lesions = deficits in trunk and proximal, lateral lesions = deficits in distal
- Cerebellum is ipsilateral, not contralateral control because it is double crossed
 - First cross is when superior peduncle decussates, 2nd cross occurs as rubrospinal and corticospinal tracts descend to the spinal cord
- Input to cerebellum is also ipsilateral for the same reason (right side controls right side)
- Lesions to vermis do not cause unilateral deficits as medial motor systems influence trunk muscles bilaterally
- Lateral cerebellar hemisphere projects to dentate nucleus, which in turn projects to the superior peduncle
 - Then decussates in the midbrain, and reaches its contralateral (compared to source) ventral lateral nucleus (VL) of the thalamus
 - Fibers entering thalamus are called the thalamic fasciculus
 - Most anterior parts of the thalamic fasciculus also include projections from the basal ganglia
 - Outputs from basal ganglia terminate in anterior VL, while cerebellar outputs terminate in the posterior VL
 - VL in turn projects to motor cortex and premotor cortex, supplementary motor area, and parietal lobe to influence motor planning in the corticospinal systems
 - Some evidence indicates that outputs from lateral cerebellum are also projected to the prefrontal association cortex, suggesting a role in cognitive function

- Some fibers from the dentate nucleus also terminate in the parvocellular division of the red nucleus
 - In the midbrain
 - Parvocellular division involved in cerebellar circuitry
 - Smaller caudal magnocellular division gives rise to the rubrospinal tract
 - Rubrospinal tract projects information to spinal cord, stimulates flexor muscles
 - The projects to the inferior olive (related to climbing fibers?)
- Intermediate hemisphere controls distal limb movement and projects to interposed (emboliform and globose nuclei)
 - Interposed nuclei project to superior peduncle which projects to the contralateral VL, which projects to motor cortex and premotor cortex, supplementary motor area to influence the lateral corticospinal tract
 - Inputs do not overlap with the dentate or basal ganglia to the VL
 - May also project to contralateral magnocellular division of red nucleus, influences rubrospinal tract
 - Thus influences lateral movement
- Cerebellar vermis and flocculonodular lobes influence proximal trunk muscles through connections to medial motor pathways (anterior corticospinal, reticulospinal, vestibulospinal, tectospinal tracts)
 - Vermis projects to fastigial nucleus
 - Outputs from fastigial nucleus are to a small extent carried by superior peduncle, but mainly carried by fiber pathways called the uncinate fasciculus and juxtarestiform body
 - Run along the superior and inferior peduncles respectively
 - Juxtarestiform body (next to restiform body, or inferior peduncle) lies on the lateral wall of the fourth ventricle, just medial to the inferior peduncle
 - Carries fibers in both directions between cerebellum and vestibular nuclei
 - Uncinate fasciculus (hook bundle) loops over sup peduncle and sends fibers to the contralateral vestibular nuclei via the contralateral juxtarestiform body

● Vermis output pathways

Carried by	Reach	Influence
Fastigial nucleus → Superior peduncle (contralateral)	Thalamic VL → motor cortex	1. Anterior corticospinal tract 2. Tectal area
Juxtarestiform body (ipsilateral)	Reticular formation and vestibular nuclei	Reticulospinal and vestibulospinal tracts

- Flocculonodular lobes and vermis sometimes referred to as vestibulocerebellum because they project mainly to vestibular nuclei
 - Reciprocal connections between cereb and vestibular nuclei are important for

equilibrium and balance

- Signals from vestibular nuclei are relayed by the medial longitudinal fasciculus and other eye movement pathways
 - Influence vestibulo-ocular reflexes

Cerebellar input pathways

- Fasciculus: small bundle of nerve, muscle, or tendon fibers
- Inputs reach cerebellum from
 - Virtually all regions of cerebral cortex
 - Multiple sensory modalities, eg. vestibular, visual, auditory, somatosensory
 - Brainstem nuclei
 - Spinal cord
- Has a rough somatotopic organization, with the rough ipsilateral body being represented in both anterior and posterior lobes
- Review: all inputs come from mossy fibers or from climbing fibers (which in turn come from the inferior olivary nucleus)
 - Most inputs give rise to collateral branches that synapse with deep cerebellar nuclei
- Corticopontine fibers
 - Major input from frontal, temporal, parietal, and occipital lobes
 - Travel in internal capsule and cerebellar peduncles
 - Sensory, motor, and visual cortices are largest contributors to the corticopontine fibers
 - Fibers travel to the ipsilateral pons and synapse in the pontine nuclei
 - Pontocerebellar fibers then cross the midline to enter the contralateral middle cerebellar peduncle and give rise to mossy fibers
- Another major input is spinocerebellar fibers
 - Travel in four tracts
 - Dorsal and ventral spinocerebellar tracts for lower extremities
 - Cuneocerebellar and rostral spinocerebellar tracts for upper extremities and neck
 - Provides two kinds of feedback information
 - Afferent information about limb movement conveyed to cerebellum by dorsal spinocerebellar tract for lower extremities and by cuneocerebellar tract for upper extremity
 - Information about spinal cord interneurons, reflecting the amount of activity in descending pathways, is carried by ventral spinocerebellar for lower and rostral spinocerebellar for upper
- Dorsal spinocerebellar tract ascends in the dorsolateral funiculus, near surface of spinal cord, lateral to the corticospinal tract
 - Myelinated axons of sensory neurons carrying proprioceptive, touch, and pressure sensation from lower extremities ascend the gracile fasciculus

- Via juxtarestiform (remember it is both input and output)
- Connections between vestibular system and cerebellum important in balance and equilibrium, as well as optical reflexes
- Flocculus also receives visual inputs related to retinal slip (disparity between target and perceived images) that are important for smooth pursuit eye movement
- Noradrenergic inputs from locus coeruleus and serotonergic inputs from the raphe nuclei project diffusely through the cereb cortex, but are not conveyed by mossy or climbing fibers
 - Thought to play a neuromodulatory effect

Blood supply to the brain

- Blood is provided by three branches of the vertebral and basilar arteries
 - Posterior inferior cerebellar artery (PICA)
 - Anterior inferior cerebral artery (AICA)
 - Superior cerebellar artery (SCA)
- PICA arises from the vertebral artery
- AICA from the lower basilar artery
- SCA from top of the basilar artery
- PICA supplies medulla, most of the inferior portion of cereb, and inferior vermis
- AICA supplies inferior lateral pons, middle cereb peduncle, and a strip of the cereb between the PICA and SCA, including the flocculus
- SCA supplies upper lateral pons, sup peduncle, most of the superior half of the cerebellar, and superior vermis

MRI Physics

MRI Physics - JHU Video

- Macromolecules in body have hydrogen protons, as does water
- Polarity of hydrogen atom allows it to act like bar magnet
- Arrangement of protons is usually random, but can be influenced by an external magnetic field
- MRI generates its own magnetic field, referred to as B_0
 - In the magnetic field, protons in the body will line up as either parallel or antiparallel to the field
 - Small majority of protons are parallel
 - Generates the net magnetization factor along the z axis (long axis of patient's body)
- Protons in the body are also spinning along their axes like tops
 - Movement known as precession, or nuclear spin
 - Frequency of precession depends on the magnetic field, and can be expressed by the Larmor Equation
 - $\omega = \gamma \times \Delta B_0$
 - ω is the angular Larmor frequency

- γ is the gyromagnetic ratio
 - A constant unique to each specific nucleus or element
 - B_0 is the strength of the magnetic field in Tesla (T)
 - Applies to all protons because all protons have same mass
- Protons in the magnetic field are aligned, but this alignment can be disrupted by a radiofrequency (RF) pulse
 - When this happens, the protons are knocked down into an alternate plane
 - Also precess together in phase
 - Angle depends on strength and duration of RF pulse
- Knocking protons down to another plane is a change in their longitudinal magnetization (up down)
- Normally the protons follow the magnetic field
 - With excitation (extra energy in the form of an RF pulse), protons have the ability to go against the current and orient themselves in the opposite direction
 - Will precess together, which can be thought of as the transverse magnetization of the protons
 - Does not last for long, and will soon release the extra energy as the baseline state of disorder is restored
- Protons will return to a state of orientation with the magnetic field and asynchronous procession
- Spin echo sequence
 - At the beginning of a sequence, a 90 degree RF pulse is applied
 - The net magnetization vector becomes perpendicular to its original orientation
 - Achieved by eliminating longitudinal magnetization and generating a transverse magnetization vector by synchronizing proton precession
 - During recovery, the longitudinal magnetization increases, and the transverse magnetization decreases
 - The protons dephase
 - Looks like the spiraling of the net magnetic vector along the z axis
 - This induces an electrical signal by a process called free induction decay
 - Current can be induced by rotating a magnetic field
 - As the proton returns to its alpha state, energy is released
 - The point at which 63% of the longitudinal magnetization has been recovered is called T1
 - The time at which 63% of the transverse magnetization has been lost is called T2
 - T1 and T2 is unique to each tissue type
 - Analogous to a group of runners in a race, each will recover to their baseline at a different rate

- MRI can take advantage of T1 and T2 by altering the sequences to highlight them
- Drawbacks
 - Free induction decay
 - Only applies to 90 degree pulses
 - Signal decays very rapidly
 - Dephasing of protons occurs at a speed known as the T2* constant
 - This is an exponential decay of proton synchronization of spins
 - Due to the fact that each proton experiences the magnetic field at a slightly different strength, meaning there is never true synchronization of precession
 - Differences in precession end up compiling, leading to increasingly asynchronous spins
 - Any inhomogeneity in the magnetic field makes de-phasing and signal drop out even worse
 - Shows up as black holes on MRI scans, and are known as T2* effects
 - T2* effects can be combated with the addition of another rf pulse
 - A 180 degree refocusing RF pulse can be applied to instruct all the protons to turn around and process in the opposite direction
 - Even if one proton is moving significantly faster, forcing them to change direction in precession will send both protons back into sync
 - Tortoise and hare; if the hare is much ahead and is forced to turn back to the start, the tortoise and hare will reach the start at the same time
 - When the protons go back in sync, more energy can be released
- Summary
 - Protons are aligned with the magnetic field with asynchronous precession
 - 90 degree RF pulse applied, eliminating longitudinal magnetization and producing a transverse magnetization vector
 - Protons start precessing in phase
 - Longitudinal recovery and transverse decay occurs
 - Produces a signal by a free induction decay (echo), which is susceptible to T2* effects
 - 180 degree RF pulse temporarily rephases proton precession
 - Produces an echo, which can be read out by the MR scanner
 - Multiple refocusing pulses can be applied, though the echoes become successively weaker until the echo dies out completely and the sequence must be restarted

More In Depth

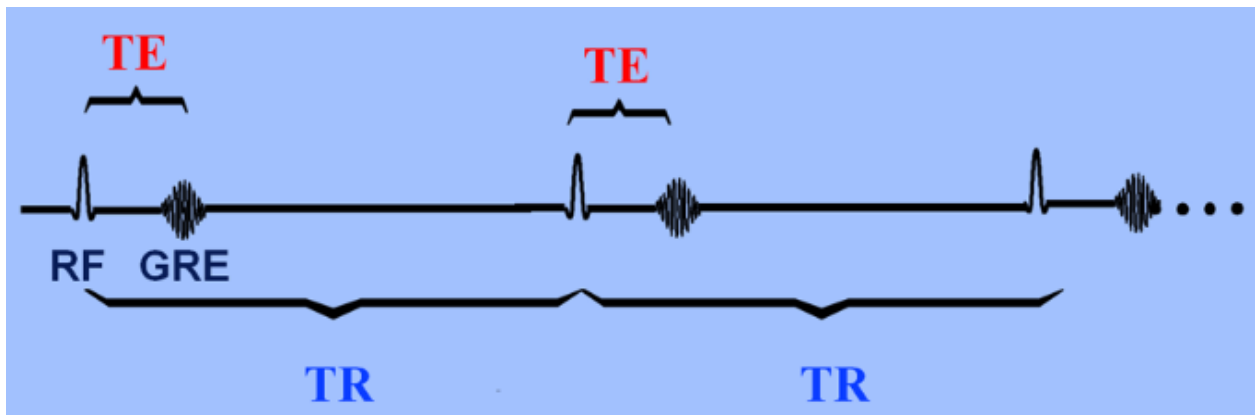
- Purpose
 - Provides images of body tissues and their chemical compositions with exceptional clarity and little risk to patient
 - Uses magnetic fields and emits waves with freq in radio wave region
 - Particularly used in cases where x ray may be harmful

- Originally known as nuclear magnetic resonance imaging because it is a form of nuclear magnetic resonance spectroscopy
- Nuclear magnetic resonance
 - Resonance refers to equivalent frequencies
 - When a magnetized species exists, it can absorb the energy from a magnetic field of equal strength
 - NMR exploits the fact different protons placed in a uniform magnetic field will feel slightly different levels of magnetism based on their location relative to the source
 - Phenomenon known as shielding
 - Some protons feel less of the applied magnetic field because they are in an environment rich with electrons, and their attraction to electrons override the applied magnetic field
 - Same also true for protons in electron deficient areas
 - Varying strength of magnetic field can reveal structural information
 - Absorption frequency is equal to the frequency experienced by the species
 - Absorption of low frequency suggest heavily shielded species
 - Absorption of high frequency suggest lightly shielded species
 - NMR often calculated in relation to a specific compound
 - Tetramethylsilane (TMS) often used as a reference
 - Highly shielded and the frequency of radiation it absorbs is often set to 0 on NMR instruments
 - Since frequency absorbed is proportional to the applied field, the shift or difference between the two values is recorded, and not the exact frequency
 - Protons in close proximity to electron donating groups (generally higher concentration of electrons) will be more shielded and vice versa
 - NMR can also indicate tendency of electrons in an area
 - Result is a spectrograph, displaying data from high fields to low fields
- Atomic structure
 - Nucleus has a net positive charge
 - Each proton and neutron in the nucleus has its own spin
 - Net net of these spins is represented by spin number, I
 - I describes the angular momentum of the spinning charge
 - If mass or atomic number is odd, I has a non-zero value
 - If mass number and atomic number are both even, then the spin of the neutrons and protons will cancel out, resulting in zero net spin
 - Nucleus must possess overall spin to respond to NMR
 - Species must have non-zero I value as well as a magnetic field for NMR to work
 - H-1 and C-13 both meet these criteria, but C-12 and O-16 do not
 - H-1 found in macromolecules all over the body

- As a result, NMR can be used for imaging of human bodies
 - The allowed spins for a given value is represented by $2I+1$
 - When $I=0$, there is only one spin state
 - NMR requires more than one possible spin state
 - Frequency to cause a change in the spin state or to cause a flip is what is detected by NMR
 - H-1 has $I=1/2$, meaning it has two possible spin states
 - When placed in an applied magnetic field, they will absorb the magnetic radiation when the freq of that radiation is = to that required cause the nucleus to flip to its other spin state
- Magnetization
 - Charged particles such as nuclei exhibit electric fields, which includes magnetic fields
 - Atomic particles possess magnetic moments
 - I values >1 means that the magnetic moments can take on more than one orientation
 - In the absence of external forces, these varying spin states are of equal energy (degenerate)
 - Systems tend towards low energy to maximize stability
 - Spin state of the particles is random without external force as each state is degenerate with each other
 - When atomic nuclei are exposed to a magnetic field they will tend to orient themselves with the field to maximize stability and minimize energy use
 - Lower energy means N aligns to N
 - When the magnetic field is applied, many of the protons (which are not aligned with magnetic field) will want to flip orientation from high energy to low energy
 - Due to the law of conservation of energy, when these protons flip from high energy to low energy, energy must be released
 - Change in energy will be equal to the energy difference between high and low states
 - Random flipping is therefore unlikely (energy input is needed)
 - Only occurs with random collisions between particles
 - If a far-from equilibrium magnetic field is applied, most collisions result in protons flipping from high to low energy states
 - Results in build up of low energy configurations
 - If high energy proton is surrounded by a large number of low-energy protons, the effect of the magnetic field on the remaining high energy protons is diminished by their surroundings, and thus will not flip from high to low energy
 - Not all protons will flip to low energy state
 - Longitudinal magnetization is the net excess magnetization
 - System's approach to equilibrium is logarithmic

- Initially quick but slows as it reaches equilibrium
 - Process is called magnetic recovery
 - Time it take to achieve magnetic recovery is dependent on its T1 value and the strength of the magnetic field
 - T1 value is dependent on the material's characteristics and calculated as the time to reach 63% longitudinal magnetization
 - If a second magnetic field is applied perpendicular to the original magnetic field, and the second magnetic field rotates around the Z axis at the same rate as the protons precess about their z axis, the protons will feel as if the orientation of the second magnetic field is constant
 - Protons will still precess around the perpendicular magnetic field as well, the degree to which the protons do is determined by the strength of magnetic field
 - As a result, when B1 (second magnetic field) is applied, the cone of magnetization is flipped and rotated
 - Longer the B1 is left on for and the stronger it is, the faster the protons will rotate
 - Also will cause the protons to rotate so it spins on the xy axis rather than the z axis
 - Returns protons to a state where equal high energy and low energy protons
 - When B1 is removed, the protons will return to their lower energy configuration oriented along the z axis
 - Return, or relax, to their magnetized state
 - MRI measures this relaxation
- T1
 - Applied magnetic field B1 that causes the flipping is in the radiofrequency range, known as RF pulses
 - Two types of relevant water types in the human body
 - Free water is that which has a high degree of freedom of motion such as urine and CSF
 - Bound water is water that has much less freedom of movement
 - Water found in brain, liver, cells,
 - Since MR signals are those created when precessing protons that have been exposed to an RF pulse relaxes, these MR signals require energy to be exchanged as the protons move from high to low energy (spin lattice relaxation)
 - Different molecules have different T1 values, and the T1 value depends on how tightly bound the H is bound to molecules
 - Water has longer T1 relaxation time, and thus appears as dark on a T1 weighted image
 - Fat has a short T1 value and appears as bright spots
- T2

- Transverse magnetization starts to disappear and the protons fall out of the xy axis alignment
- T2 is the time it takes for only 37% of the transverse magnetization vector to remain
- Many causes for loss of coherence in protons, including spin-spin interaction, magnetic field inhomogeneity, Magnetic susceptibility, and chemical shift artifact
 - T2* effects
 - Inhomogeneity in tissue causes proton's spin to be influenced by small magnetic fields created by the spin from a nearby proton - result is longer t2
 - T2 decay is a characteristic specific to each tissue
 - Molecules in free water have far apart molecules, meaning longer T2 time
 - Tissues are closer together, meaning shorter T2
- While transverse to longitudinal is happening, spins within the B1 are decaying from their aligned precession
 - T2 captures captures the differences in decay, which is useful given different tissues have different decay times
-
- T1 and T2 weighting



- Time to echo TE is the difference between the peak of the 90 degree RF pulse and the peak of the echo formed
- TR is time to run a pulse sequence at one time
- TE and TR control weighting effects in an MR image
- Images created predominantly using differences between T1 times is known as a T1-weighted image
 - Fat relaxes a lot faster than water
 - A short TR ensure that not all tissues have the chance to return to full relaxation, meaning the tissues that have returned to this point will have released more energy than the ones who haven't (released a greater echo)

- Fat releases more energy in the TR time than water, which is why it appear brighter on T1 weighted images
 - If TR time is too long, the image will be uniform and useless
- When T1 effects are minimized by having a long TE and TR, T2 weighted images are produced
- More information below, see scanned document

MRI intro

Flair T2

- CSF is no longer white

T2

- Shows axial view - CSF glows
- White matter shows as black
- grey = grey
- lower res than T1

T1 structural

- structure
- high res
- used by surgeons for volume coils

- most studies have both T1 and T2

fMRI

- BOLD signal - how oxygenated brain hemoglobin is
 - more deoxy hemoglobin
 - high activity = high BOLD
 - Network = build signal varies in a task dependent method
- clinically - used in epilepsy ~~brain~~ presurgery to identify language center

- 3 Tesla static magnetic field

- molecules become parallel or antiparallel to the field
- based on Heisenberg
- Apply magnetic, causing the molecules to fall out of formation
- when they come back together, they release an electrical impulse

Diffusing scanning

- diffusivity is different in different structure
- shows different tracts - allows mapping networks
- Areas of restricted diffusion can be identified for certain disorders

- FMRI
 - Based on BOLD, blood oxygenation level dependent, effect
 - Exploits the fact deoxyhemoglobin creates magnetic field gradients that decrease MR signal
 - Brain activation characterized by drop in OEF
 - local oxygen extraction fraction
 - The relative difference in oxygen concentration between arterial (Y_a) and venous (Y_v) blood
 - Decrease in OEF = decrease in deoxyhemoglobin, which means higher brain activity

Analysis Programs

- FSL
 - Stands for FMRIB Software Library
 - Library of analysis tools for FMRI, MRI and diffusion brain imaging data
 - BET - brain extraction tool
 - Segments brain from non-brain in structural and functional data
 - FAST - FMRIB's Automated Segmentation Tool
 - Brain segmentation by tissue type
 - FLIRT - FMRIB's Linear Image Registration Tool
 - linear inter- and intra-modal registration
 - will translate, rotate, zoom and shear one image to match it with another
 - FNIRT
 - Register different brains to each other

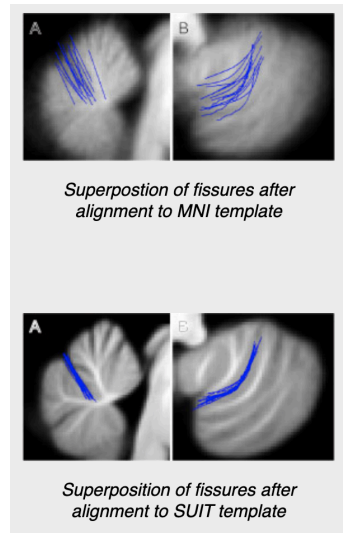
Voxel-based morphometry

- Statistical mapping parameter (SPM) approach to analysis of functional neuroimaging data (eg. PET or fMRI) has been adapted to other neuroimaging modalities, including the analysis of structural changes
- Voxel-based morphometry can be used to investigate local changes in tissue volume
- Pathology that affects the intensity of tissue (but not volume) may alter the segmentation tissue, a limitation
- Input to the statistical analysis stage of VBM is the result of segmentation of a particular tissue class, such as gray matter
 - Probability of a voxel containing gray matter is determined by intensity and the location of said voxel in the brain
 - Referenced with existing atlases
- Can lead to misclassification of voxels which can lead to an erroneous volume change value for the affected parts of the brain

SUIT

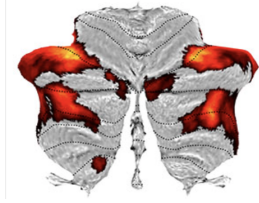
- MATLAB toolbox dedicated to the analysis of human cerebellum
- Contains high resolution atlas of human cerebellum and brainstem

- Allows you to
 - Automatically isolate cerebellar structures from the cerebrum in an anatomical image
 - Achieve accurate normalization of the cerebellum into the atlas space using the dartel algorithm
 - Display data on a surface-based flatmap representation
 - Use VBM to determine patterns of growth or shrinkage
 - Uses atlas to assign probable locations to the different cerebellar lobules and nuclei
- Most commonly used atlas template for brain imaging is the ICBM152 template
 - Defines the MNI space
 - Template created by averaging 152 brains after affine normalization (corrections to size, translation, rotation, etc.
 - This regular template does not show any clear differentiation for the cerebellum making analysis of specific regions of the cerebellum difficult to impossible
 - The normalization of the template leads to large spatial spread of cerebellar folia, whereas the SUIT template is much closer together



- Diedrichsen lab developed a new atlas based on the average anatomy of 20 healthy individuals aged 22-45
 - Template specifically based on brainstem and cerebellum
 - Preserves the anatomical accuracy of the cerebellum to a far greater extent than the ICBM152 template
 - Reduces spatial variance and improves overlap of deep cerebellar nuclei (although these are not visible on a T1 scan)
- SUIT database was developed to be spatially unbiased in reference to MNI space
 - When normalizing the same brain to the MNI whole-brain template and the SUIT atlas, the same structure would end up in the same space on average

- Also includes a surface-based representation of the cerebellum
 - Allows to display volume-averaged cerebellar data on a group flatmap



- Intuitive way to communicate results
- Understanding of the contents of the program
 - First use isolation function to isolate the cerebellum from the rest of the brain
 - Creates a cerebellar mask, as well as gray and white matter probability images
 - Works best on T1 weighted images
 - The isolation function is performed in the native space of the original image, meaning that the image needs to be normalized to the cerebellar atlas in order to compare between various images
 - Normalization function deforms image from native space to suit space, changing location but not size
 - Dartel algorithm uses the tissue segmentation maps (in this case white matter and gray matter maps) to find the nonlinear deformation (change from voxel in scan to voxel in the atlas) in the form of a flowfield (no idea what this is)
 - Does not reslice the image into the atlas space, only calculates the changes that would be necessary
 - Reslicing using dartel
 - Uses flow field and affine transformations from normalizing to the images into the atlas space
 - Inverse reslicing
 - Takes an image in SUIT space and reslices it into the native space
 - After going through the suit atlas, the specific regions in the cerebellum can be identified
 - By inverse reslicing, it becomes possible to find the volumes of specific cerebellar regions in each subject (eg. can find the volume of the vermis)
 - SUIT volume function can then be used find the volumes of each layer

Literature Review

- Voxel based morphometry
 - Studied interaction between brain volume and amphetamine-type stimulants (ATS) (eg. methylphenidate) and cocaine
 - Focus on young occasional, not chronic users
 - Gray matter lower in right dorsolateral cerebellum

- How was a robust regression used to identify voxels related to lifetime amount of ats and cocaine
- Brain Apoptosis Signaling pathways
 - Chronic treatment of methylphenidate and its effect on pro-apoptotic protein, Bax, and anti-apoptotic protein, Bcl-2, caspase-3, and cytochrome c
 - Cortex
 - MPH at all doses increase Bax
 - Bcl-2, caspase-3 were increased at 1 mg/kg
 - Bcl-2, caspase-3 were decreased at 2 mg/kg
 - Cytochrome c reduced in cortex at all doses
 - Cerebellum
 - Increase of Bax with MPH at all doses
 - Reduction of anti-apoptotic proteins at 2 and 10 mg/kg
 - Treatment with MPH (2 and 10) increased Bax and decreased Bcl-2 in the hippocampus
 - Caspase-3 and cytochrome c reduced in the hippocampus at 10 mg/kg
 - MPH can activate the initial cascade of apoptosis by increasing Bax and reducing Bcl-2
 - Can also inhibit by reducing caspase-3 and cytochrome c
- Effects of acute doses of MPH on inflammation and oxidative stress in hippocampus and cerebral cortex
 - At 10 and 20 mg/kg, rats demonstrated depression and anxiety-like behavior
 - Increased levels of inflammatory factors in isolated tissues
 - Acute administration of MPH causes oxidative and inflammatory changes in brain cells, neurodegeneration in hippocampus and cerebral cortex
- Increased risk of diseases in cerebellum of patients with ADHD history
 - Patients with ADHD (n=31769) had a 2.4-fold times increased risk of basal ganglia and cerebellum increases compared with non-ADHD
 - Patients (21-69 age) prescribed with psychostimulants had a 8.6 fold risk for diseases
 - Retrospective cohort study using state-wide records from the Utah Population Database
- Long term administration of high dose MPH-induced cerebellar morphology and function damage
 - MPH in the form of the Ritalin was given to the treatment group for 3 weeks
 - At the end of each week, rotarod performance test was performed
 - Assesses motor coordination and balance in rats
 - At the end of the third week tissues in the cerebellum were separated and tested for inflammation parameters
 - Ritalin at high doses (20 mg/kg) results in significant increases of bax and caspase-8 genes
 - High increase of TNF- α and IL-1 β in isolated cerebellar cells

- Decreased mean volumes of granular layer, white matter, as well as molecular layers of cerebellum
 - Also reduced number of Purkinje cells
- Lower coordination in rats receiving Ritalin
- Increased dose of Ritalin could lead to inflammation and neurodegeneration in the cerebellum of adult rats
- MPH alter monoaminergic and metabolic pathways in the cerebellum
 - Investigates chronic and acute effects of MPH in adolescent rats on monoaminergic and metabolic markers in the cerebellum
 - Monoaminergic = working on monoamine transporters
 - Dopamine, epinephrine, serotonin
 - Acute MPH (2 mg/kg) decreased cerebellar vesicular monoamine transporter (VMAT2) density
 - Chronic treatment caused an increase
 - Regulates the packaging and subsequent release of dopamine and other monoamines from neuronal vesicles into the synapse
 - Levels of tyrosine hydroxylase and dopamine D1 receptor did no change
 - Tyrosine hydroxylase helps convert tyrosine into dopamine
 - Chronic treatment increased dopamine turnover in the cerebellum
 - Dopamine turnover = ratio of dopamine metabolites to dopamine itself
 - Acute MPH (5 mg/kg) altered levels of cerebellar metabolites
 - Acute MPH = decrease cerebellar metabolites from excitatory neurotransmission, decrease in metabolites from inhibitory neurotransmission
- MPH induces lipid and protein damage in prefrontal cortex, not cerebellum or hippocampus
 - Effects of prolonged MPH use on brain development
 - Increased activity of superoxide dismutase (SOD) and catalase (CAT)
 - Breaks down oxygen molecules that could harm the cell, protects the cell from radical attacks
 - Did not alter the activity of thiobarbituric acid reactive substance levels and sulfhydryl group in the cerebellum
 - In the striatum and hippocampus, MPH treated rats showed decreased thiobarbituric acid reactive substance levels (TBARS)
 - Indicator for increased lipid peroxidation
 - In the prefrontal cortex, MPH promoted an increase in reactive species formation, SOD/CAT ratio, and increased lipid peroxidation and protein damage
 - Structures respond differently to MPH when administered chronically in young rats

ADHD and Methylphenidate Critical Review

- Medication-naïve ADHD patients normally undergo structural changes in the brain, such as the thinning of the cortex

- Medications like MPH normalize and reduce some, but not all, of these structural changes
- Suggests that MPH may have a normalizing effect on cerebellum and striatum activation in boys with ADHD during rest
- Some studies surmise there is no evidence showing that MPH has a long term effect on brain activation patterns
- Effects of MPH may be specific to the specific neuronal changes caused by ADHD in each patient

Synthesis

Attention Deficit Hyperactivity Disorder (ADHD)

Attention deficit hyperactivity disorder (ADHD) is a chronic and debilitating disorder that affects individuals in areas such as academic and professional achievements, interpersonal relationships, and daily functioning (Harpin, 2005). Estimates suggest that 8.4% of children have ADHD, while a lower proportion, 2.5% of adults have the condition. In particular, the disorder leads to decreases in executive function and changes motivation patterns. While some theories postulate the genetic basis for the condition, the true cause remains unknown. With the exclusion of Parent-Child Interaction Therapy (PCIT) for preschool-aged children, the most commonly prescribed medications for ADHD are psychostimulants, usually amphetamines and methylphenidates. Twin studies show heritability estimates of 0.6 to 0.9, with the most studied genetic variations being those occurring in the dopamine D4 receptor and dopamine transporter (DAT1). A literature review from 1991 to 2004 show the four most associated genes are the dopamine D4 and D5 receptors, and the dopamine and serotonin transporters, although new findings suggest the role of COMT, an enzyme that is involved in metabolizing catecholamine neurotransmitter, val 158/108 met variant in influencing conduct problems. The most consistent finding between individuals with the condition is an overall reduction in total brain size that continues into adolescence, as well as reduced dimensions of specific brain regions, including: the caudate nucleus, prefrontal cortex white matter, corpus callosum and the cerebellar vermis. The structures with decreased size are most commonly those with a high density of dopamine receptors, such as the caudate nucleus. In addition, decreased blood flow to the striatum and changes in its affinity for dopamine has also been observed. A regional decrease in cortical thickness has been associated with the DRD4-7 repeat allele, which is commonly associated with the diagnosis of ADHD.

Dopamine Reward Pathway

The mesolimbic system, or reward system, is composed of brain structures responsible for mediating the physiological and cognitive processing of rewards. Usually, rewards result in an adjustment of an individual's behavior so that they search for a particular stimulus. Though the mesolimbic system requires the coordinated release of many heterogeneous neurotransmitters, dopamine plays a key role in the reward value of food, drink, sex, social interaction, and substance abuse. As such, the mesolimbic system primarily refers to the dopaminergic pathway, which is formed by projections of midbrain dopamine neurons of the ventral tegmental area (VTA) to the striatum, prefrontal cortex, amygdala, hippocampus, and

many structures of the limbic system. When a reward is obtained, the dopamine neurons will release dopamine to the desired target nuclei. The striatum is a key area of the dopaminergic pathway. The ventral striatum, which includes the nucleus accumbens (NAcc), a structure known for its role in evaluation and incentive based learning. Similarly, the dorsal striatum is critically involved in action selection and habitual behavior. Virtually all outputs from the striatum are medium spiny neurons (MSNs), which produce γ -aminobutyric acid (GABA). The striatum gives rise to two main pathways: the direct pathway is formed by dopamine D1 receptor (D1R) expressed in medium spiny neurons (dMSNs), while the indirect pathway is formed by dopamine D2 receptor (D2R) expressed in medium spiny neurons (iMSNs). The coordinated dopamine signaling to dMSNs and iMSNs within the striatum helps with integrating and responding to rewards. The remaining neurons in the striatum are interneurons, which regulate MSN activity. Majority of these interneurons are inhibitory GABAergic interneurons, which control reward by signaling to MSNs and expressing a variety of modulatory peptides. 1-2% of the neurons in the striatum are formed by tonically active cholinergic interneurons, which are critical in regulating MSNs despite their low abundance

Some abnormalities exist in the mesolimbic system for individuals with ADHD. Usually, the repetition of a positive stimulus means the time of the reward (dopamine release) transfers to earlier and earlier predictors of the reward. If the reward is silenced in some trials, dopamine cells stop firing to the point where an expected reward is no longer developed. The dopamine transfer deficit theory suggests that the transfer of the cell's response to dopamine fails to predict the reinforcement that will occur in children with ADHD. Some genetic basis exists for this change, but these differences do not appear major enough to result in the behavior of children with ADHD. The free diffusion of dopamine from synaptic cleft into surrounding extracellular tissue is the main mechanism by which dopamine acts on cells. Dopamine transporters (DATs) are responsible for terminating the dopamine signal. In many diagnosed with ADHD, the dopamine transporter 1 (DAT1) gene varies in length due to a variable number tandem repeat (VNTR) of a 40 base pair repeat. A VNTR is a location in DNA where a short nucleotide sequence is organized as a tandem repeat, or a sequence of DNA bases that are repeated numerous times in a head-to-tail manner on a chromosome, with variations in length between individuals. The alleles with 10 copies (10R) have been associated with ADHD. In vitro, it was found that DAT binding site density for the 10R polymorphism was elevated 50% over that of the 9R allele. In addition, individuals homozygous for the 10R allele showed significantly hypoactivation in the left dorsal anterior cingulate cortex (dACC), a structure found in the cerebral cortex associated with executive function, compared to 9R carriers. Hypoactivation was also shown in the left cerebellar vermis and right lateral prefrontal cortex.

Five dopamine receptors have been identified and classified into D1-like and D2-like groups, with the former group containing D1 and D5 receptors, and the latter group containing D2, D3, and D4 receptors. It is important to note that dopamine receptors are GPCRs, and each have different biochemical properties, as well as selective agonists and antagonists. D1 and D2 receptors are more or less uniformly expressed throughout the striatum at high levels, and can

be found in lower levels in the prefrontal cortex. Polymorphisms, or the presence of two or more variant forms of a specific DNA sequence that can occur among different individuals or populations, of D4 and D5 are associated with ADHD. D4 is expressed at very low levels in the striatum but at moderate levels in the prefrontal cortex. D4 is expressed presynaptically in the terminals of the corticostriatal afferents, giving it regulatory powers over both the presynaptic and postsynaptic neuron. This receptor is associated with the rapid translocation of the Ca²⁺/calmodulin-dependent protein kinase II (CaMKII) from the cytosol to postsynaptic sites in prefrontal cortex neurons, which activates synaptic proteins responsible for developing plasticity. In contrast, D5 receptors are expressed in cortex, hippocampus, and striatum. Coupled to adenylyl cyclase, D5 receptors will result in increased cyclic AMP levels upon activation. This process is key for the development of plasticity for the dopamine pathway, as well as the development of long term potentiation between the cerebral cortex and striatum.

Methylphenidate

Methylphenidate is FDA approved for treating ADHD in children (>6 years of age) and adults (Verghese & Abdijadid). The basic mechanism blocks the reuptake of norepinephrine (NE) and dopamine (DA) in presynaptic neurons, increasing the concentration of DA and NE in the synaptic cleft, and thereby increases the effect of both neurotransmitters on the next firing. Methylphenidate chemically derives from phenethylamine and benzylpiperazine, and undergoes metabolism by the liver to form ritalinic acid through de-esterification via carboxylesterase CES1A1. In addition, methylphenidate is a weak agonist at the 5HT1A receptor, which helps contribute to higher dopamine levels. Amphetamines (AMP) and Methylphenidates (MPH) seem to have comparable efficacy, though some studies state AMP has slightly greater effect. In preclinical studies, it was found that direct effects of the drug included inhibition of NET and DAT, affinity for agonist activity at 5-HT1A receptor, inhibition of MAO, and redistribution of VMAT-2. The cumulative effect of these changes is elevated extracellular DA and NE levels. Activation of α_2 adrenergic receptors was also observed, leading to stimulation in cortical excitability. In neuroimaging studies, MPH increases activation of the parietal and prefrontal cortices and increases deactivation of the insula and posterior cingulate cortex during visual attention and working memory tasks. When study participants were placed in an uncertain environment, MPH resulted in increased activation in left and right parahippocampal regions and cerebellar regions. In addition, it was found MPH resulted in increased regional CBF in the prefrontal cortex and increased CBF in the thalamus and precentral gyrus. MPH-associated improvements in working memory tasks corresponded with decreased oxy-hemoglobin levels in the right lateral prefrontal cortex, again indicating lower neural activation.

Cerebellum Anatomy

The cerebellum has no direct connections to lower motor neurons, but instead exerts influence through connections with the motor cortex and brainstem. As the largest structure in posterior fossa, the cerebellum is attached to dorsal pons and rostral medulla by three peduncles: the superior, middle, and inferior peduncles. The superior cerebellar peduncle carries output from the cerebellum, and decussates in the midbrain. In contrast, the inferior and middle peduncle carry inputs. The cerebellum consists of the midline vermis situated in between two larger cerebellar hemispheres, which are in turn divided into anterior and posterior lobes by the primary fissure, as well as the flocculonodular lobe by the posterolateral fissure.

There are three functional regions of the cerebellum. The vermis and flocculonodular lobes are respectively important in proximal and trunk muscle control and in vestibulo-ocular control. The intermediate part of the cerebellar hemisphere is involved in control of distal appendicular muscles in arms and legs, while the lateral part of the cerebellar hemisphere controls motor planning. All outputs of the cerebellum pass through the four deep cerebellar nuclei, starting from most lateral to most medial: dentate, emboliform, globose, and fastigial. The dentate nucleus is the largest of the cerebellar nuclei, and receives projections from the lateral hemispheres. The interposed nuclei consists of the emboliform and globose nucleus, which receive input from the intermediate parts of the cerebellum. Lastly the fastigial nucleus receives input from the vermis, as well as a lesser input from the flocculonodular lobe.

Cerebellar Circuitry

The cerebellar cortex has three layers. Starting from the innermost layer, the granule cell layer is tightly packed with small granule cells so numerous that they rival the total number of cells in the nervous system. Above the granule layer is the purkinje layer, which, as the name suggests, contains flask-shaped purkinje cells. Lastly is the molecular layer, which contains the unmyelinated axons of granule cells, dendrites of purkinje cells, as well as several types of interneurons. There are two types of synaptic inputs to the cerebellum, mossy fibers and climbing fibers. Mossy fibers ascend from various regions and pass through cerebellar white matter to form excitatory synapses with dendrites of granule cells. In turn, granule cells send axons into the molecular layer, which bifurcate, forming parallel fibers that run perpendicular to the dendrites of the purkinje cells. These fibers form many excitatory synapses with the purkinje cells they pass.

All outputs from cerebellar cortex carried by axons of purkinje fibers into the cerebellar white matter. Purkinje cells form inhibitory synapses with deep cerebellar and vestibular nuclei, which convey information from the cerebellum to other regions through excitatory synapses, regulating information exiting so as to avoid overstimulation. The other kind of input to cerebellum is climbing fibers, which arise exclusively from neurons in the contralateral inferior olivary nucleus. Climbing fibers wrap around the cell body and proximal dendritic tree of purkinje fibers, forming excitatory synapses. These cells have a strong modulatory effect on purkinje, and can cause significant decline in response to parallel fiber stimulation. Basket cells

and stellate cells are located in the molecular layer, and are excited by synaptic input from granule cell parallel fibers. Signals then travel in the rostral-caudal direction, perpendicular to the parallel fibers, where they cause inhibition of adjacent purkinje cells. Golgi cells can be found at the granule cell layer. These cells receive excitatory signals from the parallel fibers, providing feedback inhibition on granule cell dendrites. The result of golgi cell's inhibitory property is regulation of the temporal domain of signals, leading to enhanced signal resolution. Similarly, the result of stellate and basket cell inhibitory property is regulation of the spatial domain of signals, also leading to enhanced signal resolution. Complex synaptic interactions occur in the granule cell layer in a specialized region called the cerebellar glomerulus. Two types of inputs (large mossy fiber axon terminals and golgi cell axon terminals), which form synapses onto one type of postsynaptic cell (granule cell dendrites), which in turn excite inhibitory purkinje cells.

Table 1: Summary of Cerebellum Circuitry terms

Name	Acts on	Effect	Originates
Mossy Fibers	Granule cells	Excitatory	White matter
Granule cells	Purkinje as parallel fibers in molecular layer	Excitatory (on purkinje cells)	Granule layer
Purkinje cells	Deep Cerebellar and Vestibular Nuclei	Inhibitory	Dendrites in molecular layer
Climbing fibers	Molecular layer (purkinje dendrites)	Inhibitory	contralateral inferior olivary nucleus
Basket & Stellate Cells	Purkinje fibers (cell body and dendrites respectively)	Inhibitory	Molecular layer Result = enhanced signal transmission on spatial plane
Golgi cells	Granule cell dendrites	Inhibitory	Granule layer Result = increased signal transmission on temporal plane
Cerebellar glomerulus	n/a	Site of where mossy fiber, granule cell, purkinje cell interactions take place	n/a

Cerebellar Output Pathways

Cerebellum is ipsilaterally controlled, not contralateral, because it is double crossed. The first cross occurs when the superior peduncle decussates, while the second cross occurs as rubrospinal and corticospinal tracts descend to the spinal cord. Input to cerebellum is also ipsilateral for the same reason. The lateral cerebellar hemisphere projects to dentate nucleus, which in turn projects to the superior peduncle. The superior peduncle decussates in the midbrain, and reaches its contralateral (compared to source) ventral lateral nucleus (VL) of the thalamus. The outputs from basal ganglia terminate in anterior VL, while cerebellar outputs terminate in the posterior VL. The VL in turn projects to the motor cortex and premotor cortex, supplementary motor area, and parietal lobe to influence motor planning in the corticospinal systems. Some evidence indicates that outputs from lateral cerebellum are also projected to the prefrontal association cortex, suggesting a role in cognitive function. Some fibers from the dentate nucleus also terminate in the parvocellular division of the red nucleus. The interposed nuclei project to superior peduncle which projects to the contralateral VL, which projects to motor cortex and premotor cortex, supplementary motor area to influence the lateral corticospinal tract. The cerebellar vermis and flocculonodular lobes influence proximal trunk muscles through connections to medial motor pathways (anterior corticospinal, reticulospinal, vestibulospinal, tectospinal tracts). The outputs from the fastigial nucleus are to a small extent carried by superior peduncle, but mainly carried by fiber pathways called the uncinatus fasciculus and juxtarestiform body, which lies on the lateral wall of the fourth ventricle, just medial to the inferior peduncle.

Cerebellar Input Pathways

Inputs reach cerebellum from: Virtually all regions of cerebral cortex; Multiple sensory modalities; Brainstem nuclei; and the spinal cord. The input pathways have a rough somatotopic organization, with the general ipsilateral body being represented in both anterior and posterior lobes. The corticopontine fibers are the major input from frontal, temporal, parietal, and occipital lobes. These fibers travel to the ipsilateral pons and synapse in the pontine nuclei. Pontocerebellar fibers then cross the midline to enter the contralateral middle cerebellar peduncle and give rise to mossy fibers. Another major input are the spinocerebellar fibers. These fibers travel in four tracts: dorsal and ventral spinocerebellar tracts for lower extremities, as well as cuneocerebellar and rostral spinocerebellar tracts for upper extremities and neck. Afferent information about limb movement is conveyed to the cerebellum by the dorsal spinocerebellar tract for lower extremities and by the cuneocerebellar tract for upper extremities. The dorsal spinocerebellar tract ascends in the dorsolateral funiculus, near the surface of the spinal cord, lateral to the corticospinal tract. Meanwhile myelinated axons of sensory neurons carrying proprioceptive, touch, and pressure sensation from lower extremities ascend the gracile fasciculus. Some of these fibers form synapses with the nucleus dorsalis of Clark, which is a long column of cells that run in the dorsomedial spinal cord gray matter intermediate zone, from C8 to L2. Fibers arising from the nucleus dorsalis of Clark ascend ipsilaterally in the dorsal spinocerebellar tract, and give rise to mossy fibers that travel to the ipsilateral cerebellar cortex via the inferior peduncle. Fibers from upper extremities enter the cuneate fasciculus and ascend ipsilaterally to synapse in the external cuneate nucleus in the

medulla. From the external cuneate nucleus, cuneocerebellar fibers ascend in the inferior cerebellar peduncle to the ipsilateral cerebellum. The inferior olivary complex gives rise to olivocerebellar fibers that cross the medulla to enter the contralateral cerebellum. These fibers form a major portion of the inferior peduncle and terminate as climbing fibers. Additionally, connections between vestibular system and cerebellum are important in balance and equilibrium, as well as optical reflexes. To be more specific, the flocculus also receives visual inputs related to retinal slip (disparity between target and perceived images) that are important for smooth pursuit eye movement.

MRI Physics

MRI provides images of body tissues and their chemical compositions with exceptional clarity and little risk to the patient. MRI was originally known as nuclear magnetic resonance imaging because it is a form of nuclear magnetic resonance spectroscopy. When a magnetized species exists, it can absorb the energy from a magnetic field of equal strength. NMR exploits the fact that different protons placed in a uniform magnetic field will feel slightly different levels of magnetism based on their location relative to the source, in a phenomenon called shielding. Some protons feel less of the applied magnetic field because they are in an environment rich with electrons, and their attraction to electrons override the applied magnetic field. The varying strengths of a magnetic field can reveal structural information, with absorption of low frequency suggesting heavily shielded species, and absorption of high frequency suggesting lightly shielded species. NMR is often calculated in relation to a specific compound, such as tetramethylsilane (TMS), which is highly shielded and the frequency of radiation it absorbs is often set to 0 on NMR instruments. Since frequency absorbed is proportional to the applied field, the shift or difference between the two values is recorded, and not the exact frequency. Protons in close proximity to electron donating groups (generally higher concentration of electrons) will be more shielded and vice versa.

The nucleus has a net positive charge, with each proton and neutron in the nucleus having its own spin. Net spin is represented by the spin number, I , which describes the angular momentum of the spinning charge. If the mass or atomic number is odd, I has a non-zero value. In contrast, if the mass and atomic number are both even, then the spin of the neutrons and protons will cancel out, resulting in zero net spin. A nucleus must possess overall spin to respond to NMR. The isotopes H-1 and C-13 both meet these criteria, but C-12 and O-16 do not. H-1 is found in macromolecules all over the body, which allows for NMR to be used for imaging of human bodies. The allowed spins for a given value are represented by $2I+1$. When $I=0$, there is only one spin state. In contrast, H-1 has an I value of $\frac{1}{2}$, meaning it has two possible spin states.

Charged particles such as nuclei exhibit electric fields, which includes magnetic fields. An I value greater than one means that the magnetic moments can take on more than one orientation. In the absence of external forces, these varying spin states are of equal energy. When atomic nuclei are exposed to a magnetic field they will tend to orient themselves with

the field to maximize stability and minimize energy use. When the magnetic field is applied, many of the protons (which are not aligned with the magnetic field) will want to flip orientation from high energy to low energy. Due to the law of conservation of energy, when these protons flip from high energy to low energy, energy must be released. This change in energy will be equal to the energy difference between high and low states. If a second magnetic field is applied perpendicular to the original magnetic field, and the second magnetic field rotates around the Z axis at the same rate as the protons precess about their z axis, the protons will feel as if the orientation of the second magnetic field is constant. Protons will still precess around the perpendicular magnetic field as well, though the degree to which the protons do so is determined by the strength of the magnetic field. As a result, when B1 (second magnetic field) is applied, the cone of magnetization is flipped and rotated. When B1 is removed, the protons will return to their lower energy configuration oriented along the z axis, releasing energy as they do so. This energy, or relaxation, is what MRI measures.

In T1 MRIs, the applied magnetic field B1 that causes the flipping is in the radiofrequency range, known as an RF pulse. The T1 value is dependent on the material's characteristics and calculated as the time to reach 63% longitudinal magnetization. Since MR signals are those created when precessing protons that have been exposed to an RF pulse releases energy during relaxation, these MR signals require energy to be exchanged as the protons move from high to low energy (spin lattice relaxation). Different molecules have different T1 values, and the T1 value depends on how tightly bound the H is bound to molecules. For example, water has a longer T1 relaxation time, and thus appears as dark on a T1 weighted image, while fat has a short T1 value and appears as bright spots. T2 is the time it takes for only 37% of the transverse magnetization vector to remain. Inhomogeneity in tissue causes the proton's spin to be influenced by small magnetic fields created by the spin from a nearby proton - the result of which is a longer T2 value. Time to echo (TE) is the difference between the peak of the 90 degree RF pulse and the peak of the echo formed, while repetition time (TR) is time to run a pulse sequence at one time. Images created predominantly using differences between T1 times is known as a T1-weighted image. A short TR ensures that not all tissues have the chance to return to full relaxation, meaning the tissues that have returned to this point will have released more energy than the ones who haven't (released a greater echo). When T1 effects are minimized by having a long TE and TR, T2 weighted images are produced.

Method

Using SUIT Toolbox to Find Cerebellar Volumes

Installation

Suits installation instructions: https://www.diedrichsenlab.org/imaging/suit_download.htm

Download "source code.zip" from git hub (linked in the SUIT download page)

Unzip the archive and place the SUIT folder in the <SPM_HOME>/toolbox/ directory.

Start Matlab and SPM12. Select fMRI. SUIT should now be present as an option under the toolbox drop down menu

- The template images can be found in <SPM_HOME>/toolbox/SUIT/templates. If you like, create a copy of these templates at a more accessible place.

Download python package for SUITs [SUITPy] from git hub here:

<https://github.com/diedrichsenlab/SUITPy/releases/tag/v.1.3.1>

Or use pip install SUITPy <done in terminal; may need to use pip3 if that is the version you are using>

Unzip the archive (or clone directly) and place it in a good location – I put in documents/MATLAB

Adjust your environmental variable \$PYTHONPATH to include the folder that contains the SUITPy package. You can do this by adding the line PYTHONPATH=/
MY PATH>:\${PYTHONPATH}

Download cerebellar atlases : https://github.com/diedrichsenlab/cerebellar_atlases

Probabilistic atlas for cerebellar lobules and nuclei: Diedrichsen (2009)

Functions

User guide: https://www.diedrichsenlab.org/imaging/suit_function.htm

To use SUIT make sure Matlab path is set to the folder where the SUITPy folder is located. Ensure SPM12 is running

To isolate the cerebellum simply type suit_isolate_seg in the matlab command window and then select the appropriate scan to be analysed using the SPM interface (all steps of analyses require that SPM is also running). If you want to use different channels, then select all images to be used. The T1 must be selected first and the following images must have the same

dimensions and be coregistered to the first channel. To select more than one subject, click in create new subject and then select the corresponding image(s).

This produces for each subject:

- The gray matter probability map (<name>_seg1.nii)
- The white matter probability map (<name>_seg2.nii)
- The (possibly hand-corrected) isolation mask c_<name>_pcereb_corr.nii

Which is used for normalization

To normalize the individual cerebellum to the SUI template use `suit_normalize_dartel`. Need to first specify the grey, white matter probability maps and the isolation files in Matlab command window. (need to be in the directory with the named files in the matlab window)

EXAMPLE (for structure called temp):

```
job.subjND.gray={'T1_seg1.nii'};  
job.subjND.white={'T1_seg2.nii'};  
job.subjND.isolation={'c_T1_pcereb.nii'};
```

THEN to do normalization to template:

```
suit_normalize_dartel(job)
```

The normalization will produce:

- The affine transformation matrix for the linear part of the normalization:
Affine_<name>.mat
- The non-linear flowfield (a 4-D nifti): u_<name>.nii

<If there is an error in the normalization with a message that images are too far apart reset the origin of the T1 using instructions here

https://andysbrainbook.readthedocs.io/en/latest/SPM/SPM_Short_Course/SPM_07_SettingTheOrigin.html

and rerun the segmentation >>

`suit_normalize_dartel` does not reslice the image into the template space. i.e. just calculates the change, does not make the change. To reslice image into SUI space use `suit_reslice_dartel`.

`suit_reslice_dartel_inv` -- This takes an image in SUI space and reslices it into the space of the individual subject (native space). This is useful in connection with group atlases to differentiate neuroanatomical areas/landmarks in the individual's native space.

To reslice back from SUI space to native space, please specify for each Subject:

- The Affine transformation file created by `suit_normalize_dartel` (Affine_<name>.mat).
 - Example temp.Affine={'Affine_T1_seg1.mat'}

- The flow field also created by `suit_normalize_dartel (u_a_<name>_seg1.nii)`.
 - `temp.flowfield={'u_a_T1_seg1.nii'}`
- The reference image for the final geometry (This can be your original or cropped T1 image).
 - `job.ref={'T1.nii'}` OR `job.ref={'c_T1.nii'}`
- The image(s) to reslice. If this field is empty the function will automatically reslice the probabilistic atlas into the subject space.
 - `job.resample={'MDTB_10Regions.nii'}` Where `MDTB_10Regions.nii` is an atlas.

complete example

```
job.Affine={'Affine_T1_seg1.mat'};
job.flowfield={'u_a_T1_seg1.nii'};
job.ref={'c_T1.nii'};
job.resample={'MDTB_10Regions.nii'};
suit_reslice_dartel_inv(temp)
```

NEED TO DOUBLE CHECK FROM HERE >

To get lobular volumes you can call `suit_reslice_dartel_inv(job)`

https://www.youtube.com/watch?v=VtIFnd_CpW8

If is the field 'resample' is empty it will automatically produce the SUIT atlas resliced into native space for the individual. For this to work – need to download cerebellar atlases from the SUIT website, rename folder 'cerebellar atlases' and put the folder in SPM12/toolbox folder.

Example

```
job.Affine={'Affine_T1_seg1.mat'};
job.flowfield={'u_a_T1_seg1.nii'};
job.ref={'T1.nii'};
suit_reslice_dartel_inv(job);
```

Should produce a file `iw_Lobules-SUIT_u_a_T1_seg1.nii`

Then can use the function `suit_vol` to get volumes of each lobule

Example

```
V=suit_vol('iw_alt_Anatom_space-SUIT_dseg_u_a_T1_seg1.nii','Atlas')
```

V will be a matlab structure

Output: Structure including the following fields:

name: Filename of the source

dir: Directory of the source
vox: Number of voxels per region
vmm: Volume in mm³ per region
Vsize: Volume of one voxel
reg: List of regions of SUIT atlas

SECTION III: METHOD

Overview

Data Collection

Data Extraction

Data Analysis

Overview

T1 weighted images from individuals between the ages of 5 and 18 were gathered or repurposed from two sources: a neuromelanin study and the TAGIT demographics study. Using the SUI toolbox developed by Diedrichsen Lab for MATLAB, the volumes of the various regions of the cerebellum were extracted and analyzed.

Data Collection

Table 1: Demographic information for population sample used in MRI study

	ADHD	NT	Both
Number	12	5	17
Age	10.43	10.96	10.56
Sex (Female/Male)	6/6	2/3	8/9
Medication (Yes/No)	9/3	0/5	9/8
Past medication (Yes/No)	8/4	0/5	8/9
Other Diagnoses (Yes/No)	6/6	0/5	6/11

Phase I: Pilot Study

Table _: Exclusion Criteria Planning

Calculation Relevant	<ul style="list-style-type: none"> ● Study_ID ● ADHD_Diagnosis ● Med_Dose ● Med_Start Med_Date_Stop_Study
Exclusion Criteria Relevant	<ul style="list-style-type: none"> ● Current_Meds Med_Type ● Previous_Meds <ul style="list-style-type: none"> ○ List_Past_Meds ● Other_Diagnoses_Present <ul style="list-style-type: none"> ○ Other_Diagnoses ● Recent_HI ● Amnesia ● Previous_Conc
Potential Confounding Variable	<ul style="list-style-type: none"> ● Assessments_Completed_By: Test_Date ● Birth_Date ● Age

	<ul style="list-style-type: none"> ● Sex ● Gender ● Height ● Weight ● BMI ● Handedness ● Ethnicity ● Other_SpecifyLanguage_Exposure ● Languages ● Lang_Freq_Set ● Describe_HA ● ADHD_Professional_Type ● ADHD_Diagnosis_Age
<p>No Direct Relavence</p>	<ul style="list-style-type: none"> ● Diagnosis_Email ● Parent1_Highest_Ed ● Parent2_Highest_Ed ● Parent_Relationship ● Gross_Income Sport_Activities ● Sport_Type ● Why_Stopped_Past_Meds ● Bedtime_Weeknight ● Bedtime_Weekend ● Waketime_Weeknight ● Waketime_Weekend ● ADHD_Diagnosis_Who ● Other_Diagnoses_Who ● Other_Diagoses_When ● Other_Diagoses_TYPE ● Time_HI Location_HI Cause_HI ● Loss_Conc ● Follow-up ● Type_FU ● Number_Past_Conc Length_Past_CS ● School_Missed Sports_MissedHistory_HA ● Current_CS ● ADHD_Diagnosis_Year ● Sleep_Length Allergies List_Allergies ● Food/Env_Factors List_Food/Env Family_History ● History_ECD History_ECD_Who ● Med_Name

To gain a better insight into the correlation between methylphenidate use and duration with cerebellar structure changes, a pilot study using eight T1 MR images was first conducted. These eight images were originally collected for a separate study at BrainKids Lab, but was reused given it: (1) contains structural image data of children with ADHD, (2) includes children who both use and do not use methylphenidate, (3) comes with detailed patient information including duration and dose of the drug, and (4) was reliably collected and reused with the consent of the subjects. All eight of the images did not contain defects that prevented the data from being usable. It should be noted that subject number four had a metal retainer in their mouth during the MRI scan, but the distortion in the image mostly applies to the areas under the frontal lobes and does not disturb the cerebellum or brainstem. As such, this scan was not excluded.

Phase II: TAG-IT Demographics Data

Table 2: Exclusion criteria information used, organized by reason and category

Reason	Number	Category
Previous concussions	1	ADHD
	1	NT
Previous head injuries	2	ADHD
	0	NT
Other diagnoses	5	ADHD
	0	NT
Unrecorded medication start date	3	ADHD
	0	NT
Unrecorded medication dose	1	ADHD
	0	NT
Incorrect medication type (eg. amphetamines)	8	ADHD
	1	NT
Total	22	n/a

In order to conduct many inferential statistics tests in an accurate manner, as well as to mitigate the effects of outliers, a larger sample size is required. In total, the TAG-IT study provided forty anatomical images. However, certain exclusion criteria must be applied to the

scans in order when gathering data on methylphenidate-using individuals: (1) no artifacts or distortions may be present in the cerebellum in any of the three dimensions, (2) subject must currently be taking a methylphenidate stimulant medication for ADHD, (3) subject must include dose and duration of their current medication. Other exclusion factors may be implemented on a case-by-case basis, and will be noted if such a circumstance occurs (Table 2). A similar exclusion criteria must be applied when selecting data for the non-methylphenidate-using subjects: (1) no artifacts or distortions may be present in the cerebellum in any of the three dimensions, (2) subject must not be currently taking a methylphenidate stimulant medication for ADHD, or have taken the medication for an extended period of time in the past, (3) subject must not be on any additional psychostimulant medication, including amphetamines, (4) must explicitly state no prior medication history. Lastly, the TAG-IT demographics also includes data from non-ADHD patients which can be used as a negative control when interpreting results. Exclusion criteria for this group include: (1) no artifacts or distortions may be present in the cerebellum in any of the three dimensions, (2) subject must not be currently taking a methylphenidate stimulant medication for ADHD, or have taken the medication for an extended period of time in the past, (3) subject must not be on any additional psychostimulant medication, including amphetamines, (4) must not have a diagnosis for ADHD or any other neurocognitive disability (must be neurotypical).

Data Extraction

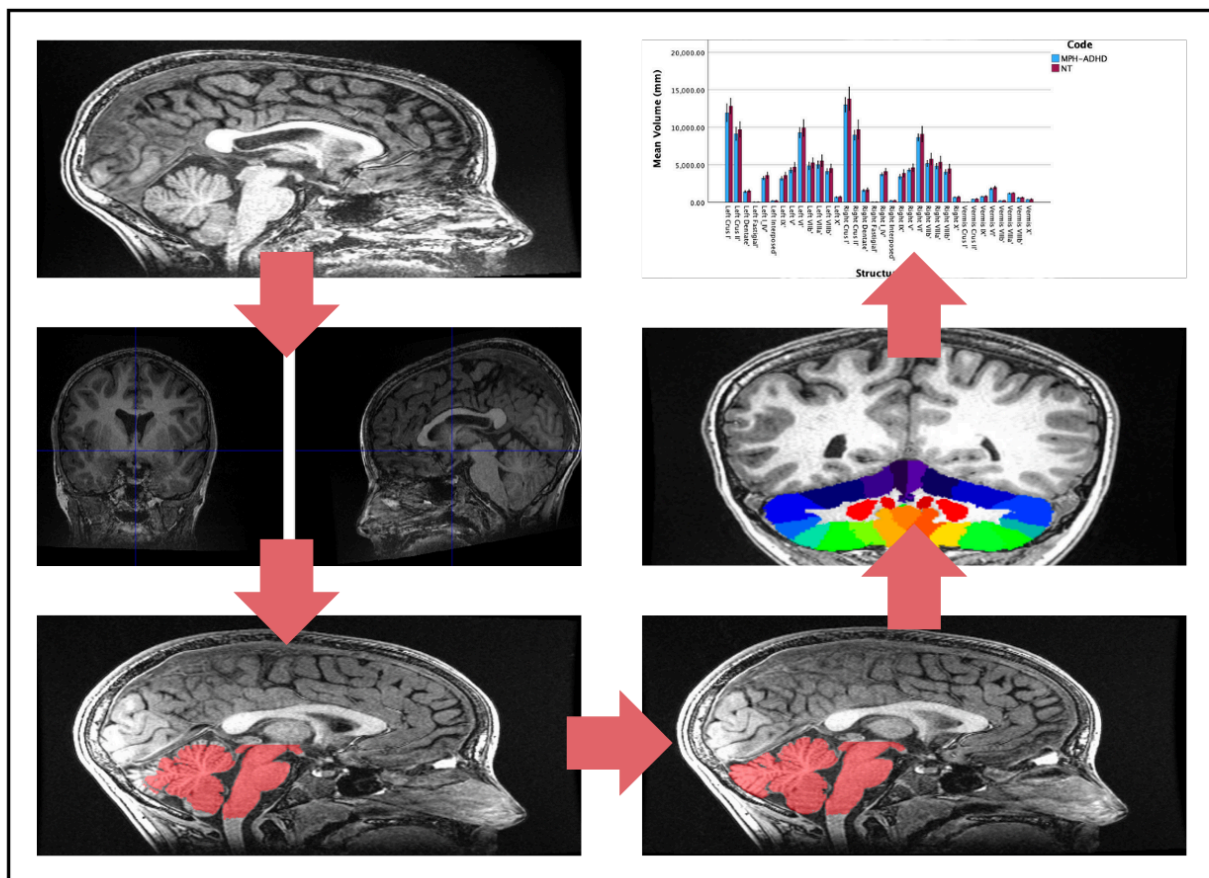


Fig. __: Summary of SUIT Toolbox Processes. MRI anatomical images (Panel 1) are reoriented by setting the origin to the anterior commissure in SPM (Panel 2). The cerebellum is isolated from the rest of the brain using SUIT (Panel 3), and the cerebellar mask is edited by hand to correct for program errors in MRIcron (Panel 4). The cerebellum is normalized to the atlas and resliced into native space with different regions identified (Panel 5). SUIT provides volume measurements for each region, which are then graphed in SPSS 29 (Panel 6).

Choosing a software

SUIT is a specialized program developed by Diedrichsen Lab using voxel-based morphometry to analyze the cerebellum from one individual to another. Specialized cerebellar atlases are provided as part of the SUIT MATLAB toolbox, focused on the human cerebellum and brainstem. The brainstem is important as this is where the cerebellar peduncles link to the rest of the brain. SUIT was chosen as the software for analysis because it can: (1) Automatically isolate cerebellar structures from the cerebrum in an anatomical image; (2) Achieve accurate normalization of the cerebellum into the atlas space using the Dartel algorithm; (3) Display data on a surface-based flatmap representation; (4) Use VBM to determine patterns of growth or shrinkage; and (5) Uses atlas to assign probable locations to the different cerebellar lobules and nuclei. The most commonly used atlas template for brain imaging is the ICBM152 template, which was created by averaging 152 brains after affine normalization (corrections to size, translation, rotation, etc.). This regular template does not show any clear differentiation for the cerebellum making analysis of specific regions of the cerebellum difficult to impossible. In addition, the normalization of the template leads to large spatial spread of cerebellar folia, whereas the SUIT template places the folia much closer together and in a manner that is accurate. In order to do this, Diedrichsen lab developed a new atlas based on the average anatomy of twenty healthy individuals aged 22-45. Certain characteristics about this template enable it to be specialized to the cerebellum, such as how it: (1) is specifically based on brainstem and cerebellum, (2) preserves the anatomical accuracy of the cerebellum to a far greater extent than the ICBM152 template, and (3) reduces spatial variance and improves overlap of deep cerebellar nuclei.

Using the SUIT Program

Prior to using the SUIT program, all images must be reoriented so the origin is set to the anterior commissure. This process can be done in SPM 12 and ensures proper normalization. To use the suit program, the first function used is "suit_isolate_seg". This function takes the original T1 weighted image and produces gray and white matter probability maps, representing the distribution of white and gray matter in the subject, as well as a cerebellar mask. In most cases, this cerebellar mask must be edited in MRIcron. The isolation function is performed in the native space of the original image, meaning that the image needs to be normalized to the cerebellar atlas in order to compare between various images. As such, the Normalization function "suit_normalize_dartel" deforms the image from the native space to suit space, changing location but not size. The Dartel algorithm uses the tissue segmentation maps -- in

this case white matter and gray matter maps -- to find the nonlinear deformation in the form of a three-dimensional mathematical model known as a flowfield. The normalization function may encounter the common error message stating the image is stated too far apart, in which the origin of the original T1 weighted image must be reset to a bundle of white matter in the brain known as the anterior commissure. This normalization function produces an affine matrix and non-linear flowfield. It is important to note that the normalization feature does not reslice the image into the atlas space, but only calculates the changes that would be necessary to make such a change. The next step in the process is to reslice the image into SUIT space using the "suit_reslice_dartel_inv". This function uses the products from the normalization function, as well as the SUIT cerebellar atlases and the original T1 weighted image, to reslice the image. This, in turn, produces a file that has split the cerebellum up into its specific volumes. Using the product of the reslice function as the input for the "suit_vol" function, the program generates the following information: number of voxels per region, volume in mm³ per region, and volume of one voxel. The key information here is the volume in mm³ per region, which should be recorded in a separate data table. Once both groups have been analyzed, a surface-based representation of the cerebellum can be created, which will allow for the display and comparison of volume-averaged cerebellar data between groups.

Editing Masks in MRICron

Oftentimes, the cerebellar mask created during the isolation function is inaccurate, failing to account for the many fissures and contours of the cerebellum. As such, to ensure proper results, the cerebellar mask must be properly edited in a MRI viewing software. In this case, MRICron was used. To edit masks in MRICron, they must first be opened as a VOI under the drawings section. A regular T1 image has around 350 slices within the image, all of which must be edited. For the most accurate editing, it is recommended that the sagittal image be used for the drawing of new masks, while the axial and coronal views be used as a reference point to ensure accuracy.

Data Analysis

Finding Significant Regions of Interest

```
# Python program to demonstrate how to
# perform two sample T-test

# Import the library
import numpy as np
import scipy.stats as stats

# Creating data groups
data_group1 = np.array([242.7239547,
205,
212])

data_group2 = np.array([234.2314157,
186.6420949,
193.5475373,
193.4126337,
241,
196,
220.2143668,
203.8274423,
213.1927764,
224.3260696])

# Perform the two sample t-test with equal variances
stats.ttest_ind(a=data_group1, b=data_group2, equal_var=True)

TtestResult(statistic=0.7388474447923281, pvalue=0.47546986149871473, df=11.0)
```

Fig. __: Code for conducting a two-sample t-test performed in Google Colaboratory

After preliminary graphical analysis of the data, structures from each comparison group were identified as having the greatest change from methylphenidate-using individuals to psychostimulant-negative individuals with ADHD, assuming change has occurred. Graphical analysis was completed in SPSS 29, where the volumes of each cerebellar region were plotted against its respective structure in a clustered bar graph. Three bar graphs were plotted to compare: (1) ADHD and medication-free vs. MPH-using individuals with ADHD; (2) ADHD vs. neurotypical individuals; and (3) MPH-using individuals with ADHD vs. neurotypical individuals. In order to determine likely statistical significance within each structure, error bars representing a 95% confidence interval were used. Overlap between these error bars could be subsequently analyzed, with lower overlap corresponding to higher levels of significance. Statistical significance was further confirmed or refuted using a two-sample t-test with an alpha level of 0.05.

Analysis of Medication Dosage and Duration

Each region with statistically significant differences were represented visually using three graphs. The first scatterplot compared medication dosage (mg) against regional volume (mm³). The second scatter plot compared methylphenidate medication duration (years) against regional volume (mm³). The third graph involved a coding system, in which letters correspond to medication dosage and numbers correspond to medication duration. For the letter system, code A refers to no medication, code B refers to <30mg, code C refers to >30mg and <60mg, and code D refers to >60mg. For the number system, number 1 refers to <2 years, number 2 refers to >2 years and <4 years, and number 3 refers to >4 years. Each letter and number will be uniquely paired, forming ten medication and dosage categories in total (A, B1, B2, B3, C1, C2, C3, D1, D2, D3). The average volume of the region of interest for all subjects meeting the criteria for each distinct category were then plotted as a bar graph with the aim of elucidating which combination of dosage and medication period have the greatest effect on cerebellar

structure. A least-squares regression line was created for each scatterplot, allowing for the Pearson's correlation coefficient (r value) and the R^2 value, revealing the nature and strength of the correlation.

Analysis of Whole-Cerebellar Volume

Total cerebellar volume was calculated by using the sum tool in Excel. These values were used to create a boxplot for each group (ADHD, MPH-ADHD, NT) in SPSS with the goal of displaying distribution skews and potential outliers, as well as variability.

OLD VERSION

Method

Overview

T1 weighted images from individuals between the ages of 5 and 18 will be gathered or repurposed from two sources: a neuromelanin study, a study completed as part of the TAG-IT demographics project. Remaining gaps will be filled out by collecting data from volunteers. Using the SUIT toolbox in MATLAB, the volumes of the various regions of the cerebellum will be extracted. After preliminary analysis of the data, three to five main structures will be identified as having the greatest change from methylphenidate-using individuals to psychostimulant-negative individuals with ADHD, assuming change has occurred. To identify relevant structure, SUIT's ability to create a surface-based representation of the cerebellum will be used. Each of these regions is represented visually using three graphs. The first scatterplot will plot medication dosage (mg) against regional volume (mm^3). The second scatter plot will plot methylphenidate medication duration (years) against regional volume (mm^3). The third graph will involve a coding system, in which letters correspond to medication dosage and numbers correspond to medication duration. For the letter system, code A refers to no medication, code B refers to $<30\text{mg}$, code C refers to $>30\text{mg}$ and $<60\text{mg}$, and code D refers to $>60\text{mg}$. For the number system, number 1 refers to <2 years, number 2 refers to >2 years and <4 years, and number 3 refers to >4 years. Each letter and number will be uniquely paired, forming ten medication and dosage categories in total (A, B1, B2, B3, C1, C2, C3, D1, D2, D3). The average volume of the region of interest for all subjects meeting the criteria for each distinct category is then plotted as a bar graph, which can elucidate which combination of dosage and medication period have the greatest effect on cerebellar structure.

Data Collection

Phase I: Pilot Study

To gain a better insight into the correlation between methylphenidate use and duration with cerebellar structure changes, a pilot study using eight T1 MR images will first be conducted. These eight images were originally collected for a separate study at BrainKids Lab, but was reused given it: (1) contains structural image data of children with ADHD, (2) includes children who both use and do not use methylphenidate, (3) comes with detailed patient information including duration and dose of the drug, and (4) was reliably collected and reused with the consent of the subjects. All eight of the images did not contain defects that prevented the data from being usable. It should be noted that subject number four had a metal retainer in their mouth during the MRI scan, but the distortion in the image mostly applies to the areas under the frontal lobes and does not disturb the cerebellum or brainstem. As such, this scan was not excluded.

Phase II: TAG-IT Demographics Data

In order to conduct many inferential statistics tests in an accurate manner, as well as to mitigate the effects of outliers, a larger sample size is required. A recent study conducted in conjunction with BrainKids Lab contained T1 weighted images from children with a mean age

of around 11 to 12. In total, there were forty MRIs conducted for this study. However, certain exclusion criteria must be applied to the scans in order when gathering data on methylphenidate-using individuals: (1) no artifacts or distortions may be present in the cerebellum in any of the three dimensions, (2) subject must currently be taking a methylphenidate stimulant medication for ADHD, (3) subject must include dose and duration of their current medication. Other exclusion factors may be implemented on a case-by-case basis, and will be noted if such a circumstance occurs. A similar exclusion criteria must be applied when selecting data for the non-methylphenidate-using subjects: (1) no artifacts or distortions may be present in the cerebellum in any of the three dimensions, (2) subject must not be currently taking a methylphenidate stimulant medication for ADHD, or have taken the medication for an extended period of time in the past, (3) subject must not be on any additional psychostimulant medication, including amphetamines, (4) must explicitly state no prior medication history. Lastly, the TAG-IT demographics also includes data from non-ADHD patients which can be used as a negative control when interpreting results. Exclusion criteria for this group include: (1) no artifacts or distortions may be present in the cerebellum in any of the three dimensions, (2) subject must not be currently taking a methylphenidate stimulant medication for ADHD, or have taken the medication for an extended period of time in the past, (3) subject must not be on any additional psychostimulant medication, including amphetamines, (4) must not have a diagnosis for ADHD or any other neurocognitive disability (must be neurotypical).

Phase III: Volunteer-based Data

Depending on the number of participants that meet the exclusion criteria from the TAG-IT study, additional and specific data may be required. The precise requirements and criteria for study participants will be similar to those mentioned in Phase II, although groups underrepresented in the Phase II data may be emphasized during recruitment. In order to obtain this data, this study will first have to be approved by the University of Calgary's Internal Review Board. In addition, this phase of the study cannot proceed until the Alberta Children's Hospital's research MRI is finished renovating in mid-2024. A CAIR Level 0 certification, which is required to assist in the operation of an MRI and to be present in the MRI suite, has already been obtained. In order to schedule MRI use, however, a CAIR Level 1 certification must be obtained. This cannot occur until the research MRI is once again available for use, meaning Phase III will be implemented after the completion of the science fair.

Data Extraction

Choosing a software

SUIT is a specialized program developed by Diedrichsen Lab using voxel-based morphometry to analyze the cerebellum from one individual to another. Specialized cerebellar atlases are provided as part of the SUIT MATLAB toolbox, focused on the human cerebellum and brainstem. The brainstem is important as this is where the cerebellar peduncles link to the rest of the brain. SUIT was chosen as the software for analysis because it can: (1) Automatically isolate cerebellar structures from the cerebrum in an anatomical image; (2) Achieve accurate

normalization of the cerebellum into the atlas space using the Dartel algorithm; (3) Display data on a surface-based flatmap representation; (4) Use VBM to determine patterns of growth or shrinkage; and (5) Uses atlas to assign probable locations to the different cerebellar lobules and nuclei. The most commonly used atlas template for brain imaging is the ICBM152 template, which was created by averaging 152 brains after affine normalization (corrections to size, translation, rotation, etc.). This regular template does not show any clear differentiation for the cerebellum making analysis of specific regions of the cerebellum difficult to impossible. In addition, the normalization of the template leads to large spatial spread of cerebellar folia, whereas the SUIT template places the folia much closer together and in a manner that is accurate. In order to do this, Diedrichsen lab developed a new atlas based on the average anatomy of twenty healthy individuals aged 22-45. Certain characteristics about this template enable it to be specialized to the cerebellum, such as how it: (1) is specifically based on brainstem and cerebellum, (2) preserves the anatomical accuracy of the cerebellum to a far greater extent than the ICBM152 template, and (3) reduces spatial variance and improves overlap of deep cerebellar nuclei.

Using the SUIT Program

To use the suit program, the first function used is "suit_isolate_seg". This function takes the original T1 weighted image and produces gray and white matter probability maps, representing the distribution of white and gray matter in the subject, as well as a cerebellar mask. In most cases, this cerebellar mask must be edited in MRIcron. The isolation function is performed in the native space of the original image, meaning that the image needs to be normalized to the cerebellar atlas in order to compare between various images. As such, the Normalization function "suit_normalize_dartel" deforms the image from the native space to suit space, changing location but not size. The Dartel algorithm uses the tissue segmentation maps -- in this case white matter and gray matter maps -- to find the nonlinear deformation in the form of a three-dimensional mathematical model known as a flowfield. The normalization function may encounter the common error message stating the image is stated too far apart, in which the origin of the original T1 weighted image must be reset to a bundle of white matter in the brain known as the anterior commissure. This normalization function produces an affine matrix and non-linear flowfield. It is important to note that the normalization feature does not reslice the image into the atlas space, but only calculates the changes that would be necessary to make such a change. The next step in the process is to reslice the image into SUIT space using the "suit_reslice_dartel_inv". This function uses the products from the normalization function, as well as the SUIT cerebellar atlases and the original T1 weighted image, to reslice the image. This, in turn, produces a file that has split the cerebellum up into its specific volumes. Using the product of the reslice function as the input for the "suit_vol" function, the program generates the following information: number of voxels per region, volume in mm³ per region, and volume of one voxel. The key information here is the volume in mm³ per region, which should be recorded in a separate data table. Once both groups have been analyzed, a surface-based representation of the cerebellum can be created, which will allow for the display and comparison of volume-averaged cerebellar data between groups.

Editing Masks in MRICron

Oftentimes, the cerebellar mask created during the isolation function is inaccurate, failing to account for the many fissures and contours of the cerebellum. As such, to ensure proper results, the cerebellar mask must be properly edited in a MRI viewing software. In this case, MRICron was used. To edit masks in MRICron, they must first be opened as a VOI under the drawings section. A regular T1 image has around 350 slices within the image, all of which must be edited. For the most accurate editing, it is recommended that the sagittal image be used for the drawing of new masks, while the axial and coronal views be used as a reference point to ensure accuracy. The redrawn file must be saved as a NIFTI (.nii) file and the .nii extension must be added to the end of the file name in order for saving to occur properly.

Data Analysis

In order to establish the relationship, or the lack of one, between methylphenidate and changes in cerebellar structures, multiple forms of data analysis must be performed. Before commencing data analysis, outliers within each group should be identified and removed using the 1.5 IQR rule. A least-squares regression line will be created for each scatterplot, allowing for the Pearson's correlation coefficient (r value) and the R^2 squared value. In turn, this will allow for the nature of the correlation, as well as the strength of the correlation, to be revealed. After calculating the sample means and standard deviations for each region in both methylphenidate-using and medication-free individuals with ADHD, a standard t test can be conducted. Setting the confidence interval to 95%, any differences must have a p -value of less than 0.05 in order to show statistical significance. Comparisons can be made using all regions, as well as between each ADHD medication level and the negative control (individual without ADHD). The use of a t test will allow for the comparison between the use of methylphenidate and medication free individuals. Further analysis can be conducted using an ANOVA test. Analysis of variance tests can show how the dependent variable changes with varying levels of the independent variable. In this case, the dependent variable is the cerebellar regional volume, while the independent variable levels are the dosage and duration of medication. A one way ANOVA test can be used to gain a better understanding how each independent variable affects cerebellar structure, but a two-way ANOVA test will also be used to understand how both dosage and duration of methylphenidate use will impact the cerebellum.

Problem

Attention deficit hyperactivity disorder (ADHD) is a neurodevelopmental disorder classified by differences in executive functioning and motivation, with estimates suggesting the condition affects up to 8.4% of children and 2.5% of adults (Harpin, 2005). From a neuroimaging standpoint, ADHD is classified by changes in overall brain volume, although these changes can be partially localized to some regions. Methylphenidate (MPH), a psychostimulant, is the most commonly used medication prescribed for ADHD treatment, oftentimes under brand names such as Ritalin. As a reuptake inhibitor, MPH increases the concentration of dopamine in the synapse, which has dramatic effects on the dopaminergic pathway in the mesolimbic system.

Despite the many benefits of MPH as a medication, existing literature demonstrates that particular doses and usage durations of MPH can have a variety of effects on brain structure and composition, many of which are still not fully understood. In particular, some existing works highlight the effects of MPH on the cerebellar structures, especially in the context of apoptosis pathways, cortical thickness, and increased disease risk (Raofi et al., 2020; Bahcelioglu et al., 2009; 2017; Reus et al., 2014; Quansah et al., 2018; Curtin et al., 2018; Mackey et al., 2013). The effects of MPH also appear to extend to the prefrontal cortex, hippocampus, and striatum (Motaghinejad et al., 2016; Schmitz et al., 2012; Lizanne et al., 2012). Much of this existing literature, however, is still contradictory and little consistency exists in the results from one study to another. Given the prevalence of MPH use in children with ADHD, as well as the continued gaps in scientific knowledge, these findings are cause for concern. As such, this project aims to examine the correlation between methylphenidate dosage and usage duration by performing volumetric analyses on T1 weighted MR images. To differentiate itself from the inconsistency existing in existing literature, results from the volumetric analysis will be coupled with detailed medication history to eliminate confounding variables. Ultimately, this project aims to (1) elucidate the structural changes that occur in the cerebellum; (2) identify how dosage and duration impact these structural changes, and (3) illuminate the possible mechanisms for harmful effects as a result of cerebellar degeneration.

SECTION IV: DATA

Raw Data

Participant	Code	Structure	Volume (mm)
1	NT	Left I_IV'	3510.79035
1	NT	Right I_IV'	4094.3919
1	NT	Left V'	4481.38088
1	NT	Right V'	4385.23993
1	NT	Left VI'	9497.34009
1	NT	Vermis VI'	2033.16457
1	NT	Right VI'	8786.93642
1	NT	Left Crus I'	12297.3803
1	NT	Vermis Crus I'	13.3384742
1	NT	Right Crus I'	13758.3763
1	NT	Left Crus II'	9380.23868
1	NT	Vermis Crus II'	461.823016
1	NT	Right Crus II'	9440.52165
1	NT	Left VIIb'	5114.87179
1	NT	Vermis VIIb'	228.832785
1	NT	Right VIIb'	5590.03328
1	NT	Left VIIIa'	5440.53843
1	NT	Vermis VIIIa'	1199.07686
1	NT	Right VIIIa'	5118.50956
1	NT	Left VIIIb'	4522.95535
1	NT	Vermis VIIIb'	620.325664
1	NT	Right VIIIb'	4539.93159
1	NT	Left IX'	3565.18361
1	NT	Vermis IX'	821.268912
1	NT	Right IX'	3825.89015
1	NT	Left X'	716.639842
1	NT	Vermis X'	358.06008
1	NT	Right X'	742.277428

1	NT	Left Dentate'	1528.72773
1	NT	Right Dentate'	1679.26194
1	NT	Left Interposed'	208.73846
1	NT	Right Interposed'	219.305303
1	NT	Left Fastigial'	40.3618765
1	NT	Right Fastigial'	38.976061
2	NT	Left I_IV'	4035.41075
2	NT	Right I_IV'	4565.96068
2	NT	Left V'	5404.52143
2	NT	Right V'	5166.17353
2	NT	Left VI'	11093.0799
2	NT	Vermis VI'	2135.57641
2	NT	Right VI'	10383.9428
2	NT	Left Crus I'	13624.7447
2	NT	Vermis Crus I'	18.0671883
2	NT	Right Crus I'	15794.1971
2	NT	Left Crus II'	10628.371
2	NT	Vermis Crus II'	472.179018
2	NT	Right Crus II'	11364.0877
2	NT	Left VIIb'	5792.44481
2	NT	Vermis VIIb'	216.111368
2	NT	Right VIIb'	6643.16617
2	NT	Left VIIIa'	6144.75499
2	NT	Vermis VIIIa'	1222.4885
2	NT	Right VIIIa'	6143.88637
2	NT	Left VIIIb'	4998.87831
2	NT	Vermis VIIIb'	644.164753
2	NT	Right VIIIb'	5124.13257
2	NT	Left IX'	3774.8263

2	NT	Vermis IX'	852.458588
2	NT	Right IX'	4227.37462
2	NT	Left X'	797.562131
2	NT	Vermis X'	487.640362
2	NT	Right X'	817.887718
2	NT	Left Dentate'	1686.32882
2	NT	Right Dentate'	1968.62864
2	NT	Left Interposed'	246.68661
2	NT	Right Interposed'	267.18592
2	NT	Left Fastigial'	44.6468019
2	NT	Right Fastigial'	48.9898761
3	NT	Left I_IV'	3759.80817
3	NT	Right I_IV'	4173.50764
3	NT	Left V'	4842.79731
3	NT	Right V'	4750.07156
3	NT	Left VI'	10436.2316
3	NT	Vermis VI'	1909.36913
3	NT	Right VI'	9350.35539
3	NT	Left Crus I'	13696.9171
3	NT	Vermis Crus I'	13.9258444
3	NT	Right Crus I'	13952.1677
3	NT	Left Crus II'	10425.5325
3	NT	Vermis Crus II'	484.517489
3	NT	Right Crus II'	9929.80638
3	NT	Left VIIb'	5697.70829
3	NT	Vermis VIIb'	231.474707
3	NT	Right VIIb'	6060.45956
3	NT	Left VIIIa'	6073.53627
3	NT	Vermis VIIIa'	1250.26911

3	NT	Right VIIIa'	5803.17109
3	NT	Left VIIIb'	4816.30424
3	NT	Vermis VIIIb'	635.833677
3	NT	Right VIIIb'	4564.95973
3	NT	Left IX'	4011.66216
3	NT	Vermis IX'	831.474808
3	NT	Right IX'	4219.53086
3	NT	Left X'	762.355068
3	NT	Vermis X'	436.626171
3	NT	Right X'	723.974082
3	NT	Left Dentate'	1419.58699
3	NT	Right Dentate'	1540.16443
3	NT	Left Interposed'	187.659245
3	NT	Right Interposed'	201.245435
3	NT	Left Fastigial'	35.4939205
3	NT	Right Fastigial'	38.7206406
4	NT	Left I_IV'	3156.88626
4	NT	Right I_IV'	3621.63806
4	NT	Left V'	4065.62655
4	NT	Right V'	4132.41516
4	NT	Left VI'	8770.4166
4	NT	Vermis VI'	1766.78354
4	NT	Right VI'	8218.80501
4	NT	Left Crus I'	11824.0055
4	NT	Vermis Crus I'	14.1882529
4	NT	Right Crus I'	12560.2374
4	NT	Left Crus II'	8662.96654
4	NT	Vermis Crus II'	381.871635
4	NT	Right Crus II'	8746.88486

4	NT	Left VIIb'	4439.53893
4	NT	Vermis VIIb'	186.869672
4	NT	Right VIIb'	5023.8527
4	NT	Left VIIIa'	4593.87943
4	NT	Vermis VIIIa'	1126.23583
4	NT	Right VIIIa'	4612.5664
4	NT	Left VIIIb'	3792.76223
4	NT	Vermis VIIIb'	563.204428
4	NT	Right VIIIb'	3783.59177
4	NT	Left IX'	3106.01618
4	NT	Vermis IX'	690.379621
4	NT	Right IX'	3317.45576
4	NT	Left X'	591.580933
4	NT	Vermis X'	321.485047
4	NT	Right X'	582.410477
4	NT	Left Dentate'	1351.34457
4	NT	Right Dentate'	1434.57079
4	NT	Left Interposed'	175.276831
4	NT	Right Interposed'	200.192787
4	NT	Left Fastigial'	33.3943025
4	NT	Right Fastigial'	35.8166871
5	NT	Left I_IV'	3477.34833
5	NT	Right I_IV'	4064.0727
5	NT	Left V'	4624.24458
5	NT	Right V'	4668.27032
5	NT	Left VI'	9767.37621
5	NT	Vermis VI'	1964.88425
5	NT	Right VI'	8662.45002
5	NT	Left Crus I'	12753.5891

5	NT	Vermis Crus I'	14.3897364
5	NT	Right Crus I'	13033.5038
5	NT	Left Crus II'	9424.07821
5	NT	Vermis Crus II'	416.788437
5	NT	Right Crus II'	9062.62173
5	NT	Left VIIb'	5205.31584
5	NT	Vermis VIIb'	224.582672
5	NT	Right VIIb'	5435.20901
5	NT	Left VIIIa'	5401.97557
5	NT	Vermis VIIIa'	1276.74649
5	NT	Right VIIIa'	5014.82314
5	NT	Left VIIIb'	4446.94247
5	NT	Vermis VIIIb'	626.467453
5	NT	Right VIIIb'	4332.50981
5	NT	Left IX'	3437.60525
5	NT	Vermis IX'	789.379826
5	NT	Right IX'	3666.64188
5	NT	Left X'	659.186973
5	NT	Vermis X'	310.92109
5	NT	Right X'	645.311156
5	NT	Left Dentate'	1538.84527
5	NT	Right Dentate'	1634.94815
5	NT	Left Interposed'	233.147991
5	NT	Right Interposed'	246.509889
5	NT	Left Fastigial'	40.9422262
5	NT	Right Fastigial'	46.9379497
6	ADHD	Left I_IV'	3936.85987
6	ADHD	Right I_IV'	4575.47799
6	ADHD	Left V'	5492.22095

6	ADHD	Right V'	5137.33575
6	ADHD	Left VI'	12723.8175
6	ADHD	Vermis VI'	2427.59005
6	ADHD	Right VI'	10931.6911
6	ADHD	Left Crus I'	16522.2284
6	ADHD	Vermis Crus I'	16.8241875
6	ADHD	Right Crus I'	16001.3796
6	ADHD	Left Crus II'	12603.2442
6	ADHD	Vermis Crus II'	496.488782
6	ADHD	Right Crus II'	11532.8053
6	ADHD	Left VIIb'	6918.77185
6	ADHD	Vermis VIIb'	243.074459
6	ADHD	Right VIIb'	7013.0574
6	ADHD	Left VIIIa'	7179.89726
6	ADHD	Vermis VIIIa'	1498.22895
6	ADHD	Right VIIIa'	6648.70859
6	ADHD	Left VIIIb'	5612.96955
6	ADHD	Vermis VIIIb'	725.893589
6	ADHD	Right VIIIb'	5186.05579
6	ADHD	Left IX'	3560.76918
6	ADHD	Vermis IX'	820.880147
6	ADHD	Right IX'	3811.02897
6	ADHD	Left X'	893.78496
6	ADHD	Vermis X'	434.800095
6	ADHD	Right X'	858.033561
6	ADHD	Left Dentate'	1770.04472
6	ADHD	Right Dentate'	1875.8969
6	ADHD	Left Interposed'	233.786105
6	ADHD	Right Interposed'	242.723955

6	ADHD	Left Fastigial'	45.0397519
6	ADHD	Right Fastigial'	48.194287
7	ADHD	Left I_IV'	3081
7	ADHD	Right I_IV'	3465
7	ADHD	Left V'	4194
7	ADHD	Right V'	3989
7	ADHD	Left VI'	8923
7	ADHD	Vermis VI'	1759
7	ADHD	Right VI'	8069
7	ADHD	Left Crus I'	11609
7	ADHD	Vermis Crus I'	11
7	ADHD	Right Crus I'	11736
7	ADHD	Left Crus II'	8883
7	ADHD	Vermis Crus II'	369
7	ADHD	Right Crus II'	8202
7	ADHD	Left VIIb'	4509
7	ADHD	Vermis VIIb'	196
7	ADHD	Right VIIb'	4634
7	ADHD	Left VIIIa'	4637
7	ADHD	Vermis VIIIa'	1170
7	ADHD	Right VIIIa'	4142
7	ADHD	Left VIIIb'	3653
7	ADHD	Vermis VIIIb'	545
7	ADHD	Right VIIIb'	3607
7	ADHD	Left IX'	2764
7	ADHD	Vermis IX'	673
7	ADHD	Right IX'	3067
7	ADHD	Left X'	583
7	ADHD	Vermis X'	245

7	ADHD	Right X'	548
7	ADHD	Left Dentate'	1290
7	ADHD	Right Dentate'	1520
7	ADHD	Left Interposed'	180
7	ADHD	Right Interposed'	205
7	ADHD	Left Fastigial'	28
7	ADHD	Right Fastigial'	38
8	ADHD	Left I_IV'	3275
8	ADHD	Right I_IV'	3817
8	ADHD	Left V'	4358
8	ADHD	Right V'	4303
8	ADHD	Left VI'	9072
8	ADHD	Vermis VI'	1838
8	ADHD	Right VI'	8333
8	ADHD	Left Crus I'	11698
8	ADHD	Vermis Crus I'	10
8	ADHD	Right Crus I'	12062
8	ADHD	Left Crus II'	9756
8	ADHD	Vermis Crus II'	421
8	ADHD	Right Crus II'	9114
8	ADHD	Left VIIb'	5488
8	ADHD	Vermis VIIb'	233
8	ADHD	Right VIIb'	5609
8	ADHD	Left VIIIa'	5583
8	ADHD	Vermis VIIIa'	1387
8	ADHD	Right VIIIa'	5155
8	ADHD	Left VIIIb'	4464
8	ADHD	Vermis VIIIb'	677
8	ADHD	Right VIIIb'	4240

8	ADHD	Left IX'	3968
8	ADHD	Vermis IX'	820
8	ADHD	Right IX'	3805
8	ADHD	Left X'	714
8	ADHD	Vermis X'	455
8	ADHD	Right X'	711
8	ADHD	Left Dentate'	1348
8	ADHD	Right Dentate'	1529
8	ADHD	Left Interposed'	199
8	ADHD	Right Interposed'	212
8	ADHD	Left Fastigial'	38
8	ADHD	Right Fastigial'	42
9	MPH-ADHD	Left I_IV'	3339.23003
9	MPH-ADHD	Right I_IV'	3937.10993
9	MPH-ADHD	Left V'	4186.84443
9	MPH-ADHD	Right V'	4577.11778
9	MPH-ADHD	Left VI'	9054.81359
9	MPH-ADHD	Vermis VI'	1779.65322
9	MPH-ADHD	Right VI'	9170.58121
9	MPH-ADHD	Left Crus I'	10560.1296
9	MPH-ADHD	Vermis Crus I'	12.9754094
9	MPH-ADHD	Right Crus I'	13253.1168
9	MPH-ADHD	Left Crus II'	8581.96945
9	MPH-ADHD	Vermis Crus II'	385.386509
9	MPH-ADHD	Right Crus II'	8889.16648
9	MPH-ADHD	Left VIIb'	4397.48419
9	MPH-ADHD	Vermis VIIb'	192.440487
9	MPH-ADHD	Right VIIb'	4867.29512
9	MPH-ADHD	Left VIIIa'	4525.21614

9	MPH-ADHD	Vermis VIIIa'	1127.51252
9	MPH-ADHD	Right VIIIa'	4548.63928
9	MPH-ADHD	Left VIIIb'	3807.01881
9	MPH-ADHD	Vermis VIIIb'	567.04224
9	MPH-ADHD	Right VIIIb'	3697.31762
9	MPH-ADHD	Left IX'	3107.86331
9	MPH-ADHD	Vermis IX'	746.67583
9	MPH-ADHD	Right IX'	3327.77122
9	MPH-ADHD	Left X'	627.200956
9	MPH-ADHD	Vermis X'	376.792407
9	MPH-ADHD	Right X'	585.410028
9	MPH-ADHD	Left Dentate'	1535.3111
9	MPH-ADHD	Right Dentate'	1729.26819
9	MPH-ADHD	Left Interposed'	202.719707
9	MPH-ADHD	Right Interposed'	234.231416
9	MPH-ADHD	Left Fastigial'	41.7909289
9	MPH-ADHD	Right Fastigial'	39.2632517
10	MPH-ADHD	Left I_IV'	2568.89534
10	MPH-ADHD	Right I_IV'	3106.26974
10	MPH-ADHD	Left V'	3226.43427
10	MPH-ADHD	Right V'	3634.72437
10	MPH-ADHD	Left VI'	7335.58971
10	MPH-ADHD	Vermis VI'	1494.48314
10	MPH-ADHD	Right VI'	7326.33334
10	MPH-ADHD	Left Crus I'	8747.607
10	MPH-ADHD	Vermis Crus I'	10.9393473
10	MPH-ADHD	Right Crus I'	10056.9627
10	MPH-ADHD	Left Crus II'	6784.7515
10	MPH-ADHD	Vermis Crus II'	344.673589

10	MPH-ADHD	Right Crus II'	6992.5991
10	MPH-ADHD	Left VIIb'	3415.43253
10	MPH-ADHD	Vermis VIIb'	167.119567
10	MPH-ADHD	Right VIIb'	3937.15525
10	MPH-ADHD	Left VIIIa'	3509.67921
10	MPH-ADHD	Vermis VIIIa'	999.183154
10	MPH-ADHD	Right VIIIa'	3743.10806
10	MPH-ADHD	Left VIIIb'	3032.21878
10	MPH-ADHD	Vermis VIIIb'	510.11018
10	MPH-ADHD	Right VIIIb'	3152.04671
10	MPH-ADHD	Left IX'	2460.84825
10	MPH-ADHD	Vermis IX'	645.084896
10	MPH-ADHD	Right IX'	2581.68597
10	MPH-ADHD	Left X'	510.11018
10	MPH-ADHD	Vermis X'	323.636383
10	MPH-ADHD	Right X'	526.771648
10	MPH-ADHD	Left Dentate'	1199.79395
10	MPH-ADHD	Right Dentate'	1445.17193
10	MPH-ADHD	Left Interposed'	150.962993
10	MPH-ADHD	Right Interposed'	186.642095
10	MPH-ADHD	Left Fastigial'	29.7886842
10	MPH-ADHD	Right Fastigial'	33.4912325
11	MPH-ADHD	Left I_IV'	3041.56112
11	MPH-ADHD	Right I_IV'	3553.0297
11	MPH-ADHD	Left V'	4015.23799
11	MPH-ADHD	Right V'	4074.9792
11	MPH-ADHD	Left VI'	8512.07396
11	MPH-ADHD	Vermis VI'	1602.53169
11	MPH-ADHD	Right VI'	8133.36362

11	MPH-ADHD	Left Crus I'	11006.0073
11	MPH-ADHD	Vermis Crus I'	11.7036868
11	MPH-ADHD	Right Crus I'	12095.4983
11	MPH-ADHD	Left Crus II'	8172.84172
11	MPH-ADHD	Vermis Crus II'	367.356021
11	MPH-ADHD	Right Crus II'	8540.37243
11	MPH-ADHD	Left VIIb'	4350.62722
11	MPH-ADHD	Vermis VIIb'	178.699576
11	MPH-ADHD	Right VIIb'	5131.97933
11	MPH-ADHD	Left VIIIa'	4670.99382
11	MPH-ADHD	Vermis VIIIa'	1032.54467
11	MPH-ADHD	Right VIIIa'	4662.95845
11	MPH-ADHD	Left VIIIb'	3819.24491
11	MPH-ADHD	Vermis VIIIb'	534.35191
11	MPH-ADHD	Right VIIIb'	3815.22722
11	MPH-ADHD	Left IX'	2972.56177
11	MPH-ADHD	Vermis IX'	687.897294
11	MPH-ADHD	Right IX'	3297.29541
11	MPH-ADHD	Left X'	595.665255
11	MPH-ADHD	Vermis X'	343.075238
11	MPH-ADHD	Right X'	598.460165
11	MPH-ADHD	Left Dentate'	1286.35746
11	MPH-ADHD	Right Dentate'	1407.06265
11	MPH-ADHD	Left Interposed'	176.079348
11	MPH-ADHD	Right Interposed'	193.547537
11	MPH-ADHD	Left Fastigial'	36.3338337
11	MPH-ADHD	Right Fastigial'	37.2072432
12	MPH-ADHD	Left I_IV'	3176.46992
12	MPH-ADHD	Right I_IV'	3663.41266

12	MPH-ADHD	Left V'	4258.14798
12	MPH-ADHD	Right V'	4262.41193
12	MPH-ADHD	Left VI'	8983.62455
12	MPH-ADHD	Vermis VI'	1693.98084
12	MPH-ADHD	Right VI'	8204.17505
12	MPH-ADHD	Left Crus I'	11827.5066
12	MPH-ADHD	Vermis Crus I'	14.4974196
12	MPH-ADHD	Right Crus I'	12412.6907
12	MPH-ADHD	Left Crus II'	8844.61988
12	MPH-ADHD	Vermis Crus II'	366.699438
12	MPH-ADHD	Right Crus II'	8423.51248
12	MPH-ADHD	Left VIIb'	4815.53113
12	MPH-ADHD	Vermis VIIb'	173.457362
12	MPH-ADHD	Right VIIb'	4988.30626
12	MPH-ADHD	Left VIIIa'	5148.97178
12	MPH-ADHD	Vermis VIIIa'	1076.04965
12	MPH-ADHD	Right VIIIa'	4849.47215
12	MPH-ADHD	Left VIIIb'	4318.86659
12	MPH-ADHD	Vermis VIIIb'	574.609491
12	MPH-ADHD	Right VIIIb'	4197.25882
12	MPH-ADHD	Left IX'	3379.60435
12	MPH-ADHD	Vermis IX'	726.235445
12	MPH-ADHD	Right IX'	3594.16616
12	MPH-ADHD	Left X'	624.241834
12	MPH-ADHD	Vermis X'	354.419271
12	MPH-ADHD	Right X'	621.854023
12	MPH-ADHD	Left Dentate'	1228.18728
12	MPH-ADHD	Right Dentate'	1335.46819
12	MPH-ADHD	Left Interposed'	162.200542

12	MPH-ADHD	Right Interposed'	193.412634
12	MPH-ADHD	Left Fastigial'	32.4059968
12	MPH-ADHD	Right Fastigial'	29.8476287
13	MPH-ADHD	Left I_IV'	3326
13	MPH-ADHD	Right I_IV'	3714
13	MPH-ADHD	Left V'	4597
13	MPH-ADHD	Right V'	4390
13	MPH-ADHD	Left VI'	10255
13	MPH-ADHD	Vermis VI'	1810
13	MPH-ADHD	Right VI'	9216
13	MPH-ADHD	Left Crus I'	13221
13	MPH-ADHD	Vermis Crus I'	13
13	MPH-ADHD	Right Crus I'	14198
13	MPH-ADHD	Left Crus II'	9952
13	MPH-ADHD	Vermis Crus II'	435
13	MPH-ADHD	Right Crus II'	9569
13	MPH-ADHD	Left VIIb'	5123
13	MPH-ADHD	Vermis VIIb'	207
13	MPH-ADHD	Right VIIb'	5494
13	MPH-ADHD	Left VIIIa'	5315
13	MPH-ADHD	Vermis VIIIa'	1157
13	MPH-ADHD	Right VIIIa'	4981
13	MPH-ADHD	Left VIIIb'	4196
13	MPH-ADHD	Vermis VIIIb'	550
13	MPH-ADHD	Right VIIIb'	4191
13	MPH-ADHD	Left IX'	3038
13	MPH-ADHD	Vermis IX'	686
13	MPH-ADHD	Right IX'	3260
13	MPH-ADHD	Left X'	682

13	MPH-ADHD	Vermis X'	382
13	MPH-ADHD	Right X'	695
13	MPH-ADHD	Left Dentate'	1611
13	MPH-ADHD	Right Dentate'	1849
13	MPH-ADHD	Left Interposed'	217
13	MPH-ADHD	Right Interposed'	241
13	MPH-ADHD	Left Fastigial'	30
13	MPH-ADHD	Right Fastigial'	30
14	MPH-ADHD	Left I_IV'	2960
14	MPH-ADHD	Right I_IV'	3479
14	MPH-ADHD	Left V'	3876
14	MPH-ADHD	Right V'	4053
14	MPH-ADHD	Left VI'	8697
14	MPH-ADHD	Vermis VI'	1807
14	MPH-ADHD	Right VI'	8269
14	MPH-ADHD	Left Crus I'	10628
14	MPH-ADHD	Vermis Crus I'	15
14	MPH-ADHD	Right Crus I'	12152
14	MPH-ADHD	Left Crus II'	8298
14	MPH-ADHD	Vermis Crus II'	369
14	MPH-ADHD	Right Crus II'	8504
14	MPH-ADHD	Left VIIb'	4528
14	MPH-ADHD	Vermis VIIb'	219
14	MPH-ADHD	Right VIIb'	4855
14	MPH-ADHD	Left VIIIa'	4709
14	MPH-ADHD	Vermis VIIIa'	1183
14	MPH-ADHD	Right VIIIa'	4374
14	MPH-ADHD	Left VIIIb'	3892
14	MPH-ADHD	Vermis VIIIb'	574

14	MPH-ADHD	Right VIIIb'	3699
14	MPH-ADHD	Left IX'	2884
14	MPH-ADHD	Vermis IX'	703
14	MPH-ADHD	Right IX'	3026
14	MPH-ADHD	Left X'	541
14	MPH-ADHD	Vermis X'	298
14	MPH-ADHD	Right X'	564
14	MPH-ADHD	Left Dentate'	1219
14	MPH-ADHD	Right Dentate'	1339
14	MPH-ADHD	Left Interposed'	171
14	MPH-ADHD	Right Interposed'	196
14	MPH-ADHD	Left Fastigial'	35
14	MPH-ADHD	Right Fastigial'	33
15	MPH-ADHD	Left I_IV'	3498.56142
15	MPH-ADHD	Right I_IV'	3968.83229
15	MPH-ADHD	Left V'	4474.77652
15	MPH-ADHD	Right V'	4457.79737
15	MPH-ADHD	Left VI'	9763.69446
15	MPH-ADHD	Vermis VI'	1919.50093
15	MPH-ADHD	Right VI'	9000.66197
15	MPH-ADHD	Left Crus I'	13662.5521
15	MPH-ADHD	Vermis Crus I'	12.5199757
15	MPH-ADHD	Right Crus I'	14156.4909
15	MPH-ADHD	Left Crus II'	10430.3403
15	MPH-ADHD	Vermis Crus II'	413.330704
15	MPH-ADHD	Right Crus II'	9916.50677
15	MPH-ADHD	Left VIIb'	5509.81834
15	MPH-ADHD	Vermis VIIb'	211.810548
15	MPH-ADHD	Right VIIb'	5682.5254

15	MPH-ADHD	Left VIIIa'	5680.12431
15	MPH-ADHD	Vermis VIIIa'	1246.16635
15	MPH-ADHD	Right VIIIa'	5309.15572
15	MPH-ADHD	Left VIIIb'	4703.3947
15	MPH-ADHD	Vermis VIIIb'	632.859045
15	MPH-ADHD	Right VIIIb'	4458.14038
15	MPH-ADHD	Left IX'	3458.94342
15	MPH-ADHD	Vermis IX'	757.544282
15	MPH-ADHD	Right IX'	3705.05527
15	MPH-ADHD	Left X'	795.790235
15	MPH-ADHD	Vermis X'	343.870565
15	MPH-ADHD	Right X'	696.316456
15	MPH-ADHD	Left Dentate'	1484.3889
15	MPH-ADHD	Right Dentate'	1631.54149
15	MPH-ADHD	Left Interposed'	204.264261
15	MPH-ADHD	Right Interposed'	220.214367
15	MPH-ADHD	Left Fastigial'	37.3884205
15	MPH-ADHD	Right Fastigial'	39.1034857
16	MPH-ADHD	Left I_IV'	3512.13024
16	MPH-ADHD	Right I_IV'	3909.57645
16	MPH-ADHD	Left V'	4758.97281
16	MPH-ADHD	Right V'	4473.649
16	MPH-ADHD	Left VI'	10212.3086
16	MPH-ADHD	Vermis VI'	1970.27427
16	MPH-ADHD	Right VI'	9275.1868
16	MPH-ADHD	Left Crus I'	13146.87
16	MPH-ADHD	Vermis Crus I'	12.8041008
16	MPH-ADHD	Right Crus I'	14293.8752
16	MPH-ADHD	Left Crus II'	10185.6622

16	MPH-ADHD	Vermis Crus II'	419.420815
16	MPH-ADHD	Right Crus II'	9892.37906
16	MPH-ADHD	Left VIIb'	5511.12722
16	MPH-ADHD	Vermis VIIb'	220.265139
16	MPH-ADHD	Right VIIb'	5801.1228
16	MPH-ADHD	Left VIIIa'	5612.86791
16	MPH-ADHD	Vermis VIIIa'	1274.52711
16	MPH-ADHD	Right VIIIa'	5208.84662
16	MPH-ADHD	Left VIIIb'	4600.65184
16	MPH-ADHD	Vermis VIIIb'	636.052358
16	MPH-ADHD	Right VIIIb'	4414.64632
16	MPH-ADHD	Left IX'	3651.24507
16	MPH-ADHD	Vermis IX'	892.826488
16	MPH-ADHD	Right IX'	3988.13134
16	MPH-ADHD	Left X'	731.217972
16	MPH-ADHD	Vermis X'	415.960247
16	MPH-ADHD	Right X'	706.820969
16	MPH-ADHD	Left Dentate'	1562.61938
16	MPH-ADHD	Right Dentate'	1721.97853
16	MPH-ADHD	Left Interposed'	206.768925
16	MPH-ADHD	Right Interposed'	203.827442
16	MPH-ADHD	Left Fastigial'	36.3359617
16	MPH-ADHD	Right Fastigial'	37.8932172
17	MPH-ADHD	Left I_IV'	3438.774
17	MPH-ADHD	Right I_IV'	4002.07858
17	MPH-ADHD	Left V'	4760.56922
17	MPH-ADHD	Right V'	4770.93157
17	MPH-ADHD	Left VI'	9854.94226
17	MPH-ADHD	Vermis VI'	1812.22354

17	MPH-ADHD	Right VI'	9017.79963
17	MPH-ADHD	Left Crus I'	13514.3835
17	MPH-ADHD	Vermis Crus I'	12.9104789
17	MPH-ADHD	Right Crus I'	13783.4651
17	MPH-ADHD	Left Crus II'	9479.689
17	MPH-ADHD	Vermis Crus II'	420.439938
17	MPH-ADHD	Right Crus II'	9099.16962
17	MPH-ADHD	Left VIIb'	5038.82401
17	MPH-ADHD	Vermis VIIb'	203.679792
17	MPH-ADHD	Right VIIb'	5264.24777
17	MPH-ADHD	Left VIIIa'	5303.6587
17	MPH-ADHD	Vermis VIIIa'	1234.47961
17	MPH-ADHD	Right VIIIa'	5102.35716
17	MPH-ADHD	Left VIIIb'	4535.31533
17	MPH-ADHD	Vermis VIIIb'	603.564888
17	MPH-ADHD	Right VIIIb'	4467.53532
17	MPH-ADHD	Left IX'	3517.426
17	MPH-ADHD	Vermis IX'	759.170134
17	MPH-ADHD	Right IX'	3928.6927
17	MPH-ADHD	Left X'	747.788527
17	MPH-ADHD	Vermis X'	333.46408
17	MPH-ADHD	Right X'	727.063811
17	MPH-ADHD	Left Dentate'	1431.36441
17	MPH-ADHD	Right Dentate'	1614.65924
17	MPH-ADHD	Left Interposed'	207.247161
17	MPH-ADHD	Right Interposed'	213.192776
17	MPH-ADHD	Left Fastigial'	41.9590564
17	MPH-ADHD	Right Fastigial'	39.4109356
18	MPH-ADHD	Left I_IV'	3304.19496

18	MPH-ADHD	Right I_IV'	3845.80357
18	MPH-ADHD	Left V'	4529.59067
18	MPH-ADHD	Right V'	4237.41802
18	MPH-ADHD	Left VI'	10050.9387
18	MPH-ADHD	Vermis VI'	2018.26946
18	MPH-ADHD	Right VI'	8896.3828
18	MPH-ADHD	Left Crus I'	13052.1521
18	MPH-ADHD	Vermis Crus I'	13.8021229
18	MPH-ADHD	Right Crus I'	13671.751
18	MPH-ADHD	Left Crus II'	10592.0484
18	MPH-ADHD	Vermis Crus II'	416.059174
18	MPH-ADHD	Right Crus II'	9774.89624
18	MPH-ADHD	Left VIIb'	5718.56872
18	MPH-ADHD	Vermis VIIb'	207.863297
18	MPH-ADHD	Right VIIb'	5632.26388
18	MPH-ADHD	Left VIIIa'	5684.14656
18	MPH-ADHD	Vermis VIIIa'	1333.98349
18	MPH-ADHD	Right VIIIa'	5276.40192
18	MPH-ADHD	Left VIIIb'	4309.42186
18	MPH-ADHD	Vermis VIIIb'	658.510923
18	MPH-ADHD	Right VIIIb'	4268.51437
18	MPH-ADHD	Left IX'	3108.1383
18	MPH-ADHD	Vermis IX'	700.083583
18	MPH-ADHD	Right IX'	3370.54493
18	MPH-ADHD	Left X'	723.696853
18	MPH-ADHD	Vermis X'	377.978618
18	MPH-ADHD	Right X'	703.741977
18	MPH-ADHD	Left Dentate'	1503.59994
18	MPH-ADHD	Right Dentate'	1625.32469

18	MPH-ADHD	Left Interposed'	212.685725
18	MPH-ADHD	Right Interposed'	224.32607
18	MPH-ADHD	Left Fastigial'	40.2423342
18	MPH-ADHD	Right Fastigial'	43.4018563

SPREADSHEET USED:

https://docs.google.com/spreadsheets/d/1KyxXjACgOGFxbLg_4eRep-ilrXngkma8j_6jhTLUsM4/edit?usp=sharing

SECTION V: ANALYSIS

Cerebellar Structures

Duration vs. Dosage

Analysis of Cerebellar Structures

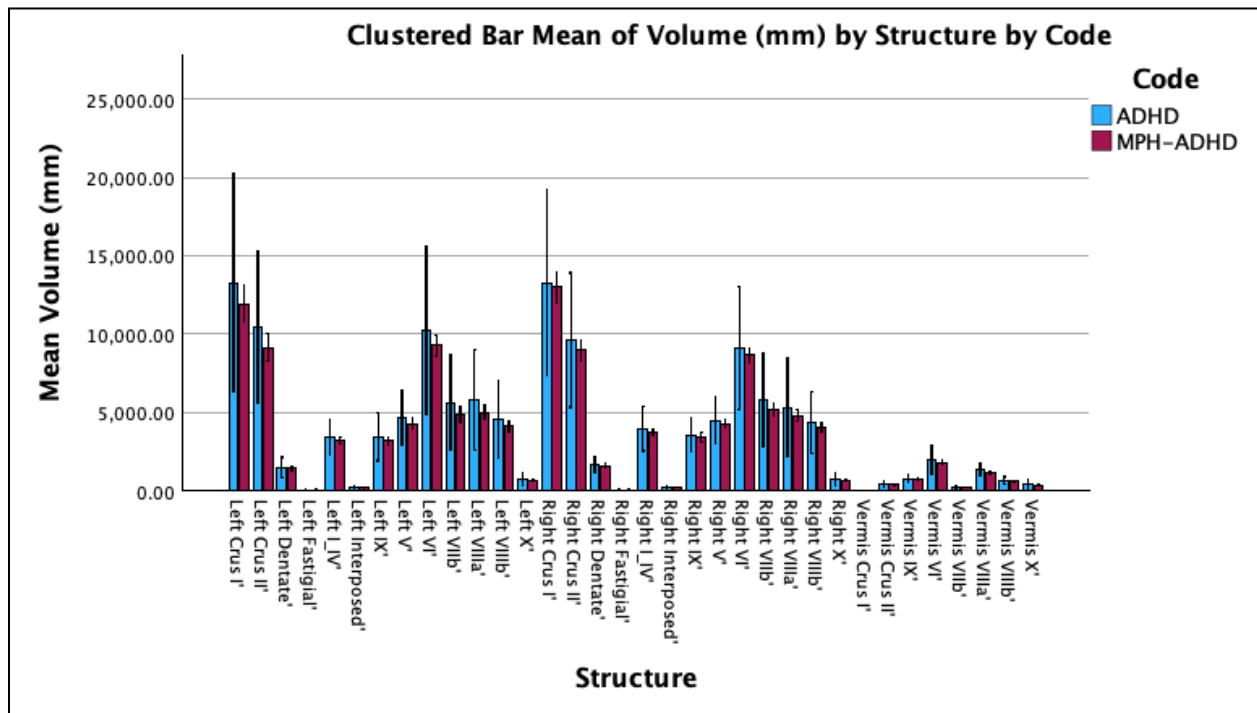


Fig. 1: Clustered bar graph of mean volumes of cerebellar structures (mm^3), organized by subjects with ADHD and using methylphenidate (MPH-ADHD), and subjects with ADHD and not using any medication; 95% confidence intervals used for error bars.

Fig. 1 displays the mean volume of each cerebellar structure for the treatment groups of individuals with ADHD and individuals who use MPH and have ADHD. The 95% confidence interval shown in the error bars represents the range in which there is 95% confidence to state the parameter exists in this range. In other words, the true value for each volume value is represented almost entirely by the error bars. In all structures, some overlap exists between the error bars. Medium to minimal overlap in the error bars were identified in the following structures through visual analysis: Left crus II, Left L_IV, Left IX, Left V, Left VI, Left VIIa, Left VIIIb, Right crus II, Right L_IV, Right IX, Right V, Right VIIb, Right VIIa, and Right VIIIb. A notable feature of this graph is the large range encompassed by the 95% confidence intervals for ADHD treatments. In general, such an occurrence brings into question the validity and reliability of the data, possibly suggesting a need for a larger sample size.

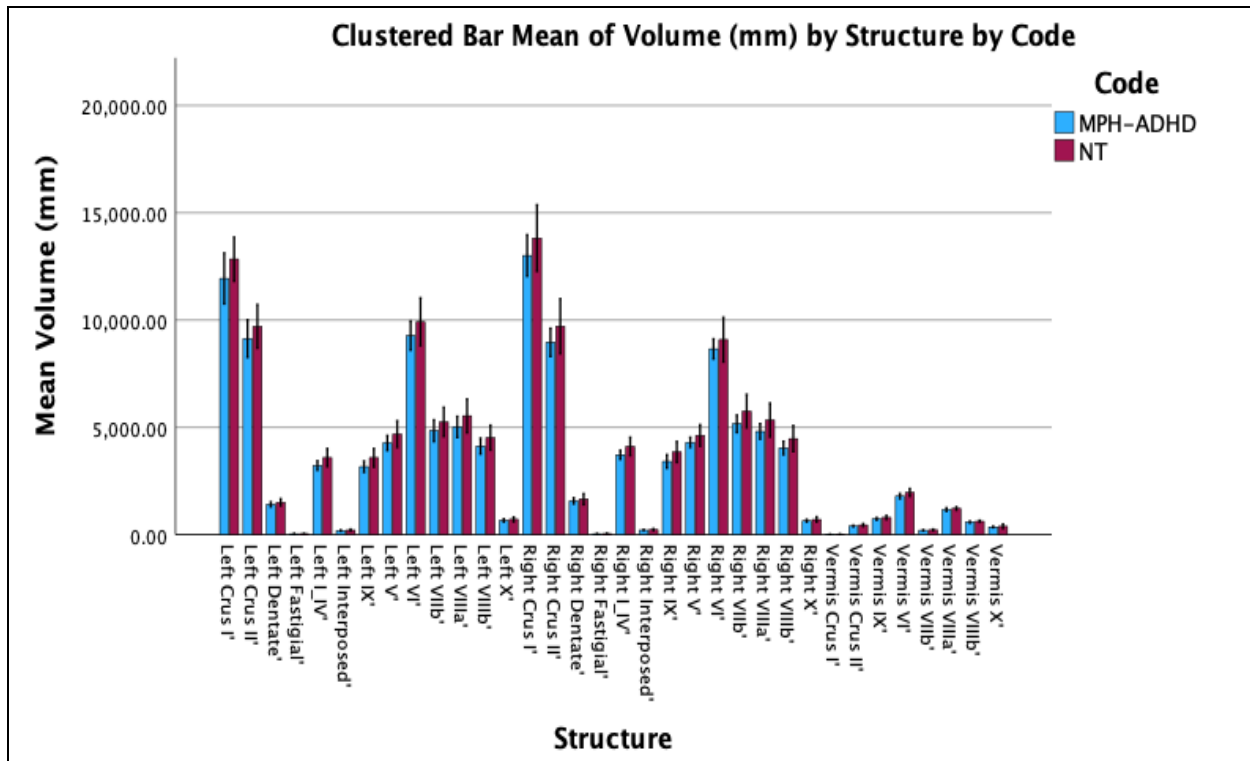


Fig. 2: Clustered bar graph of mean volumes of cerebellar structures (mm³), organized by subjects with ADHD and using methylphenidate (MPH-ADHD), and neurotypical subjects (NT); 95% confidence intervals used for error bars.

Fig. 2 displays the mean volume of each cerebellar structure for the treatment groups of neurotypical individuals and individuals who use MPH and have ADHD. In most structures, some overlap exists between the error bars. Medium to no overlap in the error bars were identified in the following structures through visual analysis: Left crus II, Left L_IV, Left IX, Left V, Left VI, Left VIIa, Left VIIIb, Right crus II, Right L_IV, Right IX, Right V, Right VIIb, Right VIIa, Right VIIIb. In comparison to Fig. 1, the error bars shown in this graph are smaller, which may be a product of the treatments in question having larger sample sizes. Overall, results taken from this comparison may have a comparably higher accuracy.

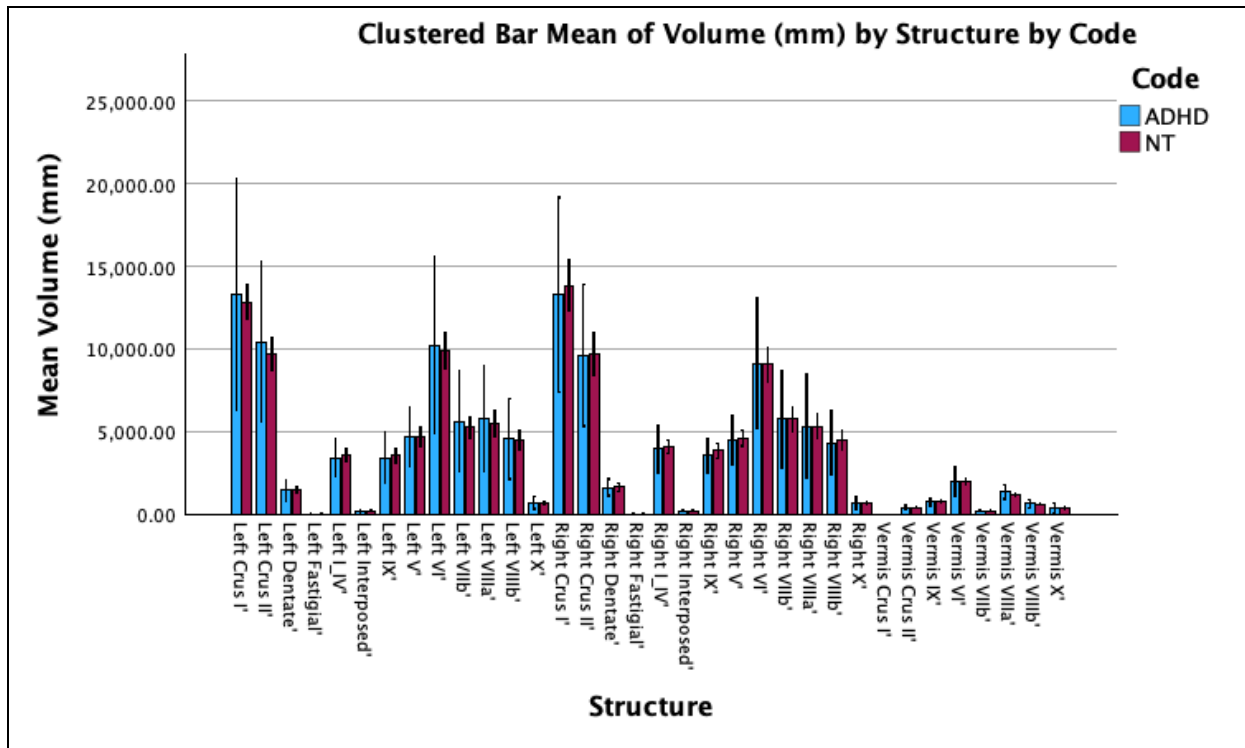


Fig. 3: Clustered bar graph of mean volumes of cerebellar structures, organized by subjects with ADHD and not using any medication (ADHD), and neurotypical subjects (NT); 95% confidence intervals used for error bars.

Fig. 3 displays the mean volume of each cerebellar structure for the treatment groups of neurotypical individuals and individuals who are medication-free and have ADHD. In most structures, some overlap exists between the error bars. Medium to no overlap in the error bars were identified in the following structures through visual analysis: Vermis VIIIa, Vermis VIIIb, Left crus II, Left VIIb, Right VIIIb. Similar to Fig. 1, error bars shown in this graph are substantial, with the ADHD treatment group again yielding an irregularly large range for the 95% confidence interval.

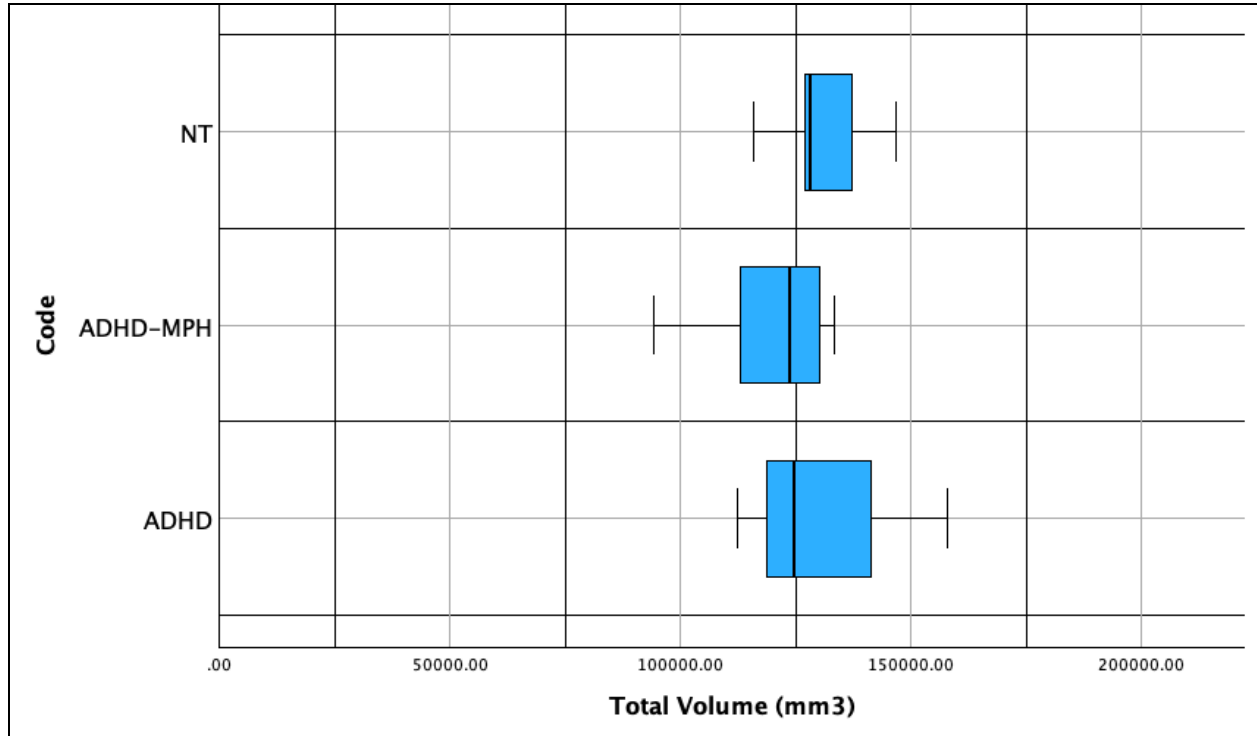


Fig. 4: Boxplot of total mean cerebellar volume, organized by subjects who: (1) have ADHD and do not use medication, (2) have ADHD and use methylphenidate, and (3) do not have ADHD and do not use medication.

Table 3: Summary statistics for overall cerebellar volume for each treatment group

Code	n	mean	SD	min	Q ₁	med	Q ₃	max
NT	5	131079.636	11627.971	115885.151	121516.859	128260.689	142051.887	146836.556
ADHD	3	131759.201	23547.348	112524	112524	124734	158019.604	158019.604
MPH-ADHD	10	120988.576	12360.127	94190.305	112954.727	123593.658	130126.747	133498.84

For neurotypical treatment, the distribution is approximately normal. No outliers were identified according to the 1.5 IQR rule. The distribution has an interquartile range (IQR) of 20535.028 and a standard deviation of 23547.348, indicating the data has a large spread. It should be noted that the software used for summary statistics, Stapplets, creates a boxplot differently from SPSS, leading to inconsistencies between the IQR in the summary statistics and the IQR in the box plot. For the ADHD-MPH treatment, the distribution is skewed to the left, with a large difference between the first quartile and minimum in comparison to the difference between the third quartile and maximum value. With additional samples, it is possible that the minimum value of 94190.305 could be considered an outlier. In the current distribution,

however, no outliers exist. Based on the summary statistics, this group has an IQR of 17172.02, which is less than the spread of the first NT group. The medication-naive ADHD group has a right skewed distribution. No outliers are present in this dataset. The has an IQR of 45495.604 and a standard deviation of 23547.348. Both of these values are significantly higher than the other groups, indicating that values are more dispersed.

Due to the skewed distribution found in both ADHD and MPH-ADHD, median is a more accurate representation of center. Based on the median, overall cerebellar volume was highest in neurotypical individuals, then in individuals with ADHD, and lowest in MPH-using individuals.

Table 4: Structures with potential significant differences, observed visually from error bars in Fig. 1, Fig. 2, and Fig. 3.

	ADHD vs. NT	MPH-ADHD vs. NT	ADHD vs. MPH-ADHD
(a) Confirmation	Vermis VIIIa Vermis VIIIb Left crus II Left VIIb	Left crus II Left L_IV Left IX Left V Left VI Left VIIIa Left VIIIb Right crus II Right I_IV Right IX Right V Right VIIb Right VIIIa Right VIIIb	Left crus I Left crus II Left I_IV Left VI Left VIIb Left VIIIa Left VIIIb Right VI Right VIIb Vermis X
(b) Not assessed	Left fastigial Left interposed Right fastigial Right interposed Vermis crus I Vermis VIIb	Left fastigial Left interposed Right fastigial Right interposed Vermis crus I Vermis VIIb	Left fastigial Left interposed Right fastigial Right interposed Vermis crus I Vermis VIIb

Through visual analysis of error bars, structural volume differences with potential significance were identified in Table 4(a). Some structures could not be analyzed visually through the graph, and were analyzed on a case-by-case basis. Structures with potentially significant differences were chosen and further evaluated using a two-sample T-test, with the results shown in Table 5, 6, and 7.

Table 5 Two sample T-test values for relevant ADHD vs. NT structures ($\alpha=0.05$)

Structure	T-statistic	p-value	Significance ($\alpha=0.05$)
-----------	-------------	---------	--------------------------------

Vermis VIIIa	-1.75	0.13	No
Vermis VIIIb	-0.714	0.50	No
Left crus II	-0.745	0.48	No
Left VIIb	-0.64	0.54	No

Table 6: Two sample T-test values for relevant MPH-ADHD vs. NT structures ($\alpha=0.05$)

Structure	T-statistic	p-value	Significance ($\alpha=0.05$)
Left crus II	0.95	0.36	No
Left L_IV	2.23	0.04	Yes
Left IX	2.20	0.047	Yes
Left V	1.59	0.14	No
Left VI	1.27	0.23	No
Left VIIIa	1.42	0.18	No
Left VIIIb	1.47	0.16	No
Right crus II	1.13	0.27	No
Right I_IV	1.11	0.29	No
Right IX	1.97	0.07	No
Right V	1.74	0.10	No
Right VIIb	1.86	0.08	No
Right VIIIa	1.82	0.09	No
Right VIIIb	1.77	0.10	No

Table 7: Two sample T-test values for relevant MPH-ADHD vs. ADHD structures ($\alpha=0.05$)

Structure	T-statistic	p-value	Significance ($\alpha=0.05$)
Left crus I	1.06	0.31	No
Left crus II	1.41	0.18	No
Left I_IV	0.99	0.34	No

Left VI	1.18	0.26	No
Left VIIIb	1.48	0.16	No
Left VIIIa	1.44	0.17	No
Left VIIIb	1.12	0.29	No
Right VI	0.78	0.45	No
Right VIIIb	1.25	0.24	No
Vermis X	0.60	0.55	No
Right Fastigial	2.14	0.05	Yes

From performing a two-sample t-test at an alpha level of 0.05, it was found that a significant difference exists between MPH-using individuals with ADHD and neurotypical individuals in the regions encompassed within the fields of Left L_IV and Left IX. When comparing medication free individuals with ADHD and MPH-using individuals, a significant difference was found in the right fastigial nucleus. It should be noted that near-significant differences exist between individuals coded MPH-ADHD and NT in the following regions: Right IX, Right VIIIb, and Right VIIIa.

Table 7: Results from further two sample t-tests on structures identified as many statistical significance, $\mu_1 > \mu_2$

Comparison	Structure	T-statistic	p-value	Significance ($\alpha=0.05$)
MPH vs. ADHD	Right Fastigial	2.10	0.027	Yes
MPH vs NT	Left IX	2.19	0.023	Yes
MPH vs NT	Left I_IV	2.23	0.021	Yes

Further testing was conducted on the structures showing significant differences. In this new analysis, a two sample t-test was conducted under the assumption that μ_1 , or the mean from the neurotypical sample, is greater than μ_2 , the mean from the MPH sample. It should be noted that μ_1 was set as ADHD for analyzing the right fastigial nucleus. These results indicate that methylphenidate is associated with a decrease in the three structures above.

Analysis of Medication Duration and Dosage

Based on the results gathered from analyzing cerebellar structure, the three regions with statistical significance were plotted for MPH-ADHD individuals in context of dosage, duration, as well as dosage and duration working conjunction. This last factor is described as medication intensity, or the product of dosage and medication. Prior to creating the graphs, no outliers were identified according to the 1.5 IQR rule.

Looking at the right fastigial nucleus to begin with (Fig. _a, 1b, 1c), there appears to be no

correlation between medication duration and volume of the right fastigial nucleus. Examining Fig. 1a, there appears to be a strong positive correlation between medication dosage and the volume of the right fastigial nucleus, with an r-value of 0.77, indicating a strong positive correlation. Similarly, the R^2 value of 0.596, suggesting 60% of the variation in volume of the right fastigial nucleus can be explained by medication dosage. When taking both medication duration and dosage into consideration, there appears to be a weak positive correlation, with an r-value of 0.32.

Looking at the Left IX region (Fig. _d, _e, _f), there appears to be no correlation between medication dosage and regional volume, with an r-value of 0.08. A weak positive correlation may exist in medication duration and regional volume, with an r-value of 0.30. A stronger positive correlation can be found between medication intensity and regional volume, with an r-value of 0.38.

Lastly, looking at the Left I_IV region (Fig. _g, _h, _i), a weak positive correlation exists between dosage and regional volume, as well as duration and regional volume, each respectively providing an r-value of 0.10 and 0.28. A stronger correlation exists between intensity and regional volume, providing an r-value of 0.58. To summarize, the right fastigial nucleus may be heavily influenced by medication dosage. The Left I_IV region may also be influenced by medication intensity, though to a lesser extent.

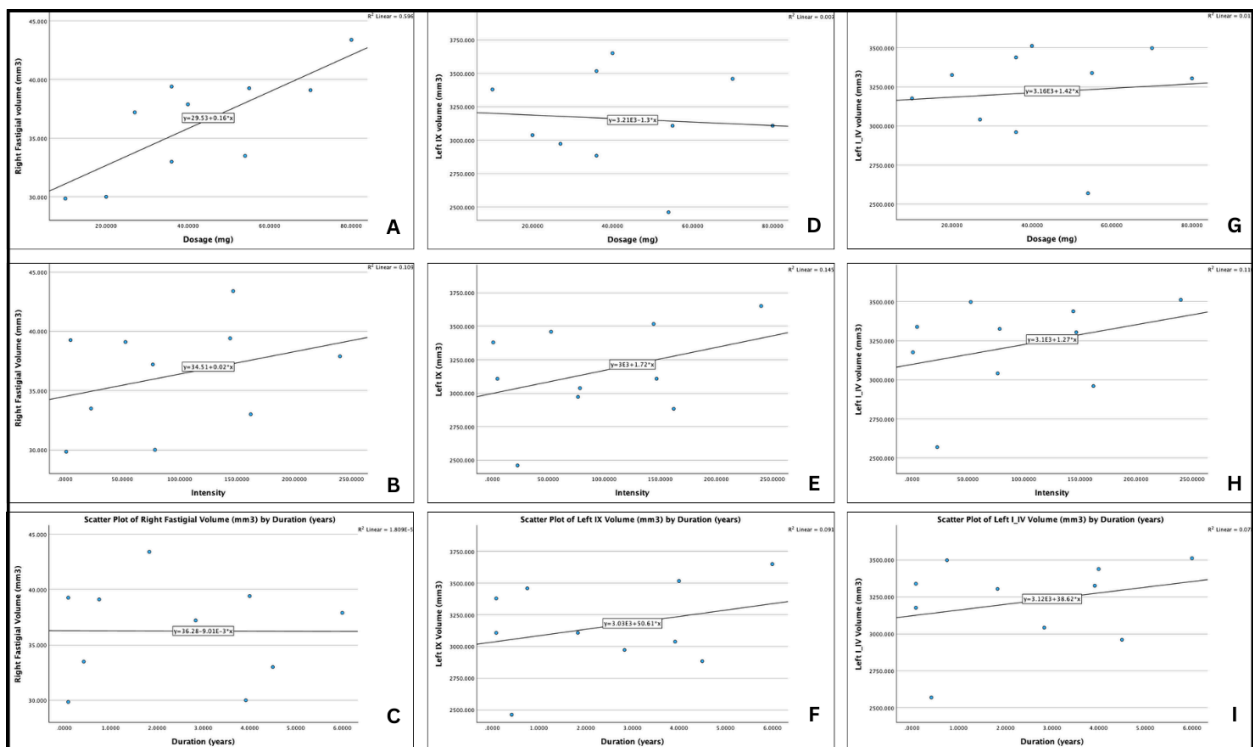


Fig. _: Graphical comparisons of duration, dosage, and intensity against three regional brain volumes. For the right fastigial nucleus, the following graphs are produced (a) dosage (mg) vs. regional volume (mm³), (b) intensity vs. regional volume (mm³), and (c) duration (years) vs. regional volume (mm³). For the Left IX region, the following graphs are produced: (d) dosage (mg) vs. regional volume (mm³), (e) intensity vs. regional volume (mm³), and (f), duration (years) vs. regional volume (mm³). For the Left I_IV region, the following graphs are produced: (g)

dosage (mg) vs. regional volume (mm^3), (h) intensity vs. regional volume (mm^3), and (i), duration (years) vs. regional volume (mm^3).

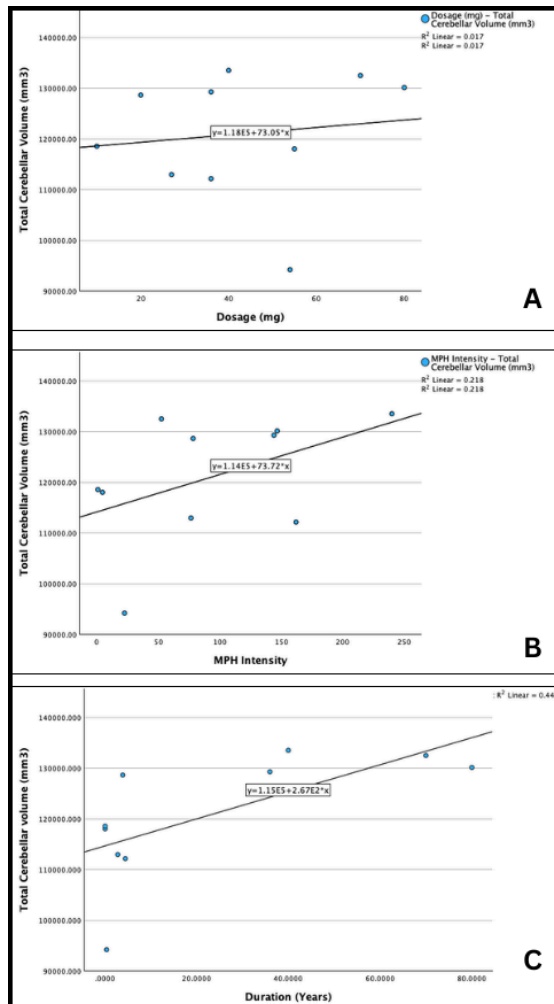


Fig. 1: Scatterplots of (a) total cerebellar volume (mm^3) versus dosage (mg), (b) total cerebellar volume (mm^3) versus intensity, and (c) total cerebellar volume (mm^3) versus duration (years).

Based on correlation coefficient values, there appears to be a medium to strong positive correlation between medication duration and total cerebellar volume ($r=0.67$). A weaker positive correlation exists between medication intensity and total cerebellar volume ($r=0.467$), while an extremely weak positive correlation exists between medication dosage and cerebellar volume ($r=0.13$).

Overall, medication characteristics either have no correlation to total and regional cerebellar volume or have a positive correlation. This suggests that as dosage, duration, and intensity increase, so does cerebellar volume.

Summary

From the various statistics and analytical tools used, the following information was obtained: (1) a statistically significant decrease ($p=0.02$) in cerebellar volume localized the Left I_IV and Left IX regions can be found between neurotypical individuals and MPH-using ADHD individuals; (2)

a statistically significant decrease ($p=0.02$) in cerebellar volume localized the right fastigial region can be found between MPH-using individuals with ADHD and drug-naive individuals with ADHD; (3) the median total cerebellar volume is lower in individuals who use MPH and highest in neurotypical individuals; (4) a strong positive correlation exists between medication dosage and the volume of the right fastigial nucleus ($r=0.77$), (5) a moderate positive correlation exists between medication intensity and regional volume in the Left I_IV region ($r=0.58$); and (6) a moderate correlation exists between medication duration and total cerebellar volume ($r=0.67$).

SECTION VI: DISCUSSION & CONCLUSION

Structural Differences

Sources of Error

Improvements

Implications

Conclusion

Structural Differences

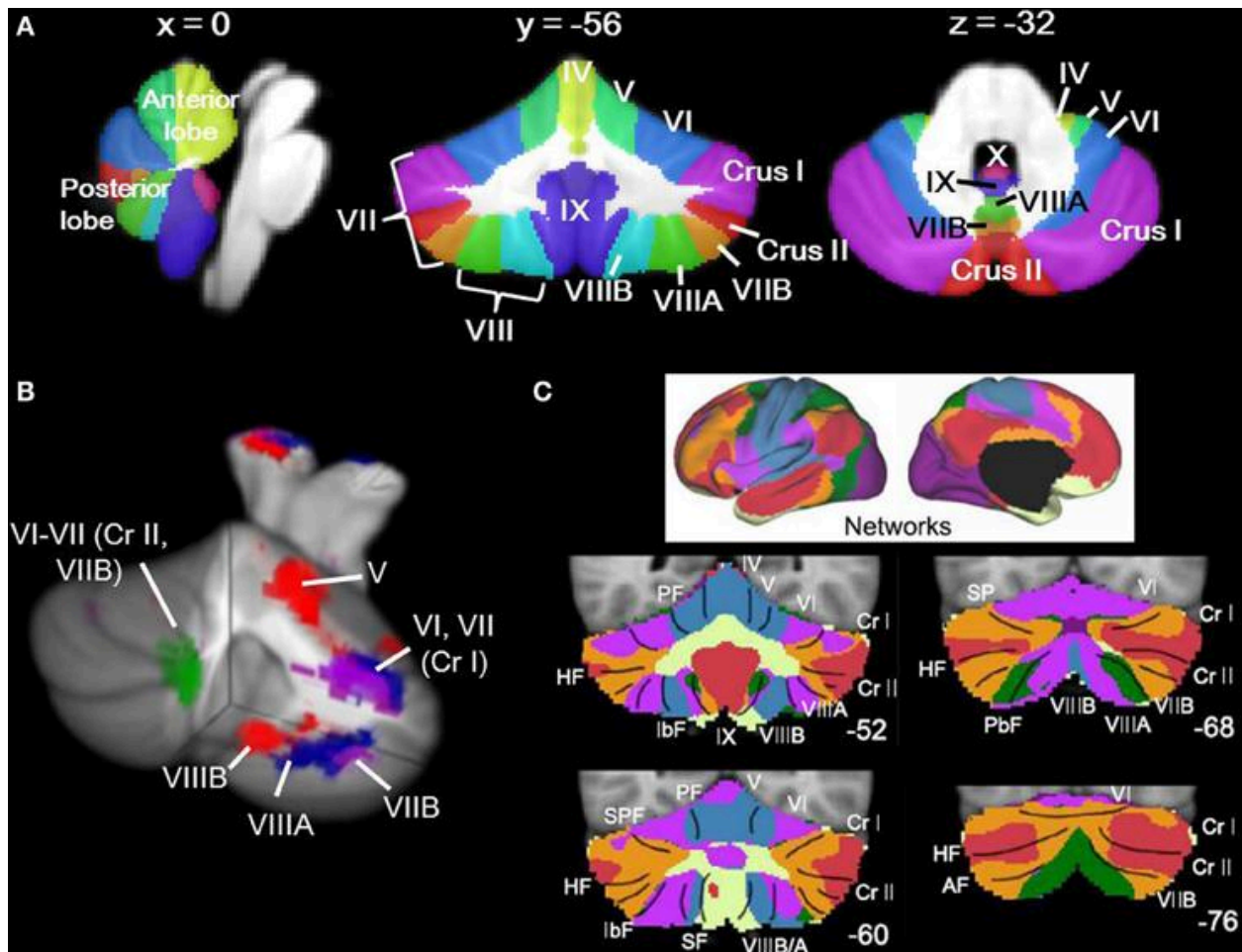


Fig. 1: Locations of Cerebellar Regions (Stoodly, 2014)

To begin, a statistically significant decrease was observed in the right fastigial nucleus from MPH-using individuals with ADHD in relation to medication-free individuals with ADHD. The reason for this change is unclear, as the fastigial nucleus is mainly responsible for carrying inputs from the vermis to the superior cerebellar peduncle, as well as the uncinate fasciculus and juxtarestiform body. The current understanding of MPH focuses on its effects on the dopamine reward system, which has sparse connections with the fastigial nuclei. A decrease in the volume in the right fastigial nucleus may have unpredictable effects on the vestibulocerebellum and spinocerebellar pathways, with the fastigial nucleus being responsible for carrying vestibular, proximal somatosensory, auditory, and visual information. This information is essential for its influence on proximal trunk muscles through connections to medial motor pathways (anterior corticospinal, reticulospinal, vestibulospinal, tectospinal tracts). In the literature review conducted, no prior study has noted differences in the volume of the fastigial nucleus. This deviation may be expected, as previous studies relied on the use of VBM or Freesurfer, which cannot map the 30–40 mm³ fastigial nucleus. That being said, results from the SUIT toolbox on an area with such a small volume should be used cautiously, as inaccuracies as small as a few millimeters in the program can be mistaken for statistical significance. As such, it is recommended further, hypothesis-driven analysis of anatomical images with a larger sample size be conducted. Moreover, it may also be pertinent to

investigate other indicators of neurodegeneration, such as specific enzymes in the area.

The region Left I_IV corresponds to the left anterolateral area of the cerebellum (Jadavid, 2022). More specifically, lobule IV of the cerebellum is part of the anterior lobe of the cerebellar hemisphere. From a functional perspective, lobule IV is a major receiver of spinocerebellum afferents. While the fastigial nucleus receives input from the vermis and flocculonodular lobe, the importance of both the fastigial nucleus and lobule IV to the spinocerebellar system may indicate a connection between MPH and the aforementioned pathway. The positioning of lobule IV as an intermediate section of the cerebellar hemispheres may also indicate differences in control of distal appendicular muscles in MPH users. Further study of this area is again recommended, with a focus on improving sample size. Clinical representations of MPH use can be evaluated, such as decrease in distal limb control. Such differences may be able to explain certain side effects associated with MPH, such as uncontrolled movement of a specific body part.

Lobule IX, the final region with a statistically significant difference, is more commonly referred to as the cerebellar tonsils (Jadavid, 2022a). The cerebellar tonsils are considered to be part of the posterior lobe, which in turn can influence the initiation, planning, and coordination of movement, as well as the strength and scope of movement (Liu et al, 2020). From a clinical perspective, chiari malformations (CM) have been associated with ADHD (DuBow et al., 2020). CM is characterized by cerebellar herniation through the foramen magnum. This herniation typically begins with the cerebellar tonsils. In an existing case study, a 28-year old woman who had been taking long-acting MPH since the age of 12 but stopped at an unknown time suffered from CM with no other relevant medical history. As such, the changes in lobule IX may be reflective of larger changes in neural networks. The change in lobule IX only is present between MPH-users and neurotypical users, and not between medication-free individuals with ADHD and neurotypical individuals. From the data, it appears MPH has an association with CM rather than ADHD, though a significant amount of further study is required to solidify this relationship.

Overall, comparisons with existing literature are difficult to examine. No existing studies utilized the SUIT Toolbox to analyze the cerebellum, leading to results stating general decreases in cerebellar volume or cortical thickness. As such, the changes in lobule IV, lobule IX, and the right fastigial nucleus cannot be confirmed through research. The lower median total cerebellar volume in individuals with ADHD does align with existing literature, which notes individuals with ADHD typically have an overall reduction in brain size (Pliszka, 2007; Tripp & Wickens, 2009). Notably, the median total cerebellar volume of MPH-using individuals was even lower than that of their medication-free counterparts, possibly indicating wide-ranging and minor structural changes. In other words, structural changes from MPH may be not only localized to the listed areas, and may minorly impact a wide range of cerebellar structures. This study does deviate from existing literature, however, which associated decreased volume of the cerebellar vermis with ADHD (Pliszka, 2007). This may indicate inaccuracies in existing literature or in the methodology used for this study, and is an area for further study.

Sources of Error

Multiple sources of errors exist in each step of the method used. To begin with data collection, the study did not account for varied MPH doses and durations. More specifically, some of the study participants used different doses of MPH over time, or would take different doses at different times in a day. Similarly, some participants took breaks from their medications, leading to gaps in duration. The possibility of misreporting, for both duration and dosage, is high, as

start dates for taking a medication are usually not explicitly remembered. In addition, some study participants had other neurological diagnoses that may have served as confounding variables. A larger population size may mitigate the effects of misreporting, and the development of a better classifying system for medication dosage and duration should be developed. From a sample size perspective, eighteen participants is not enough for conducting statistical analyses. The distribution for individuals coded ADHD and MPH-ADHD both were skewed, meaning the distribution failed one of the requirements for a two sample t-test. Skewed data can still be used so long as the sample size is greater than thirty. In order to fulfill this criteria, however, ninety participants (30 for each treatment) would have to be recruited. A study of that magnitude would require approval by the University of Calgary's IRB, as well as a large amount of funding for incentivizing the participants and MRI use. As such, it is unlikely this source of error can be completely eliminated. It may be possible to loosen the exclusion criteria implemented for this study and use covariate analysis to control for confounding variables, allowing for the study to use a greater number of anatomical scans from the TAG-IT demographics project.

In the data processing phase using the SUIIT toolbox, multiple sources of error also existed. While SUIIT has been used by multiple peer-reviewed studies, it is not as established as VBM. Understanding how the SUIIT program works and potentially making improvements to the open-access code may reduce errors in the results. The most significant source of error lies in the hand-editing portion of analyzing the SUIIT images. The cerebellum mask created by the SUIIT segregation function consistently does not encompass the entire cerebellum and must be edited by hand to do so, The editing process is time consuming and tiring, leading to errors in the new cerebellum mask. In addition, the sagittal, coronal, and axial views are not smooth post-editing, with each individual slice not directly leading into the next. Errors increase for the TAG-IT demographics data, which uses lower resolution MRI images. In multiple scans, the contrast between the cerebellum and the rest of the brain has errors, displaying a completely white mass with no border. Obtaining higher resolution MRI images could rectify this error, as could cross-checking with edited masks with another researcher.

In the data analysis phase of the project, the distributions sometime did not fulfill all the requirements to ensure accurate inferential statistics, The three requirements for a two-sample t-test are: (1) the distribution is normally distributed, (2) the distribution is independent, and (3) random sampling took place. Out of the three treatments, only neurotypical individuals had normally distributed data. It was assumed that the population cerebellar volume for individuals coded ADHD and MPH-ADHD were normally distributed. A greater sample size would nullify the requirement for normally distributed data. All three distributions were independent of each other, with the cerebellar volume of one individual having no impact on that of the next. All studies which actively recruit participants are by nature not performing random sampling as a result of participant bias. In other words, certain demographics of people may be more willing to volunteer as study participants. It could be possible to reduce the impacts of bias by taking a significantly larger sample, and then randomly selecting participant anatomical images to analyze. The funding and scale required for such a project, however, does not make it a plausible option for this study. To summarize, the distributions used did not fulfill the requirements for a t-test, which may have led to inaccurate results.

Improvements

There are two main improvements that can be made to this project: sample size and covariate analysis. The sample size of each treatment group did not exceed ten for this current study,

which exacerbates the power of outliers in skewing the distribution. In particular, the ADHD treatment used only three participants, one of which had a drastically higher overall cerebellar volume than the other two. The inappropriate size of this sample is reflected in the large error bars for the graphs comparing ADHD, possibly explaining why more significant differences were found in comparisons not involving participants coded with ADHD. It is, however, difficult to recruit medication-free individuals with ADHD, as the condition is often associated with other neurological disorders that also are treated with medication. Another reason for only three structures showing statistical significant differences is that confounding variables are changing the results. Through covariate analysis tools, such as ANCOVA, hierarchical linear modeling, and regression analysis, major confounding variables such as age, sex, ethnicity, overall cranial capacity, and ADHD type can be accounted for.

Implications

Taking into account both the prevalence of ADHD and MPH in treating ADHD, understanding the potential risks of using the drug is essential. The mechanism of MPH is still not understood and the changes the drug causes to brain structure could be expressed phenotypically given sufficient duration and dosage. By localizing the structures most impacted by MPH, as well as the general nature of these impacts, this study lays the groundwork for future research on MPH. Current literature fails to localize the effects of MPH, but the well-documented neurodegeneration is a source for concern. With MPH in the hands of so many, especially children, this study has the potential to shape treatment approaches to ADHD.

Conclusions

Through the analysis of T1 weighted MRI scans, significant ($p < 0.05$) decreases in the volume of the left lobule IV and left cerebellar tonsils were found in MPH-using individuals compared to neurotypical individuals. Similarly, a significant decrease in the right fastigial nucleus was observed in individuals using MPH relative to individuals with ADHD and not taking MPH. Further analysis revealed a strong positive correlation exists between medication dosage and the volume of the right fastigial nucleus ($r = 0.77$). Moreover, a moderate positive correlation exists between medication intensity and regional volume in the Left I_IV region ($r = 0.58$), as well as between medication duration and total cerebellar volume ($r = 0.67$). These results introduce new and specific structures for where MPH has the greatest impacts, laying the groundwork for future hypothesis-driven studies. Further analysis should focus on: (1) expanding the sample size of the study; (2) examining apoptotic and inflammatory factors in the most affected regions; (3) comparing the effect of MPH and amphetamines to see if the latter provides a suitable alternative.

OLD VERSION

Without full experimental results, it is difficult to form a conclusion on the effects of methylphenidate dosage and usage duration on cerebellar structure. Purely from conducting literature review, prior studies suggest the MPH has the most profound effects on cerebellar cortical thickness and composition, increases in cerebellar-related diseases, and increases in tissue degeneration and inflammation factors. Due to the method of this study, obtained results will only indirectly correspond to the findings in the literature review. The main reason for this is the fact that only anatomical scans are being used. Additionally, inflammation factors

cannot be tested for in subjects who are still alive. The literature review serves to elucidate the unique nature of this project. While previous studies have focused primarily on the degeneration of the outer layers of the cerebellar hemispheres, the use of SUIIT allows this study to examine medial structure as well. As such, this study has the potential to yield novel insights into the dangers of methylphenidate.

References

- Bahcelioglu, M., Gozil, R., Take, G., Elmas, C., Oktem, H., Kadioglu, D., ... Senol, S. (2009). Dose-related immunohistochemical and ultrastructural changes after oral methylphenidate administration in cerebrum and cerebellum of the rat. *World Journal of Biological Psychiatry*, 10*(4 Pt 2), 531-543.
<https://doi.org/10.1080/15622970903176683>
- Bantick, R. A., De Vries, M. H., & Grasby, P. M. (2005). The effect of a 5-HT_{1A} receptor agonist on striatal dopamine release. *Synapse (New York, N.Y.)*, 57*(2), 67-75.
<https://doi.org/10.1002/syn.20156>
- Blumenfeld, H. (2010). *Neuroanatomy Through Clinical Cases with Ebook**. Oxford University Press, Incorporated.
- Brown, A. B., Biederman, J., Valera, E. M., Doyle, A. E., Bush, G., Spencer, T., ... Seidman, L. J. (2010). Effect of dopamine transporter gene (SLC6A3) variation on dorsal anterior cingulate function in attention-deficit/hyperactivity disorder. *American Journal of Medical Genetics. Part B, Neuropsychiatric Genetics*, 153B*(2), 365-375.
<https://doi.org/10.1002/ajmg.b.31022>
- Curtin, K., Fleckenstein, A. E., Keeshin, B. R., Yurgelun-Todd, D. A., Renshaw, P. F., Smith, K. R., & Hanson, G. R. (2018). Increased risk of diseases of the basal ganglia and cerebellum in patients with a history of attention-deficit/hyperactivity disorder. *Neuropsychopharmacology*, 43*(13), 2548-2555.
<https://doi.org/10.1038/s41386-018-0207-5>
- Diedrichsen, J. (2006). A spatially unbiased atlas template of the human cerebellum. *Neuroimage*, 33, 1, p. 127-138.
- Diedrichsen, J., Balsters, J. H., Flavell, J., Cussans, E., & Ramnani, N. (2009). A probabilistic atlas of the human cerebellum. *Neuroimage*.
- Diedrichsen, J., Maderwald, S., Kuper, M., Thurling, M., Rabe, K., Gizewski, E. R., et al. (2011). Imaging the deep cerebellar nuclei: A probabilistic atlas and normalization procedure. *Neuroimage*.
- Diedrichsen, J. & Zotow, E. (2015). Surface-based display of volume-averaged cerebellar data. *PLoS One*, 7, e0133402.

DuBow, A., Mouroto, A., & Tourjman, S. V. (2020). Chiari Malformation and Attention Deficit Hyperactivity Disorder. *Case reports in medicine*, 2020, 2694956. <https://doi.org/10.1155/2020/2694956>

Faraone, S. V. (2018). The pharmacology of amphetamine and methylphenidate: Relevance to the neurobiology of attention-deficit/hyperactivity disorder and other psychiatric comorbidities. **Neuroscience and Biobehavioral Reviews*, 87*, 255-270. <https://doi.org/10.1016/j.neubiorev.2018.02.001>

Faraone, S. V., Larsson, H. (2019). Genetics of attention deficit hyperactivity disorder. **Molecular Psychiatry*, 24*, 562-575. <https://doi.org/10.1038/s41380-018-0070-0>

Harpin, V. A. (2005). The effect of ADHD on the life of an individual, their family, and community from preschool to adult life. **Archives of Disease in Childhood*, 90 Suppl 1*(Suppl 1), i2-i7.

Harpin, V., Mazzone, L., Raynaud, J. P., Kahle, J., Hodgkins, P. (2013). Long-Term Outcomes of ADHD: A Systematic Review of Self-Esteem and Social Function. **Journal of Attention Disorders*, 20*(4), 295-305.

Javaid, M. A. (2022). *Lobule IV of cerebellar hemisphere - e-Anatomy*. IMAIOS. Retrieved March 14, 2024, from <https://www.imaios.com/en/e-anatomy/anatomical-structure/lobule-iv-of-cerebellar-hemisphere-1553803868>

Javaid, M. A. (2022a). *Tonsil of cerebellum - e-Anatomy*. IMAIOS. Retrieved March 14, 2024, from <https://www.imaios.com/en/e-anatomy/anatomical-structure/tonsil-of-cerebellum-1553804124?from=2>

Jimshelishvili, S., Dididze, M. (2023). Neuroanatomy, Cerebellum. In: **StatPearls**. Available from: <https://www.ncbi.nlm.nih.gov/books/NBK538167/>

Lewis, R. G., Florio, E., Punzo, D., & Borrelli, E. (2021). The Brain's Reward System in Health and Disease. **Advances in Experimental Medicine and Biology*, 1344*, 57-69. https://doi.org/10.1007/978-3-030-81147-1_4

Liu, W. F., Shu, Y. Q., Zhu, P. W., Li, B., Shi, W. Q., Lin, Q., Liu, Y. X., Zhang, M. Y., Min, Y. L., Yuan, Q., & Shao, Y. (2019). The Cerebellum Posterior Lobe Associates with the

Exophthalmos of Primary Hyperthyroidism: A Resting-State fMRI Study. *International journal of endocrinology*, 2019, 8135671. <https://doi.org/10.1155/2019/8135671>

Loureiro-Vieira, S., Costa, V. M., Duarte, J. A., Duarte-Araújo, M., Gonçalves-Monteiro, S., Maria de Lourdes B., ... Capela, J. P. (2018). Methylphenidate clinically oral doses improved brain and heart glutathione redox status and evoked renal and cardiac tissue injury in rats. **Biomedicine & Pharmacotherapy*, 100*, 551-563. <https://doi.org/10.1016/j.biopha.2018.02.017>

Mackey, S., Stewart, J. L., Connolly, C. G., Tapert, S. F., Paulus, M. P. (2014). A voxel-based morphometry study of young occasional users of amphetamine-type stimulants and cocaine. **Drug and Alcohol Dependence*, 135*, 104-111. <https://doi.org/10.1016/j.drugalcdep.2013.11.018>

Mahmud, A. (2023, November 6). *T1 weighted image | Radiology Reference Article*. Radiopaedia. Retrieved February 9, 2024, from <https://radiopaedia.org/articles/t1-weighted-image>

Mahoud, A. (2023). T1 weighted image | Radiology Reference Article. *Radiopaedia*. Retrieved February 9, 2024, from <https://radiopaedia.org/articles/t1-weighted-image>

Motaghinejad, M., Motevalian, M., Shabab, B. (2016). Effects of chronic treatment with methylphenidate on oxidative stress and inflammation in hippocampus of adult rats. **Neuroscience Letters*, 619*, 106-113. <https://doi.org/10.1016/j.neulet.2015.12.015>

Motaghinejad, M., Motevalian, M., Shabab, B. (2017). Effects of acute doses of methylphenidate on inflammation and oxidative stress in isolated hippocampus and cerebral cortex of adult rats. **Journal of Neural Transmission*, 124*(1), 121-131. <https://doi.org/10.1007/s00702-016-1623-5>

Pai, A., Shetty, R., Hodis, B., et al. (2023 Apr 2). *Magnetic Resonance Imaging Physics*. In: *StatPearls*. Available from: <https://www.ncbi.nlm.nih.gov/books/NBK564320/>

Pliszka, S.; AACAP Work Group on Quality Issues. (2007). Practice parameter for the assessment and treatment of children and adolescents with attention-deficit/hyperactivity disorder. **Journal of the American Academy of Child and Adolescent Psychiatry*, 46*(7), 894-921.

Quansah, E., Ruiz-Rodado, V., Groot

veld, M., & Zetterström, T. S. C. (2018). Methylphenidate alters monoaminergic and metabolic pathways in the cerebellum of adolescent rats. **European Neuropsychopharmacology*, 28*(4), 513-528.
<https://doi.org/10.1016/j.euroneuro.2018.02.002>

Raofi, A., Aliaghaei, A., Abdollahifar, M. A., Eskandarian Boroujeni, M., Javadinia, S. S., Atabati, H., & Abouhamzeh, B. (2020). Long-term administration of high-dose methylphenidate-induced cerebellar morphology and function damage in adult rats. **Journal of Chemical Neuroanatomy*, 103*, 101712.
<https://doi.org/10.1016/j.jchemneu.2019.101712>

Réus, G. Z., Scaini, G., Jeremias, G. C., Furlanetto, C. B., Morais, M. O., Mello-Santos, L. M., ... Streck, E. L. (2014). Brain apoptosis signaling pathways are regulated by methylphenidate treatment in young and adult rats. **Brain Research*, 1583*, 269-276.
<https://doi.org/10.1016/j.brainres.2014.08.010>

Schmitz, F., Scherer, E. B., Machado, F. R., da Cunha, A. A., Tagliari, B., Netto, C. A., & Wyse, A. T. (2012). Methylphenidate induces lipid and protein damage in prefrontal cortex, but not in cerebellum, striatum and hippocampus of juvenile rats. **Metabolic Brain Disease*, 27*(4), 605-612. <https://doi.org/10.1007/s11011-012-9335-5>

Schweren, L. J., de Zeeuw, P., & Durston, S. (2013). MR imaging of the effects of methylphenidate on brain structure and function in attention-deficit/hyperactivity disorder. **European Neuropsychopharmacology*, 23*(10), 1151-1164.
<https://doi.org/10.1016/j.euroneuro.2012.10.014>

Stoodley C. J. (2014). Distinct regions of the cerebellum show gray matter decreases in autism, ADHD, and developmental dyslexia. *Frontiers in systems neuroscience*, 8, 92.
<https://doi.org/10.3389/fnsys.2014.00092>

Tripp, G., & Wickens, J. R. (2009). Neurobiology of ADHD. **Neuropharmacology*, 57*(7-8), 579-589. <https://doi.org/10.1016/j.neuropharm.2009.07.026>

Tripp, G., Wickens, J. R. (2009 Dec). Neurobiology of ADHD. **Neuropharmacology*, 57*(7-8), 579-589. <https://doi.org/10.1016/j.neuropharm.2009.07.026>

Urry, L. A., Cain, M. L., Wasserman, S. A., Minorsky, P. V., & Orr, R. B. (2020). **Campbell Biology**. Pearson.

Vergheese, C., Abdijadid, S. (2023 Jan 2). *Methylphenidate*. In: *StatPearls*. Available from: <https://www.ncbi.nlm.nih.gov/books/NBK482451/>

Weseley, A. J., & McEntarffer, R. (2023). *AP Psychology Premium, 2024: Comprehensive Review With 6 Practice Tests + an Online Timed Test Option*. Barrons Educational Services.